

Aus dem Lehrstuhl für Physiologische Chemie  
im Biomedizinischen Centrum (BMC)  
der Ludwig-Maximilians-Universität München

Vorstand: Prof. Andreas Ladurner

# **Molecular mechanisms of protein translocation across mitochondrial inner membrane**

Dissertation  
zum Erwerb des Doktorgrades der Naturwissenschaften  
an der Medizinischen Fakultät der  
Ludwig-Maximilians-Universität zu München

vorgelegt von  
**Rupa Banerjee**

aus  
Allahabad, UP, India

Jahr  
2018

Mit Genehmigung der Medizinischen Fakultät  
der Universität München

Betreuerin: PD Dr. rer. nat. Dejana Mokranjac  
Zweitgutachterin: Prof. Dr. Simone Kreth  
Dekan: Prof. Dr. med. dent. Reinhard Hickel  
Tag der mündlichen Prüfung: 07.11.2018

## Acknowledgements

It gives me immense pleasure to thank and express my gratitude towards all the people who have helped me and have been instrumental in providing me with their kind support and encouragement during this journey towards obtaining my doctoral degree.

I would like to thank my mentor, **Dr. Dejana Mokranjac**, for giving me an opportunity to work in her lab and for her valuable guidance throughout my doctoral training. I have truly learnt a lot under her mentorship, not only about science but also about lessons of life. In moments of failure and frustration, she has always been there with a smile on her face saying and I quote her, "Science is fun, don't lose hope". I consider myself extremely fortunate that I got an opportunity to work under her supervision and I hope I do justice to the training received. It has been a wonderful and an enriching experience to work with her.

I thank **Umut** for being a helpful colleague, a co-operative benchmate and an awesome friend. We have had some extremely interesting and sometimes even heated discussions on scientific and non-scientific topics. It has, undoubtedly, been a pleasant experience to have him around.

I am extremely thankful to **Petra Robisch** for her technical assistance and for always managing to light up the mood even in the worst of situations.

I am grateful to **DAAD** for funding a considerable period of my PhD training.

I thank **Prof. Don Lamb** and **Vanessa** for a fruitful collaboration and insightful discussions.

I am thankful to my Thesis Advisory Committee (TAC) members, **Dr. Sigurd Braun**, **Dr. Andreas Bracher** and **Prof. Dr. Dr. Walter Neupert** for their time and consideration and for their insightful suggestions that have been beneficial for the development of my thesis project. I am grateful to **Dr. Sigurd Braun** for being a source of encouragement and for his valuable suggestions.

I thank **Prof. Andreas Ladurner** and all the past and present members of his department for a co-operative and conducive work atmosphere. I am grateful to **Christine Werner**, **Anton Eberharter** and **Corey Laverty** for their tremendous efforts in ensuring all of the administrative work is taken care of. I would like to thank **Zdenka Stanic**, **Marianne Köber**, **Petra Heckmayer**, **Heiko Germeroth**, **Karin Waegemann** and **Kathrin Aschenbrenner** for their efficient technical support and services.

I would also like to thank **Bernadette**, **Teresa**, **Ramon**, **Hari**, **Andy**, **Gytis**, **Maria H**, **Aurelio**, **Christian**, **Moritz**, **Giuliana** and **Shao-Yen** for their generous help and for a delightful time in the department. I am grateful to **Charlotte** for helping me out with German translation.

I had a great pleasure to work with some extremely talented undergrad students- **Mauricio, Justin, Grace** and **Christina G** and I am thankful to them for the experience I had working with each of them.

I want to thank **Shahaf, Nissa** and **Jyaysi** for being warm and welcoming when I was figuring things out in a new lab and in a new country. I also want to thank **Nilay, Sneha K, Ashish, Ganesh** and **Siavash** for their support and help during the whole time.

I take this opportunity to thank **Hui-Lan** for being 'my partner in crime' and for being there with me in my moments of random craziness and in my moments of despair. I am ever grateful to **Julia P** for always being a source of positivity and optimism, whenever I felt dejected. I thank **Thomas vE** for being high in spirit and spreading his infectious smile in both good and bad times. I could not thank enough - **Priyanka, Jayeeta, Aditi, Sneha S, Isha, Poorti** and **Anupama**- for sticking with me all these years.

I thank **Gopal** for being my pillar of strength and source of inspiration. It would have been impossible for me to have gone through this entire journey without his support and confidence in me.

Finally, I would like to thank **my parents and my brother**, who have always loved me and supported me unconditionally, having little or at times even no idea of what I do.

***“One’s mind, once stretched by a new idea, never regains its original dimensions.”***

– Oliver Wendell Holmes Sr.

*To all my Teachers*



# Contents

1. Introduction .....	1
1.1 Protein trafficking in eukaryotic cells .....	1
1.2 Protein translocation into mitochondria .....	1
1.3 Mitochondrial translocases .....	3
1.3.1 TOM complex .....	3
1.3.2 SAM (TOB) complex .....	4
1.3.3 Mim1 complex .....	5
1.3.4 MIA pathway .....	6
1.3.5 Small TIMs .....	7
1.3.6 TIM22 complex .....	7
1.3.7 OXA complex .....	8
1.3.8 TIM23 complex .....	9
1.4 Mitochondrial Hsp70 and its co-chaperones in TIM23 complex.....	15
1.5 mtHsp70 and its cochaperones in mitochondrial matrix.....	18
1.6 Aim of the present study .....	19
2. Materials and Methods .....	21
2.1 Molecular biology methods .....	21
2.1.1 DNA Isolation.....	21
2.1.1.1 Isolation of genomic DNA from yeast <i>S. cerevisiae</i> .....	21
2.1.1.2 Isolation of plasmid DNA from <i>E. coli</i> .....	21
2.1.2 Amplification of DNA fragments.....	22
2.1.3 Detection and analysis of DNA .....	22
2.1.3.1 Agarose gel electrophoresis .....	22
2.1.3.2 DNA extraction from agarose gels .....	23
2.1.3.3 Quantification of DNA .....	23
2.1.4 Manipulation of DNA with enzymes .....	23
2.1.4.1 Restriction Digestion .....	23
2.1.4.2 Ligation .....	23
2.1.5 Transformation of <i>E. coli</i> with plasmid DNA .....	24
2.1.5.1 <i>E. coli</i> strains used.....	24

2.1.5.2 Preparation of electrocompetent <i>E. coli</i> cells.....	24
2.1.5.3 Transformation .....	24
2.1.6 Plasmids and cloning strategies.....	25
2.1.6.1 Overview of constructs used.....	25
2.1.6.2.1 Tim44 constructs in yeast expression vectors.....	27
a) Tim44 under endogenous promoter .....	27
b) Tim44 under overexpression promoter .....	27
c) Tim44 (1-262) under endogenous promoter .....	27
d) Tim44 (1-262) under overexpression promoter .....	28
e) Tim44 (1-209) under overexpression promoter .....	28
f) Tim44 (pre-210-431) under overexpression promoter.....	28
g) Tim44 (pre-264-431) under endogenous promoter.....	28
h) Tim44 (pre-264-431) under overexpression promoter .....	29
i) His <sub>9</sub> -tagged Tim44 under endogenous promoter .....	29
j) His <sub>9</sub> -tagged Tim44 under overexpression promoter.....	29
k) Tim44 P282Q under endogenous promoter.....	30
l) Tim44 R294A and Tim44 E300A under endogenous promoter .....	30
m) Tim44 D345A, Tim44 Q372A and Tim44 I393A under endogenous promoter.....	31
n) Tim44 Bpa mutants under overexpression promoter .....	31
o) Tim44 F422Bpa mutant under overexpression promoter.....	32
2.1.6.2.2 Tim44 constructs in bacterial expression vectors .....	32
a) His <sub>6</sub> -TEV-Tim44 truncation constructs.....	32
b) His <sub>6</sub> -TEV-Tim44 P282Q .....	33
c) His <sub>6</sub> -TEV-Tim44 D345A, Q372A and His <sub>6</sub> -TEV-Tim44 D345A, Q372A, I393A .....	33
2.1.6.2.3 Ssc1 constructs in yeast expression vectors .....	34
a) Ssc1-His <sub>6</sub> under endogenous promoter.....	34
b) Ssc1-His <sub>6</sub> D341C, Q448C under endogenous promoter .....	34
2.1.6.2.3 Ssc1 construct in bacterial expression vector .....	34
2.2 Yeast genetics methods .....	35
2.2.1 <i>S.cerevisiae</i> strains used.....	35
2.2.2 Transformation of yeast cell with plasmid DNA .....	37
2.2.3 5-FOA selection by plasmid shuffling.....	38
2.3 Cell biology methods.....	38
2.3.1 Bacterial culture.....	38

2.3.1.1 Media for <i>E.coli</i> growth .....	38
2.3.1.2 Cultivation of <i>E.coli</i> .....	38
2.3.2 Yeast culture .....	38
2.3.2.1 Media for <i>S. cerevisiae</i> growth .....	38
2.3.2.2 Cultivation of liquid <i>S. cerevisiae</i> cultures .....	40
2.3.3 Assays with yeast cells .....	40
2.3.3.1 Drop dilution test .....	40
2.3.3.2 Bpa-photocrosslinking .....	40
2.3.3.3 Preparation of whole cell lysate .....	41
2.3.3.4 Ni-NTA pulldown of His-tagged proteins from yeast cell .....	41
2.3.3.5 Isolation of crude mitochondria .....	42
2.3.3.6 Large-scale mitochondria isolation from <i>S. cerevisiae</i> .....	43
2.4 Protein biochemistry methods .....	44
2.4.1 Isolation of recombinant proteins .....	44
2.4.1.1 Expression of recombinant proteins in <i>E.coli</i> .....	44
2.4.1.2 Purification of His <sub>6</sub> -tagged recombinant proteins .....	44
2.4.1.3 Purification of mature Ssc1 and its variants .....	45
2.4.1.4 Purification of presequence-containing Ssc1 and its variants .....	46
2.4.2 Protein detection and analysis .....	46
2.4.2.1 SDS-PAGE .....	46
2.4.2.2 CBB staining .....	47
2.4.2.3 Transfer of proteins to nitrocellulose membrane .....	47
2.4.2.4 Fluorescence scanning .....	48
2.4.2.5 Estimation of protein concentration .....	48
2.4.3 Assays with purified proteins .....	48
2.4.3.1 Ni-NTA pull down .....	48
2.4.3.2 Pull-down with proteins immobilized to CNBr-Sepharose beads .....	49
a) Immobilization of proteins to CNBr-Sepharose beads .....	49
b) Pull-down of interacting proteins .....	49
2.4.3.3 Thermal Shift Assay .....	50
2.4.3.4 Labelling of proteins with fluorophores .....	50
2.4.4 Assays with isolated mitochondria .....	51
2.4.4.1 Chemical crosslinking .....	51
2.4.4.2 Crosslinking of arrested precursor .....	52

2.4.4.3 Immunoprecipitation.....	52
a) Co-immunoprecipitation of protein complexes in mitochondria .....	52
b) Immunoprecipitation in harsh condition.....	53
2.4.4.4 Import of precursor proteins into isolated mitochondria .....	53
2.4.4.5 Blue Native PAGE (BN-PAGE) .....	54
2.4.4.6 Estimation of membrane potential .....	54
2.4.4.7 Immobilization of mitochondria on cover slides.....	54
2.4.4.8 Single molecule HiLo measurements .....	55
2.5 Methods in immunology .....	55
2.5.1 Affinity purification of antibodies .....	55
2.5.2 Immunodecoration with specific antibodies .....	56
2.5.3 Biotinylation of antibodies .....	56
3. Results.....	57
3.1 Role of Tim44 in communication of the translocation channel and the import motor of the TIM23 complex.....	57
3.1.1 The N-terminal domain of Tim44 extended to include the membrane-recruitment helices of the C-terminal domain is not sufficient to support the function of Tim44 .....	57
3.1.2. Two domains of Tim44 co-expressed <i>in trans</i> can support function of Tim44 .....	58
3.1.3 N+C strain is severely sick.....	61
3.1.4 Protein import in N+C strain is impaired.....	62
3.1.5 Assembly of TIM23 complex in N+C strain is normal.....	65
3.1.6 Conformation of TIM23 complex in N+C strain is altered .....	66
3.1.7 C-terminal domain of Tim44 interacts with precursor protein .....	68
3.1.8 Interaction partners of N- and Cc- domain of Tim44 in the TIM23 complex .....	70
3.2 Characterization of yeast Tim44 P282Q mutation associated with cancer in humans .....	71
3.2.1 Tim44 P282Q mutation does not affect growth in yeast .....	71
3.2.2 TIM23 complex function in Tim44 P282Q mutants is not compromised.....	72
3.2.3 Stability of Tim44 with P282Q mutation .....	74
3.3 Residues that are involved in interaction of Tim44 C-terminal domain with TIM23 complex subunits.....	76
3.3.1 Site-specific photocrosslinking between Tim44 and Tim17 .....	76
3.3.2 Functional analysis of conserved residues on the surface of C-terminal domain of Tim44 .....	77
a) Functional analysis of tim44 <sup>D345A</sup> .....	80
b) Functional analysis of tim44 <sup>Q372A</sup> .....	82

c) Functional analysis of Tim44 double and triple alanine mutants .....	83
3.3.3 Site-specific photocrosslinking of C-terminal domain of Tim44.....	84
3.4 Conformation of Ssc1 in mitochondria .....	87
3.4.1 Generation of Ssc1 construct for <i>in organello</i> FRET measurements and its functionality <i>in vivo</i> .....	87
3.4.2 Import of donor-acceptor dye pair labelled Ssc1 into isolated mitochondria .....	90
3.4.3 Characterization of mitochondria after import of pre-Ssc1-his <sub>6</sub> (ATTO 532, ATTO 647) .....	92
3.4.4 Immobilization of mitochondria .....	95
3.4.5 <i>In organello</i> conformation of Ssc1 at single molecule resolution .....	96
4. Discussion .....	98
4.1 Tim44 as the organizer of the TIM23 complex.....	98
4.2 Conformation of Ssc1 in intact mitochondria .....	103
5. Summary.....	106
6. Zusammenfassung.....	108
7. References .....	111
Abbreviations.....	123
Publications from this thesis.....	128



# 1. Introduction

## 1.1 Protein trafficking in eukaryotic cells

Eukaryotic cells contain various organelles that perform specific functions and are separated from the cytosol by intracellular membranes. With few exceptions, proteins found in all of the organelles, including proteins secreted into extracellular space, are encoded by nuclear genome and are synthesized in the cytosol with specific targeting signals. Transport of such proteins into their respective organelle in a specific and regulated manner is enabled through the action of several protein translocases (or translocons). Protein translocases are multi-subunit protein complexes present in organellar membranes where they specifically recognize and transport proteins from the cytosol across or into the membrane to their respective place of function (Blobel, 1980; Jarvis and Lopez-Juez, 2013; Smith and Aitchison, 2013; Wickner and Schekman, 2005; Wiedemann and Pfanner, 2017). How this process is achieved in a specific and regulated manner is currently under extensive research.

## 1.2 Protein translocation into mitochondria

Mitochondria have an essential role in a number of processes including energy metabolism, signalling and apoptosis (Herzig and Shaw, 2018; Nunnari and Suomalainen, 2012; Shpilka and Haynes, 2018). Defects in the mitochondrial function have been implicated in diabetes, cancer, neurodegeneration and in severe diseases like Friedrich ataxia, Leigh syndrome, and hereditary spastic paraplegia (Suomalainen and Battersby, 2018; Vafai and Mootha, 2012; Wallace, 2005). Mitochondria possess their own genome and a fully functional transcription and translation systems for its expression. However, about 99% of mitochondrial proteins are encoded by the nuclear genome and are synthesized in the cytosol. Therefore, the biogenesis of mitochondria relies on the efficient transport of proteins from the cytosol. Understanding the molecular mechanisms of mitochondrial biogenesis is therefore not only important from the basic science point of view but also has noteworthy clinical significance.

Mitochondria are comprised of two membranes- the outer (OM) and the inner mitochondrial membrane (IM). The aqueous compartment between these two membranes

is known as the intermembrane space (IMS) and the one enclosed by the inner membrane is called matrix. Proteins that are targeted to different mitochondrial compartments possess characteristic mitochondrial targeting signals. Hitherto, a number of different mitochondrial targeting signals have been identified and some likely still remain to be identified. Intricate molecular machines, mitochondrial protein translocases, that mediate recognition, transport and intra-mitochondrial sorting of proteins, are present for all mitochondrial subcompartments. Transport across the outer membrane is facilitated by a complex of various protein subunits referred to as the translocase of outer membrane (TOM) complex. At the IMS side, the TOM complex cooperates with other mitochondrial protein translocases to sort proteins to their respective compartment in the organelle

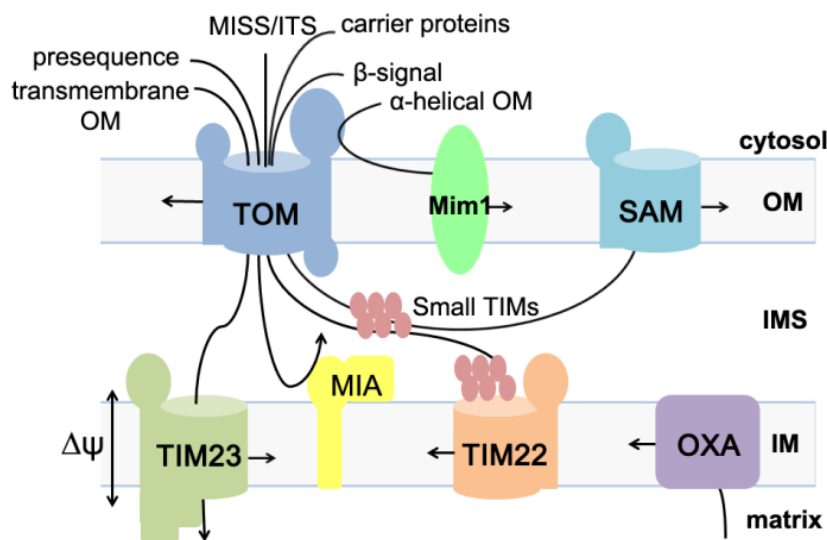


**Figure 1.1. Translocases for import of proteins into mitochondria.** Precursor proteins carrying different targeting signals are recognized by TOM complex in outer membrane (OM) and transferred to translocases residing in different mitochondrial compartments.  $\beta$ -barrel proteins in OM are transferred to SAM complex via small TIM chaperones in intermembrane space (IMS). IMS proteins with disulphide bonds having MISS/ITS signal are folded and oxidised by Mia/Erv complex. Presequence-containing proteins are transferred to TIM23 complex that sorts proteins either to mitochondrial matrix or laterally sorts them to inner membrane (IM), if a stop-transfer signal is present. TIM22 complex and OXA complex sort proteins into mitochondrial IM. Mim1 complex sorts  $\alpha$ -helical transmembrane proteins into OM.

(Chacinska et al., 2009; Endo et al., 2011; Mokranjac and Neupert, 2009; Neupert and Herrmann, 2007; Wiedemann and Pfanner, 2017).

The process of mitochondrial protein translocation is highly conserved from yeast to humans - the basic principles established using fungal model systems were subsequently confirmed in mammalian models. Mistargeting of mitochondrial precursor proteins and their accumulation in cytosol lead to activation of cell-wide stress responses (Wang and Chen, 2015; Wrobel et al., 2015).

Various mitochondrial translocases that are involved in protein translocation into mitochondrial subcompartments are discussed below in more detail (Figure 1.1).

## **1.3 Mitochondrial translocases**

### **1.3.1 TOM complex**

The TOM complex is the major translocase of the outer mitochondrial membrane and acts as the major entry gate for proteins entering mitochondria. The TOM complex mediates initial stages of translocation across the outer membrane. Depending on the targeting signals present in proteins, the TOM complex then co-ordinates with downstream translocases to sort individual proteins to their corresponding mitochondrial subcompartment. The TOM complex is comprised of the following subunits: Tom70, Tom22, Tom20, Tom40, Tom5, Tom6 and Tom7 (Endo and Yamano, 2010; Rapaport, 2005).

Tom70, Tom22 and Tom20 act as the receptors of the complex and are involved in recognition of targeting signals in proteins. Tom70 is anchored to the outer membrane through an N-terminal transmembrane domain and its C-terminal, receptor domain faces the cytosol. It mainly recognizes presequence-less target proteins through its tetratricopeptide repeats (TPR) motifs (Hines et al., 1990; Sollner et al., 1990; Wu and Sha, 2006). In addition, the C-terminal subdomain of the receptor domain of Tom70 has a binding site for Hsp70 and Hsp90 which deliver precursor proteins to the mitochondrial surface (Young et al., 2003). Tom22 is a receptor for recognition of presequence-containing precursors. It is attached to the outer membrane via its single hydrophobic transmembrane segment and has its N- and C-termini exposed to cytosol and IMS, respectively. Both N- and C-terminal domains have binding sites for presequences (Lithgow et al., 1994; Mayer et al., 1995; Nakai and Endo, 1995). Tom20 is the major receptor for presequences. The N-terminal segment of Tom20 is a transmembrane domain that anchors the protein to mitochondrial outer membrane and the C-terminal domain is a cytosol-exposed receptor domain that recognizes presequences (Moczko et al., 1993;

Sollner et al., 1989). *In vitro* studies with the recombinant receptor domains of human Tom20 and Tom22 revealed that these domains possess chaperone-like properties and play potentially a role in unfolding of entering precursors (Yano et al., 2004). Tom20 and Tom22 recognize the positively charged and the hydrophobic face, respectively, of the amphipathic helix that is characteristic for presequences (Yamano et al., 2008).

Proteins recognised by receptor subunits of TOM complex are transferred to the channel of the complex formed probably exclusively by Tom40. Tom40 has a  $\beta$ -barrel structure with an estimated pore size of 15-20 Å, through which the precursor enters the IMS from cytosol (Ahting et al., 1999; Rapaport and Neupert, 1999). An *in vivo* site-specific crosslinking approach recently revealed the architecture of the TOM complex in *Saccharomyces cerevisiae* consisting of a trimer of Tom40 interconnected by Tom22 along with small proteins, Tom5, Tom6 and Tom7. This trimeric TOM complex appears to be in an equilibrium with a dimer of Tom40 that was speculated to be an intermediate state during TOM complex assembly (Shiota et al., 2015). Electron microscopy analysis of TOM complex purified from *Neurospora crassa* (Ahting et al., 2001; Ahting et al., 1999; Bausewein et al., 2017; Kunkele et al., 1998) and *Saccharomyces cerevisiae* (Model et al., 2008; Model et al., 2002) possessed two to three pores through which precursor proteins are likely translocated.

The remaining subunits of TOM complex are three small proteins - Tom5, Tom6 and Tom7. Tom5 likely serves as an additional receptor of the complex whereas Tom6 and Tom7 appear to play a role in TOM complex assembly and stability (Dietmeier et al., 1997; Honlinger et al., 1996; Sherman et al., 2005; Shiota et al., 2015). Their exact functions are, however, still not understood.

### **1.3.2 SAM (TOB) complex**

There are two types of proteins that are found in mitochondrial outer membrane:  $\beta$ -barrel proteins and  $\alpha$ -helical transmembrane proteins. Integration and assembly of  $\beta$ -barrel proteins, such as Tom40 and porin, are carried out by sorting and assembly machinery (SAM) complex. SAM complex is also known as topogenesis of mitochondrial outer membrane  $\beta$ -barrel proteins (TOB) complex. Precursors of  $\beta$ -barrel proteins in cytosol contain hydrophobic  $\beta$ -hairpin motif that is recognized by Tom22 in the TOM complex and are subsequently translocated to the IMS where they bind to the small TIM chaperones. There, the small TIM chaperones deliver precursors of  $\beta$ -barrel proteins to

the IMS side of the SAM complex which subsequently integrates them into the outer membrane (Endo and Yamano, 2010; Jores et al., 2016; Wiedemann and Pfanner, 2017). SAM complex is comprised of three subunits: Sam35 (also known as Tom38 or Tob38), Sam50 (Tob55) and Sam37 (Mas37 or Tom37). The  $\beta$ -barrel proteins assembled by SAM complex have a characteristic short carboxy-terminal SAM complex recognition motif called  $\beta$ -signal. The recognition of  $\beta$ -barrel proteins in SAM complex is carried out by Sam35. It is not clear whether Sam35 is a peripheral protein at the cytosolic face of outer membrane or it is integrated into the membrane (Kutik et al., 2008; Milenkovic et al., 2004; Waizenegger et al., 2004). Sam50 is a  $\beta$ -barrel protein that forms a channel and belongs to BamA/Toc75 family of proteins that are conserved in gram negative bacteria, mitochondria and chloroplast (Kozjak et al., 2003; Paschen et al., 2003).  $\beta$ -strand 1 and 16 of Sam50 come together forming the lateral gate. During the gate opening, the  $\beta$ -signal present in strand 16 is replaced by the  $\beta$ -signal-containing strand of the precursor protein. Subsequently, the remaining strands of precursor protein accumulate in the lumen of Sam50 and are inserted, one  $\beta$ -hairpin after the other, in the lateral gate until the assembled  $\beta$ -barrel is released into the outer membrane (Hohr et al., 2018). In addition, Sam50 possesses N-terminal polypeptide transport-associated (POTRA) domain that is important for release of precursor protein from the SAM complex (Stroud et al., 2011). Sam37 plays a role in formation of supercomplex between SAM complex and TOM complex (Gratzer et al., 1995; Wenz et al., 2015). Formation of this supercomplex is important for efficient transfer of  $\beta$ -barrel proteins from TOM complex to SAM complex. On the other hand, Tom22 from the TOM complex side plays an important role in TOM-SAM supercomplex formation (Qiu et al., 2013).

### **1.3.3 Mim1 complex**

The assembly and insertion of several outer membrane proteins with multiple  $\alpha$ -helical transmembrane domains is carried out by the Mim1 complex. The subunits of this complex are not fully characterized; however, it is comprised of at least two outer membrane proteins, Mitochondrial Import 1 (Mim1) and Mim2. Two of transmembrane segments of Mim1 possess GxxxG motifs that are required for homo-oligomerization of Mim1 and are necessary for its function. Proteins that are targeted to Mim1 complex are recognized by receptor protein Tom70 of TOM complex and are subsequently transferred to Mim1 complex. This complex is also involved in biogenesis of Tom70 and Tom20 and

as a result, it affects the assembly of TOM complex (Becker et al., 2011; Dimmer et al., 2012; Papic et al., 2011; Popov-Celeketic et al., 2008b; Waizenegger et al., 2005).

### **1.3.4 MIA pathway**

Proteins that enter the IMS through the TOM complex follow different routes depending on their targeting signals. A number of proteins that are targeted to IMS possess characteristic signature cysteine motifs and form intramolecular disulphide bonds upon translocation into IMS. These proteins typically have an IMS-specific sorting signal called MISS/ITS signal, which contains 9 amino acids found upstream or downstream to the cysteine residues that form disulphide bonds in IMS. Once these proteins enter IMS from the reducing environment of the cytosol via TOM complex, they undergo oxidative folding by a disulphide relay system in IMS, also termed mitochondrial IMS assembly (MIA) pathway. Disulphide relay system is comprised of two proteins: Mia40 (or Tim40) and Erv1. Mia40 is a receptor and an oxidoreductase. Erv1 is a sulfhydryl oxidase that is required for regeneration of redox-activated Mia40 (Chacinska et al., 2004; Mordas and Tokatlidis, 2015; Stojanovski et al., 2012; Terziyska et al., 2007; Terziyska et al., 2005). The precursor protein in reduced state passes through the TOM complex and is recognized by receptor Mia40 in redox-active state. NMR structure of Mia40 revealed a hydrophobic binding cleft in the vicinity of its redox active CPC motif (Banci et al., 2009). The precursor protein undergoes oxidative folding characterized by formation of an intra-molecular disulphide bond with the help of Mia40 via an initial mixed disulphide between Mia40 and precursor. As a result Mia40 gets reduced and becomes redox inactive (Banci et al., 2010; Banci et al., 2009; Grumbt et al., 2007). Recovery of redox-active Mia40 is achieved with the assistance of Erv1. Erv1 reoxidizes Mia40 and as a result becomes reduced itself. Recovery of active oxidized form of Erv1 takes place by transfer of electrons to cytochrome c, which finally transfers them to molecular oxygen through complex IV (Banci et al., 2011; Bien et al., 2010). Interestingly, Mia40/Erv1 disulphide relay can function under anaerobic conditions as well, and its electron acceptor in anaerobic condition has only recently been identified as Osm1, which is a fumarate reductase that enables the transfer of electron from fumarate to succinate (Neal et al., 2017). The folded protein carrying intramolecular disulphide bonds cannot be translocated back out of the IMS into cytosol. As a result, Mia40/Erv1 disulphide relay system couples unidirectional import of proteins with their folding.

### 1.3.5 Small TIMs

A family of small translocase of inner membrane (TIM) chaperones are present in IMS that co-ordinate between the TOM complex in outer membrane and the SAM complex and the TIM22 complex in outer membrane and inner membrane, respectively. Precursor proteins belonging to  $\beta$ -barrel protein family and inner membrane carrier protein family are targeted to the SAM complex and the TIM22 complex, respectively. The precursor proteins transported from TOM complex in an unfolded state enter into the aqueous environment of IMS, where they are susceptible to misfolding or aggregation. Small TIM chaperones bind these entering proteins in order to prevent their aggregation in IMS and allow their specific targeting to either SAM or TIM22 complex. In *Saccharomyces cerevisiae*, there are five small TIM protein members: Tim8, Tim9, Tim10, Tim12 and Tim13 (Koehler, 2004; Lutz et al., 2003). Small TIMs are characterized by twin CX<sub>3</sub>C motifs that form two intramolecular disulphide bonds and are imported and assembled in IMS by MIA pathway. Tim9 and Tim10 form the major soluble heterohexameric chaperone complex in which each of the individual subunits has two helices, which are connected by a loop. This structure is stabilized by an intramolecular disulphide bond between cysteine residues in twin CX<sub>3</sub>C motifs (Baker et al., 2009; Webb et al., 2006). Similarly, Tim8 and Tim13 form a heterohexameric complex in IMS that is used by few precursor proteins (Beverly et al., 2008). Tim12, on the other hand, along with Tim9 and Tim10 is found in the inner membrane bound to the TIM22 complex (Gebert et al., 2008). The improperly folded and unassembled small TIM chaperones are degraded by i-AAA protease in IMS (Baker et al., 2012).

### 1.3.6 TIM22 complex

Insertion into inner membrane of mitochondria of hydrophobic proteins with multiple transmembrane segments, belonging to carrier and TIM families, is carried out by the TIM22 complex. This insertion requires membrane potential across the inner membrane of mitochondria (Jensen and Dunn, 2002; Rehling et al., 2004). The targeting signal recognized by the TIM22 complex is not clearly defined. TIM22 complex in yeast is comprised of following subunits: Tim9-Tim10-Tim12 chaperone complex, Tim54, Tim22, Tim18 and Sdh3. Tim9-Tim10-Tim12 forms a soluble chaperone complex in IMS that is recruited to TIM22 complex by adhering to IMS-exposed domain of Tim54. Tim22 forms the channel of the complex and structurally has multiple  $\alpha$ -helical transmembrane

segments. It allows the insertion of hydrophobic carrier or transport proteins into inner membrane. (Gebert et al., 2008; Rehling et al., 2003; Wagner et al., 2008). Study with recombinantly expressed and purified Tim22 reconstituted into liposomes showed that gating of Tim22 channel is dependent on high threshold membrane potential and targeting signal of precursor protein (Kovermann et al., 2002). Single particle electron microscopy study of purified TIM22 complex combined with electrophysiological analysis revealed that TIM22 complex is comprised of ‘twin pore’ and protein translocation through both the pores are regulated in a two-step voltage-dependent manner. In the first step, docking of the precursor to TIM22 complex takes place and in the second step gating of the Tim22 channel occurs (Rehling et al., 2003). Tim18 and Sdh3 play a role in assembly of the TIM22 complex (Gebert et al., 2011). Human homologues of yeast Tim22, Tim9, Tim10 and Tim12 have been identified as hTim22, hTim9, hTim10a and hTim10b, respectively, whereas Tim54 and Tim18 are lacking in mammalian cells. Human Sdh3 homologue, SDHC, has not been shown to interact with TIM22 complex. In addition, human TIM22 complex possesses Tim29 that plays a role in TIM22 complex stability and insertion of carrier proteins by TIM22 complex (Callegari et al., 2016; Kang et al., 2016). So far, the exact mechanism of protein insertion by TIM22 complex is not understood.

### **1.3.7 OXA complex**

The oxidase assembly (OXA) translocase is required for insertion of transmembrane proteins from mitochondrial matrix to inner membrane. There are two OXA proteins that have been identified: Oxa1 and Oxa2. Oxa1 plays a major role in protein insertion and Oxa2, on the other hand, is a paralog of Oxa1 that plays a limited role in OXA translocase function (Hell et al., 1997; Herrmann et al., 1997; Stiller et al., 2016). Oxa1 in mitochondria is related to YidC in bacteria, Alb3 in chloroplast and Get1 and TMCO1 in yeast and human ER, respectively. Substrate proteins of OXA translocase follow two different routes, based on the genome from which they originate - mitochondrial or nuclear DNA.

Proteins encoded by mitochondrial genome are synthesized in mitochondrial matrix and are co-translationally inserted into inner membrane by OXA translocase. The insertion is facilitated by recruitment of ribosomes by the C-terminal domain of Oxa1 and by Mba1. Mba1 is a peripheral membrane protein at the matrix face of mitochondrial inner

membrane that does not stably interact with Oxa1 but enables the ribosomal binding, which allows insertion of proteins into inner membrane by OXA complex (Ott et al., 2006; Pfeffer et al., 2015; Preuss et al., 2001). Recent crystal structure of YidC revealed a conserved core present in all members of the family that consists of five transmembrane segments and a hydrophilic groove, which enables insertion of proteins into bacterial membrane (Kumazaki et al., 2014a; Kumazaki et al., 2014b). Expression of YidC in yeast can rescue the function of both Oxa1 and Oxa2. YidC, however, lacks a ribosome binding domain and the rescue of Oxa1 function required fusion of YidC with the ribosome binding domain of Oxa1. Such a fusion could not rescue the function of Oxa2, suggesting that Oxa1 and Oxa2 play roles in co-translational and post-translational function, respectively (Preuss et al., 2005).

Proteins encoded by nuclear genome follow a conservative sorting pathway. It first involves presequence-dependent import of proteins into mitochondrial matrix through TOM and TIM23 complexes and is followed by subsequent integration of proteins into inner membrane from the matrix by OXA translocase (Rojo et al., 1995). A number of substrate proteins are integrated into inner membrane by OXA translocase including TIM22 complex subunits, Tim18 and Sdh3. As a result, OXA translocase also indirectly influences the import of carrier proteins into mitochondrial inner membrane (Stiller et al., 2016). In addition, insertion of some proteins with multiple transmembrane segments into the mitochondrial inner membrane takes place by co-ordinated action of TIM23 complex and OXA complex and it is postulated that the first two entering segments are laterally sorted into inner membrane by TIM23 complex, the rest by OXA complex (Bohnert et al., 2010).

### **1.3.8 TIM23 complex**

The proteins that are targeted to the mitochondrial matrix are synthesized in cytosol as preproteins and are characterized by the presence of an N-terminal positively charged matrix targeting signal (MTS) or a presequence. Presequences are typically cleaved off by different peptidases such as mitochondrial processing peptidase (MPP), MIP (Oct1), Icp55 etc. once the precursor enters mitochondrial matrix. The transport of precursor protein into the mitochondrial matrix requires a coordinated action of the TOM complex in the outer membrane and the TIM23 (translocase of the inner membrane) complex in the inner membrane (Figure 1.2) (Marom et al., 2011a; Mokranjac and Neupert, 2010). In

*Saccharomyces cerevisiae*, TIM23 complex is comprised of at least 11 subunits, namely, Tim50, Tim23, Tim17, Tim44, Ssc1 (mtHsp70), Tim16 (Pam16), Tim14 (Pam18), Mge1, Tim21, Pam17 and Mgr2, which interact with each other in a specific, highly dynamic and regulated manner. Preproteins are transferred from the TOM complex to TIM23 complex with the help of Tim50, the major receptor of TIM23 complex. Translocation

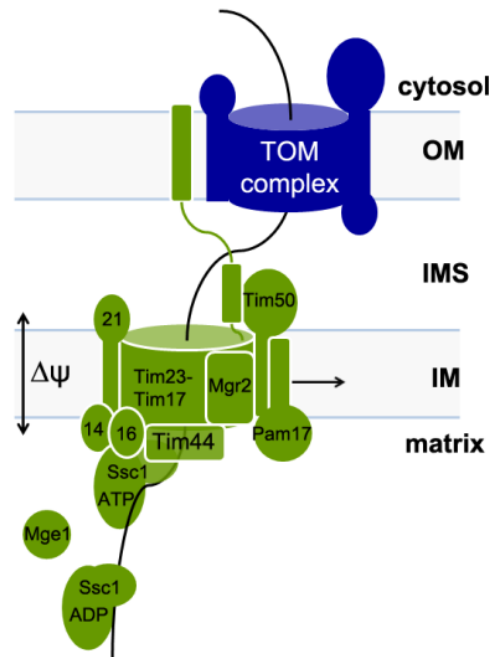


**Figure 1.2. Translocation of proteins by TIM23 complex.** Presequence-containing precursor proteins are recognized by TOM complex and transferred to the TIM23 complex. Tim50 and Tim23 recognize the precursor and transfer it to the protein conducting channel formed likely by Tim23 and Tim17 from where it is transferred to the import motor. Precursor entering the matrix binds to mitochondrial Hsp70, known as Ssc1 in yeast. Ssc1 and its co-chaperones, Tim14 and Tim16, are tethered to TIM23 complex by Tim44. Ssc1, upon binding to precursor, dissociates from TIM23 complex allowing another Ssc1 molecule to bind. Translocation of proteins to mitochondrial matrix by TIM23 complex requires membrane potential across inner membrane and energy from ATP hydrolysis. ATP hydrolysis is carried out by Ssc1 assisted by its co-chaperones, Tim14, Tim16 and Mge1. Tim21, Pam17 and Mgr2 are non-essential subunits of the complex. Mgr2 helps in lateral sorting of the proteins into inner membrane. OM- outer membrane; IMS- intermembrane space; IM- inner membrane

across the inner membrane occurs through the channel of the TIM23 complex formed by Tim23 and likely by Tim17. The initial transfer of the MTS across the inner membrane strictly depends on the membrane potential ( $\Delta\psi$ ) across the inner membrane. Complete

translocation of the preproteins into the matrix is facilitated by a number of proteins, collectively referred to as the import motor that uses energy derived from ATP hydrolysis. All of the subunits of TIM23 complex are essential for cell viability of yeast cells and all other organisms tested so far, except for Tim21, Pam17 and Mgr2, and are highly evolutionarily conserved.

TIM23 complex is also involved in transport of proteins that are laterally sorted into IM and to IMS. There are two models that describe the protein translocation including lateral insertion by TIM23 complex: single-entity model and modular model. According to single-entity model, all components of TIM23 complex are assembled together as one unit and undergo conformational changes depending on the type of entering precursor (Popov-Celeketic et al., 2008a). Modular model suggests that different modules of TIM23 complex are present that come together based on the target signal of entering precursor. According to this model, lateral sorting of entering precursor is performed by TIM23<sup>SORT</sup> complex that is comprised of Tim50, Tim23, Tim17 and Tim21, whereas targeting of proteins to matrix is carried out by TIM23 complex with assembled import motor (Chacinska et al., 2005). Laterally sorted proteins contain an additional hydrophobic stop transfer signal that enables it to laterally release and insert into the membrane, downstream to the N-terminal presequence. Lateral insertion may or may not require ATP depending on the precursor protein, however, Tim14, a subunit traditionally assigned to the import motor, appears to play an important role in this process (Chacinska et al., 2010; Popov-Celeketic et al., 2008a; Popov-Celeketic et al., 2011). Proteins that are targeted to IMS possess additional inner membrane peptidase (IMP) cleavage site downstream of the stop transfer signal. The laterally sorted protein that is inserted into mitochondrial inner membrane is subsequently cleaved by IMP, releasing the soluble protein into the aqueous IMS (Glick et al., 1992; Nunnari et al., 1993).

The central receptor of TIM23 complex is Tim50. Presequence-containing arrested precursor protein that spans through TOM complex has been found to crosslink with Tim50 (Mokranjac et al., 2003a; Yamamoto et al., 2002). Presequence-containing precursor proteins that pass through TOM complex are transferred to Tim50 in TIM23 complex (Mokranjac et al., 2009). Tim50 possesses N-terminal transmembrane segment and C-terminal globular domain that is exposed to IMS (Tim50<sup>IMS</sup>). Tim50<sup>IMS</sup> is further comprised of a conserved core of Tim50<sup>IMS</sup> and a fungi-specific C-terminal presequence binding domain. NMR study with purified subdomains of Tim50<sup>IMS</sup> revealed that core of Tim50<sup>IMS</sup> and C-terminal presequence domain interact with each other and it is

speculated that the C-terminal domain receives precursor protein from TOM complex and transfers it to the core of Tim50<sup>IMS</sup> (Rahman et al., 2014). Crystal structure of trypsin resistant core of Tim50<sup>IMS</sup> derived from *Saccharomyces cerevisiae* revealed presence of an acidic patch, which is the potential binding site for positively charged presequence (Li and Sha, 2015; Qian et al., 2011). Tim50<sup>IMS</sup> has been shown to interact with Tim23 and is speculated to form a ternary complex with Tim23 and presequence (Gevorkyan-Airapetov et al., 2009; Marom et al., 2011b). In addition, the stability of the interaction between soluble receptor domain Tim50<sup>IMS</sup> and Tim23 is dependent on presence of cardiolipin in mitochondrial inner membrane (Malhotra et al., 2017).

Tim23 is involved in formation of the protein conducting channel of TIM23 complex and also plays a role in recognition of the precursor proteins entering TIM23 complex. The dual role of Tim23 is facilitated by its two domains: the N- and the C-terminal domains. The N-terminal domain of Tim23 corresponds to the first 100 amino acid residues and is exposed to the IMS. It possesses an intrinsically disordered structure that extends to the cytosolic face of outer membrane and connects the TOM and TIM23 complexes. This insertion exposes roughly 20 amino acids of Tim23 N-terminal domain to the cytosol that can be cleaved by proteolytic enzyme (Bajaj et al., 2014; de la Cruz et al., 2010; Donzeau et al., 2000; Popov-Celeketic et al., 2008a; Waegemann et al., 2015). In addition, the N-terminal domain of Tim23 has a binding site to interact with IMS domain of Tim50. Tim23 Y70A, L71A mutant show an impaired interaction with Tim50 and is defective in protein import (Gevorkyan-Airapetov et al., 2009; Tamura et al., 2009). The C-terminal part of Tim23 is comprised of four predicted transmembrane helices that span the inner membrane of mitochondria and are involved in the formation of channel through which presequence-containing proteins translocate. The transmembrane helices possess characteristic GxxxG motifs that play an important role in maintenance of the structural integrity of the channel formed by Tim23 (Demishtein-Zohary et al., 2015; Pareek et al., 2013). Tim23 recombinantly expressed and purified from *E.coli* showed selectivity towards cation and activation by membrane potential and presequence upon reconstitution into liposomes. The channel formation is carried out by C-terminal domain itself and N-terminal domain is necessary for presequence specificity and affinity (Truscott et al., 2001). Fluorescence mapping of Tim23 further revealed that it undergoes conformational changes in energized state that regulates the gating of the channel (Alder et al., 2008; Malhotra et al., 2013).

Tim17, an integral membrane protein, is a subunit of TIM23 complex that is likely involved in formation of the translocation channel. Tim17 is far more conserved at sequence level when compared with Tim23. Tim17 is structurally similar to Tim23 but lacks an extensive IMS exposed domain that is found in Tim23. The IMS domain of Tim17 harbours a negatively charged conserved motif, truncation of which impairs precursor import (Meier et al., 2005). Tim17 has been predicted to possess four transmembrane helical segments that are embedded in inner membrane of mitochondria. Unlike Tim23, deletion of TM3 and TM4 in Tim17 renders yeast cell dead suggesting that TM1 and TM2 are not sufficient for Tim17 function (Demishtein-Zohary et al., 2017). In addition, Tim17 possesses two highly conserved cysteine residues present right before TM1 and right after TM2 that form a disulphide bond, which is important for maintenance of structural integrity and dynamic gating of TIM23 complex (Ramesh et al., 2016; Wrobel et al., 2016). Both Tim17 and Tim23 are essential and cannot rescue each other's function (Emtage and Jensen, 1993; Ryan et al., 1998; Ryan et al., 1994). This suggests that the two proteins have distinct roles in TIM23 complex. However, it is not clear what Tim17 specifically does. It is postulated that Tim17 stabilizes the channel formed by Tim23 as depletion of Tim17 leads to collapse of the reconstituted Tim23-Tim17 'twin pore' to a single pore. In addition, truncation of N- and C-termini of Tim17 causes alteration in the twin pore structure and affects the voltage gating of the channel (Martinez-Caballero et al., 2007).

The Tim23-Tim17 channel core is connected with the rest of the downstream subunits of TIM23 complex by a matrix-localized peripheral membrane protein Tim44. *In vitro* binding study with purified Tim44 suggests an interaction of Tim44 with presequence and *in organello* crosslinking suggests interaction between Tim44 and arrested precursor (Marom et al., 2011b; Popov-Celeketic et al., 2011). Likewise, Tim44 also binds Tim23-Tim17 channel and recruits mtHsp70 and Tim14-Tim16 subcomplex (D'Silva et al., 2004; Kozany et al., 2004; Mokranjac et al., 2003b; Slutsky-Leiderman et al., 2007). Chemical crosslinking of Tim44 in isolated mitochondria shows ATP-dependence, where Tim44-mtHsp70 crosslinks are stronger in the presence of ATP and Tim44-Tim16 and Tim44-Tim14 crosslinks are stronger upon ATP depletion.

Tim44 is comprised of two domains: N-terminal and C-terminal domain. The N-terminal domain of Tim44 is easily susceptible to proteolytic digestion (Josyula et al., 2006) and has recently been shown to be intrinsically disordered (Ting et al., 2017). *In vivo* analysis of Tim44 N-terminal domain mutants in yeast showed interaction of Tim44 with

mtHsp70 and Tim16 (Schilke et al., 2012; Schiller et al., 2008). The C-terminal domain, on the other hand, has a more globular structure. Crystal structures of C-terminal domain of Tim44 derived from yeast and human show a surface-exposed hydrophobic pocket that was speculated to play a role in membrane binding (Handa et al., 2007; Josyula et al., 2006). However, subsequent biochemical experiments showed that the A1 and A2 helices at the beginning of the C-terminal domain of Tim44 (amino acid residues 235-262 in yeast protein) interact with cardiolipin-containing membranes (Marom et al., 2009; Weiss et al., 1999). Hence, the function of the remaining part of C-terminal domain remains uncharacterized. Interestingly, at the primary sequence level, this part of C-terminal domain is more conserved across the eukaryotes when compared to Tim44 N-terminal domain. A mutation in the C-terminal domain of human Tim44, P308Q, predisposes the carriers of this mutation to oncocyctic thyroid carcinoma (Bonora et al., 2006).

Tim44 acts as a docking platform for recruitment of the downstream import motor components, mitochondrial Hsp70 (mtHsp70), Tim14/Tim16 and Mge1, to the translocation channel of the TIM23 complex. These import motor subunits convert the energy derived from ATP hydrolysis to unidirectional import of presequence-containing proteins from cytosol to mitochondrial matrix. The subunits of the import motor are discussed in more detail in the text that will follow later in sections 1.4 and 1.5.

TIM23 complex contains three non-essential subunits- Tim21, Pam17 and Mgr2. The N-terminal transmembrane domain of Tim21 anchors it to inner membrane and its C-terminal domain is exposed to IMS. Upon deletion of Tim21 yeast cells show impaired membrane protein insertion upon increasing concentration of CCCP treatment (van der Laan et al., 2006). Recombinantly expressed and purified IMS domain of Tim21 interacts directly with purified IMS domain of Tom22 and *in organello* crosslinking experiments revealed that IMS domain of Tim21 interacts with Tim50 suggesting a role of Tim21 in TOM-TIM23 protein transfer. In addition, Tim21 was reported to recruit respiratory chain complexes (van der Laan et al., 2006). In humans, Tim21 is involved in transfer of subunits of respiratory chain complex proteins from TIM23 complex to the assembly intermediates and their assembly in the inner membrane (Mick et al., 2012).

Pam17 plays a regulatory role in the organization of TIM23 complex. Pam17 has two transmembrane helices that span the inner membrane such that both the N- and C-termini are exposed at the matrix side (van der Laan et al., 2005). Site specific photocrosslinking studies reveal that Pam17 interacts with the channel subunit, Tim17, and chemical crosslinking studies have shown that it interacts with Tim23 (Popov-Celeketic et al.,

2008a; Ting et al., 2014). Deletion of Pam17 shows severe growth defect at high temperature and destabilizes the Tim14-Tim16 interaction (van der Laan et al., 2005). Pam17 acts antagonistically to Tim21 and alters the conformation of TIM23 complex (Popov-Celeketic et al., 2008a). In addition, interaction between Pam17 and Tim50 is required for efficient import of  $\Delta\psi$ -hypersensitive precursor proteins, in which the remaining unfolded protein downstream of the presequence also requires membrane potential across the inner membrane for translocation (Schendzielorz et al., 2017). However, the exact function of Pam17 in TIM23 complex is still unclear.

Regulation of the lateral insertion of the proteins into mitochondrial inner membrane is dependent on Mgr2 (Gebert et al., 2012; Ieva et al., 2014). However, the exact mechanism of its action is not known.

## **1.4 Mitochondrial Hsp70 and its co-chaperones in TIM23 complex**

Mitochondrial Hsp70 is a member of a highly conserved family of heat shock proteins 70 or Hsp70s that function as molecular chaperones. They are involved in maintenance of proteostasis within cell by enabling folding of proteins, preventing their aggregation and remodelling of protein complexes. Also, certain members of the family, like mtHsp70, are involved in protein translocation across membranes. So far, bacterial Hsp70, DnaK, and its cochaperones, DnaJ and GrpE, are the most extensively studied amongst all of the Hsp70s. All Hsp70s are comprised of two domains: the N-terminal nucleotide binding domain (NBD, also known as the ATPase domain) and the C-terminal substrate binding domain (SBD). The NBD and SBD are connected via a flexible interdomain linker that is highly conserved. Binding of nucleotides, ATP or ADP, to NBD of Hsp70 regulates the conformation of its SBD (Figure 1.3). SBD has a hydrophobic pocket to which short hydrophobic segments of substrate proteins can bind. The hydrophobic pocket in SBD extends to a flexible lid that can alternate between 'open' and 'close' conformations (Hartl et al., 2011; Liu and Hendrickson, 2007; Mayer, 2013; Polier et al., 2008; Zhuravleva et al., 2012). When NBD of Hsp70 is in ATP-bound state, the SBD acquires an open conformation. In the ATP-bound state, Hsp70 has high on and off rates for substrate binding and as a result substrates are easily bound but also released from SBD (Kityk et al., 2012; Qi et al., 2013). Substrate binding is followed by hydrolysis of ATP to ADP in NBD, which then closes the SBD so that substrates are tightly bound (Banerjee et

al., 2016; Zhu et al., 1996). The NBD of Hsp70s possesses a basal ATPase activity that is stimulated several fold by co-chaperones belonging to Hsp40 family (or J-proteins). Some members of J-proteins family also directly assist in transfer of substrate proteins to Hsp70s. J-proteins have a characteristic HPD motif that is required for stimulation of ATP hydrolysis by Hsp70s and thereby tight binding of their substrates. Recovery of Hsp70 for the next cycle is enabled by nucleotide exchange factors (NEF). NEFs allow exchange of ADP from the NBD and binding of ATP and release of substrate. As a result

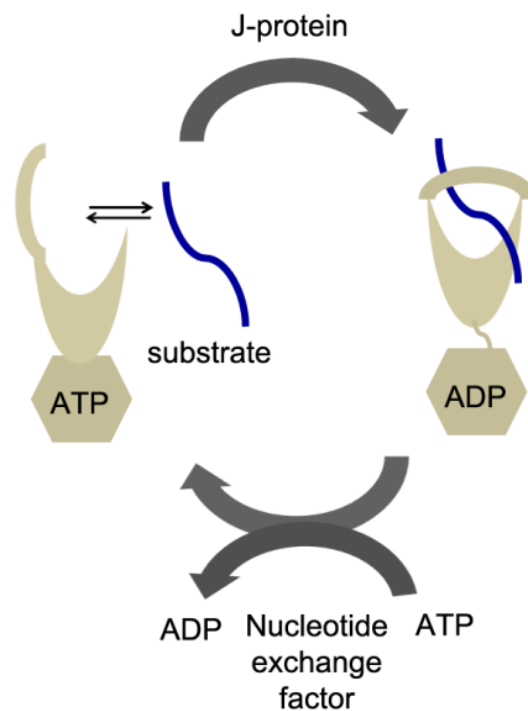


**Figure 1.3. Schematic representation of Hsp70 cycle.** Hsp70s are comprised of nucleotide binding domain (NBD) and substrate binding domain (SBD). When NBD is ATP-bound, SBD has an open conformation and has low affinity for substrate. Substrate binding induces ATP hydrolysis that is additionally stimulated by J-proteins causes the SBD to acquire a closed conformation and binds substrate tightly. Recovery of Hsp70 for next cycle is carried out by nucleotide exchange factor (NEF) that accelerates the exchange of ADP in the NBD with ATP.

the Hsp70 cycle can restart (Hartl et al., 2011; Liu and Hendrickson, 2007; Mayer, 2013; Polier et al., 2008; Zhuravleva et al., 2012).

Yeast mitochondrial Hsp70, Ssc1, performs a dual function of protein folding and protein import in mitochondria. Majority of Ssc1 is localized in mitochondrial matrix but a fraction of it is recruited to the TIM23 complex in inner membrane by Tim44. Tim14 and

Tim16 are the J-protein and J-like proteins of Ssc1 in TIM23 complex. The nucleotide exchange factor of Ssc1, Mge1, is involved in both protein folding and protein import and is described in more detail in 1.5. The temperature sensitive mutants of Ssc1 show a defect in protein import (Gambill et al., 1993). The *in vitro* conformational dynamics of Ssc1 has been analysed by ensemble and single molecule FRET (Mapa et al., 2010; Sikor et al., 2013). They showed that in the ATP-bound state, Ssc1 adopts a well-defined conformation in which two domains are tightly docked to each other and the SBD is open. On the other hand, in presence of ADP, the conformation of Ssc1 is heterogeneous, the two domains switch between docked and undocked state and the SBD partly closes. Only in the presence of substrate peptide the two domains of Ssc1 separate completely and its SBD closes.

The recruitment of Ssc1 and its co-chaperones, Tim14 and Tim16, at the TIM23 complex is carried out by Tim44. Conflicting results have been presented as to which domain of Ssc1 is involved in the interaction with Tim44. One study suggested that Ssc1 interacts with Tim44 through its SBD in an ATP-dependent manner (Moro et al., 2002). The dependence of this interaction on ATP is regulated by the  $\alpha$ -helices of the lid subdomain of SBD. On the other hand, it has also been reported that the interaction of Ssc1 with Tim44 is mediated by the NBD of Ssc1 and is regulated by the SBD (Krimmer et al., 2000). An *in vitro* study with purified proteins from yeast suggested that Tim44 interacts with both the NBD and the SBD of Ssc1 (D'Silva et al., 2004). Furthermore, the majority of studies suggested that ATP disrupts the interaction between Ssc1 and Tim44 (Krimmer et al., 2000; Moro et al., 2002), however, some studies concluded that the interaction is independent of the nature of nucleotides present (D'Silva et al., 2004; Liu et al., 2003). This could be due to hydrolysis of ATP in the conditions used, such as 1 h incubation in room temperature, prior to the experiment. Drawing any clear conclusion is further complicated by the observations that the interaction between Tim44 and Ssc1 is dependent on salt conditions as well as on the presence of substrates (Geissler et al., 2001; Schiller et al., 2008). However, it seems clear that Ssc1 and Tim44 interact in a very dynamic and tightly regulated manner.

As the precursor protein enters mitochondrial matrix, Ssc1 binds to it so that the entering precursor acts like a substrate. The hydrolysis of ATP bound at the NBD of Ssc1 is stimulated by Tim14. Tim14 is comprised of matrix-exposed C-terminal J-domain that interacts with Ssc1 and IMS exposed N-terminal domain that was shown to interact with Tim17. The C-terminal J-domain contains the characteristic HPD motif that is necessary

for stimulatory function of Tim14 on ATP hydrolysis by Ssc1 (D'Silva et al., 2003; Mokranjac et al., 2003b; Truscott et al., 2003). The C-terminal domain of Tim14 also interacts with a J-like protein, Tim16 (Kozany et al., 2004). Tim16 and Tim14 form a heterodimer through interaction of their J-like and J-domains at the mitochondrial matrix face. Tim16 shows a very high similarity with Tim14 in terms of sequence and structure. However, it is incapable of stimulating ATPase activity in Ssc1. Analysis of the crystal structure and biochemistry of the complex of truncated Tim14 (99-168 aa) and Tim16 (54-149 aa) revealed that Tim16 plays a regulatory role on Tim14 activity (D'Silva et al., 2008; Mokranjac et al., 2007; Mokranjac et al., 2006). However, study of Tim16 and Tim14 mutants suggests that Tim16 is only required for tethering of Tim14 to TIM23 complex (Pais et al., 2011). Further analysis of Tim14-Tim16 interplay is required to determine the exact role of Tim16 within the TIM23 complex.

Interestingly, yeast mitochondria contain a close homologue of Tim14, Mdj2 (Westermann and Neupert, 1997). In contrast to Tim14, deletion of Mdj2 shows no obvious growth phenotype. However, Mdj2 is a functional J-protein that can stimulate the ATPase activity of Ssc1 and forms a complex with Tim16. The abundance of Mdj2 in mitochondria is lower compared to Tim14. Upon overexpression, Mdj2 has been found to rescue the function of Tim14. This suggests that Mdj2 can compensate for Tim14 when expressed at higher levels (Mokranjac et al., 2005). However, the exact role of Mdj2 in yeast mitochondria remains unclear.

## **1.5 mtHsp70 and its cochaperones in mitochondrial matrix**

The soluble Ssc1 that localizes in mitochondrial matrix and assists in folding of newly imported proteins and misfolded proteins employs J-protein, Mdj1 for stimulation of its ATPase activity. Mdj1 possesses J-domain at its N-terminus followed by a glycine/phenylalanine (GF) rich linker, client protein binding domains and a dimerization domain at the C-terminus. Deletion of Mdj1 leads to temperature sensitive growth in yeast cells (Kubo et al., 1999; Prip-Buus et al., 1996; Rowley et al., 1994; Westermann et al., 1996).  $\Delta mdj1$  strain also shows a loss of mitochondrial DNA, which implicates Mdj1 also in mitochondrial DNA (mtDNA) maintenance. This is further confirmed by localization of Mdj1 with mitochondrial nucleoids (Ciesielski et al., 2013; Duchniewicz et al., 1999). It is speculated that Mdj1 localization at mitochondrial nucleoid enhances

the local concentration of Hsp70s, which in turn is important for mtDNA maintenance (Ciesielski et al., 2013; Duchniewicz et al., 1999).

The recovery of Ssc1 from substrate- and ADP-bound state is accomplished by matrix localized nucleotide exchange factor, Mge1. Mge1 has a high sequence homology with bacterial NEF, GrpE. Mge1 is an essential protein and the temperature sensitive mutants of Mge1 show protein import defect in mitochondria. This suggests that Mge1-mediated nucleotide exchange is essential for Ssc1 function during protein translocation via TIM23 complex (Bolliger et al., 1994; Nakai et al., 1994; Westermann et al., 1995). Mge1 releases the ADP bound to the NBD of Ssc1, which subsequently gets replaced with ATP and as a result ATP-bound Ssc1 can undergo further substrate and J-protein dependent ATP hydrolysis (Miao et al., 1997; Sakuragi et al., 1999; Westermann et al., 1995). Additionally, Mge1 can also act as a sensor of oxidative stress and can modulate the Ssc1 chaperone cycle during stress (Marada et al., 2013).

Ssc1 requires a chaperone protein, Hep1, for its own folding in mitochondrial matrix . Hep1, also referred to as Zim17 or Tim15, is known to prevent aggregation of nucleotide-free state of Ssc1 (Sichting et al., 2005). Hep1 is localized at the matrix side of the inner membrane of mitochondria. It also possesses two zinc-finger motifs that is a characteristic feature of J-proteins. However, Hep1 does not show any ATPase stimulatory function (Fraga et al., 2013; Goswami et al., 2010; Lewrenz et al., 2013). The study of temperature sensitive mutants of Hep1 showed defects in protein import and poor binding of substrate proteins to Ssc1 (Burri et al., 2004). As a result, Hep1 maintains the stability of Ssc1 structure and influences Ssc1 function (Blamowska et al., 2010; Burri et al., 2004; Sichting et al., 2005). Ssc1 shares a high sequence homology with bacterial Hsp70, DnaK. However, unlike DnaK, Ssc1 is prone to aggregation and requires co-expression of Hep1 for expression of soluble recombinant Ssc1 in *E.coli*. (Blamowska et al., 2010; Weiss et al., 2002).

## **1.6 Aim of the present study**

The aim of this study was to gain novel insight into the molecular mechanisms of function of the TIM23 complex. In particular, the focus was on elucidating the mechanisms of action of Tim44 and mtHsp70 (Ssc1). To this end, the role of uncharacterized C-terminal domain of Tim44 was to be evaluated. The work on Ssc1 was

to focus on establishing an assay that would enable the analysis of the conformation of Ssc1 in intact, physiologically active mitochondria.

## 2. Materials and Methods

### 2.1 Molecular biology methods

#### 2.1.1 DNA Isolation

##### 2.1.1.1 Isolation of genomic DNA from yeast *S. cerevisiae*

Genomic DNA was isolated from yeast cells using ‘Wizard Genomic DNA purification’ kit (Promega) according to the manufacturer’s instructions. Briefly, yeast cells were inoculated in 5 mL YPD medium (as described in 2.3.2.1) and grown overnight at 30°C, with shaking at 160 rpm. Cells were harvested by centrifuging 1 mL of culture at 3,000 x g, 5 min, RT and resuspended in 293 µL of 50 mM EDTA, pH 8.0. To the resuspended cells, 7.5 µL of 10 mg/mL of zymolase was added and incubated for 60 min at 30°C. Zymolase-treated cells were centrifuged at 16,000 x g, 2 min, RT and pellet was resuspended in 300 µL of ‘nuclei lysis solution’ followed by incubation in 100 µL of ‘protein precipitation solution’ on ice for 5 min. Centrifugation was done at 16,000 x g, 3 min, RT and supernatant was transferred to microcentrifuge tube having 300 µL of isopropanol. This was followed by centrifugation at 16,000 x g, 2 min, RT. Pellet containing DNA was washed with 70% ethanol and centrifuged at 16,000 x g, 2 min, RT. 50 µL of ‘DNA rehydration solution’ containing 100 µg/mL RNase was added to DNA pellet and incubated at 37°C for 15 min. DNA was rehydrated by incubation at 65°C, 1 h and stored at -20°C until use.

##### 2.1.1.2 Isolation of plasmid DNA from *E. coli*

Single bacterial colony was inoculated in 40 mL of LB medium (as described in 2.3.1.1) containing 100 µg/mL of ampicillin and grown overnight at 37°C, with shaking at 160 rpm. Next day, cells were harvested by centrifugation at 6,000 x g, 10 min, RT. The cells were resuspended in 3 mL of ‘Cell Resuspension Buffer’ of Pure Yield Plasmid Midiprep kit (Promega). The resuspended cells were lysed by addition of 3 mL of ‘Lysis Buffer’ followed by incubation for 2 min. The neutralization of alkali in lysis buffer was done by addition of 5 mL of ‘Neutralization Buffer’. The protein precipitate obtained in the solution was cleared up by pelleting the precipitate at 27,500 x g, 15 min, RT. The clear solution was passed through a clarification column followed by a silica membrane column using vacuum suction. The bound plasmid DNA to anion exchange column was

washed with 5 mL of ‘Endotoxin Removal Wash’ solution followed by 20 mL of ‘Column Wash’ solution. The column was then allowed to dry under vacuum suction. Plasmid DNA bound to the column was eluted with 600  $\mu$ L of sterile distilled water (dH<sub>2</sub>O). The eluted plasmid DNA was stored at -20°C until use.

## 2.1.2 Amplification of DNA fragments

Amplification of DNA sequence of interest was done by Polymerase Chain Reaction (PCR). For cloning purposes, DNA fragments were amplified either from yeast genomic DNA (gDNA) or from DNA fragments previously cloned in various cloning vectors. For analysis of individual clones after cloning reactions, the single colonies were resuspended in 10  $\mu$ L of dH<sub>2</sub>O and used as template for PCR. Phusion-HF, a commercially available high fidelity DNA polymerase from NEB, which was made by fusing *Pyrococcus*-like enzyme with a processivity enhancing domain, was used for PCR.

For each 50  $\mu$ L of PCR mix, following reagents were used in given quantities: 10  $\mu$ L of 5X Phusion-HF buffer, 1 U Phusion-HF DNA polymerase, 0.8  $\mu$ L of dNTP (10 mM each), 1.25  $\mu$ L primer (20  $\mu$ M each) and 20 ng plasmid DNA or 50 ng of gDNA. Occasionally, 5% DMSO was added in case of high GC content in DNA.

The following PCR program was used for amplifying DNA fragments, if not mentioned otherwise:

Nuclease inactivation + Denaturation of DNA	95°C, 3 min
DNA amplification cycle:	16-25 cycles
1. DNA denaturation	95°C, 30 s
2. Annealing of primers	55°C, 30 s
3. Extension of primers	72°C, 1 min/kbp
Final extension and completion of reaction	72°C, 10 min

## 2.1.3 Detection and analysis of DNA

### 2.1.3.1 Agarose gel electrophoresis

PCR products and other DNA fragments were analysed by agarose gel electrophoresis. 0.8% (w/v) of agarose was boiled in TAE buffer (40 mM Tris-acetate, pH 7.5, 20 mM Na-acetate, 1 mM EDTA) in a microwave oven. Upon cooling of agarose to 65°C, the agarose solution was poured into a cast, 0.5  $\mu$ g/mL of ethidium bromide was added and

mixed thoroughly. A comb was inserted and the cast was kept under fume hood until agarose solidified. DNA samples were pre-mixed with commercially available Gel Loading Dye, Purple (6X) from NEB in 1:5 ratio and were loaded in the wells of solidified agarose gels. Gels were run at constant voltage, 120-180 V, depending on their size. Visualization of separated DNA fragments was done under UV light (366 nm).

### **2.1.3.2 DNA extraction from agarose gels**

'mi-Gel Extraction Kit' (Metabion) was used to extract DNA from agarose gels. DNA band of interest was cut out from agarose gel using a scalpel under UV light. The cut out agarose gel was put in 2 mL microcentrifuge tube. 500  $\mu$ L of 'GEX buffer' was added to the tube and the tube was incubated with shaking at 55°C until the agarose dissolved in the buffer. The solubilized agarose solution was passed through 'GP column' to bind DNA. GP column with bound DNA was washed with 'WN buffer' followed by 'WS buffer'. The elution of DNA was done by passing 30-50  $\mu$ L of dH<sub>2</sub>O through the column. Recovery of eluted DNA was analysed by running 1-2  $\mu$ L of sample in an agarose gel. After elution, DNA sample was used immediately for further experiments.

### **2.1.3.3 Quantification of DNA**

Estimation of DNA concentration was done by measuring the absorbance of 1.5  $\mu$ L of DNA sample at 260 nm using NanoDrop.

## **2.1.4 Manipulation of DNA with enzymes**

### **2.1.4.1 Restriction Digestion**

DNA samples were digested for analytical and preparative purposes with suitable restriction endonucleases available from NEB. Up to 0.1  $\mu$ g and 3  $\mu$ g of DNA were digested for analytical and preparative purposes, respectively. 10-20 units of enzyme were used per  $\mu$ g of DNA. DNA sample with enzyme was incubated at 37°C or at a different temperature as recommended by manufacturer for 1.5 h in provided buffers. The digested products were analysed by agarose gel electrophoresis.

### **2.1.4.2 Ligation**

The insert and vector, which were used to generate plasmid clone of interest, were cut by two different restriction enzymes each to produce sticky ends on both their sides. About

5-10 fold molar excess of restriction digested insert and about 100 ng of linearized vector was ligated by 10 U of T4 DNA ligase (NEB) in T4 ligase buffer (50 mM Tris-Cl, 10 mM MgCl<sub>2</sub>, 1 mM ATP, 10 mM DTT, pH 7.5) at 25°C for 2 h. 0.5-1 µL of ligation mixture was used to transform 45 µL of electrocompetent *E. coli* cells.

## 2.1.5 Transformation of *E. coli* with plasmid DNA

### 2.1.5.1 *E. coli* strains used

MH1	The strain used for cloning	(Casadaban and Cohen, 1980)
BL21(DE3)	The strain used for recombinant protein expression	Commercially available from Novagen
BL21(DE3) $\Delta$ dnaK::52	The strain used for recombinant expression of mature and presequence form of Ssc1	A gift from Dr Matthias Mayer

### 2.1.5.2 Preparation of electrocompetent *E. coli* cells

Electrocompetent cells of bacterial strains were prepared by previously described method (Dower et al., 1988). Briefly, single bacterial colony was inoculated in 50 mL LB medium and grown overnight at 37°C, with shaking at 160 rpm. Next day, 2 mL of overnight culture was inoculated into 1 L of LB medium pre-heated at 37°C. This culture was allowed to grow until OD<sub>600</sub> reached ~0.5. The culture was kept in ice to cool down for 30 min. Cells were harvested by centrifugation at 4,400 x g, 5 min at 4°C and then successively washed with 400 mL, 200 mL and 50 mL of sterile 10% (v/v) glycerol. Finally, cells were resuspended in 1 mL of 10% glycerol and were stored in -80°C in 45 µL aliquots until use.

### 2.1.5.3 Transformation

45 µL of bacterial electrocompetent cells were transformed with 0.5-1 µL of plasmid DNA or ligation mixture by electroporation. Electrocompetent cells, freshly taken out of -80°C, were premixed with DNA and were transferred to cuvettes for electroporation.

Cells were treated with high voltage pulse through Eporator (Eppendorf) set at 2500 V. Transformed cells were resuspended in 1 mL of LB medium and incubated at 37°C, with shaking at 160 rpm, for recovery, before they were harvested by centrifugation at 10,000 x g, 5 min, RT. The cell pellet was resuspended in 100 µL of LB medium and plated on LB-Amp plates (LB medium with 2% Agar and 100 µg/mL of ampicillin). The LB-Amp plates were incubated overnight at 37°C.

## 2.1.6 Plasmids and cloning strategies

### 2.1.6.1 Overview of constructs used

<i>Construct</i>	<i>Vector</i>	<i>Reference</i>
prom-Tim44-f	pRS314	(Mapa, 2009)
prom-Tim44-f	pRS315	This thesis
prom-Tim44-f (1-262)	pRS315	This thesis
prom-Tim44-f (pre-210-431)	pRS314	(Mapa, 2009)
Tim44 (1-262)	p415 GPD	This thesis
Tim44 (pre-210-431)	p414 GPD	This thesis
Tim44 (1-209)	p415 GPD	This thesis
prom-Tim44-f (pre-264-431)	pRS314	This thesis
Tim44 (pre-264-431)	p414 GPD	This thesis
prom-pre-His <sub>9</sub> -Tim44-f (43-431)	pRS314	This thesis
prom-pre-His <sub>9</sub> -Tim44-f (43-209)	pRS315	This thesis
His <sub>6</sub> -TEV-Tim44 (43-431)	pET-Duet1	(Mapa, 2009)
His <sub>6</sub> -TEV-Tim44 (43-263)	pET-Duet1	This thesis
His <sub>6</sub> -TEV-Tim44 (211-431)	pET-Duet1	(Mapa, 2009)
His <sub>6</sub> -TEV-Tim44 (43-209)	pET-Duet1	This thesis
His <sub>6</sub> -TEV-Tim44 (264-431)	pET-Duet1	This thesis
prom-Tim44-f P282Q	pRS314	This thesis
His <sub>6</sub> -TEV-Tim44 (43-431) P282Q	pET-Duet1	This thesis
pBpa2-PGK1 + 3SUP4-tRNA <sub>CUA</sub>	-	(Chen et al., 2007)
Tim17-His <sub>9</sub> V104Bpa	p415 GPD	(Demishtein-Zohary et al.,

		2017)
Tim17-His <sub>9</sub> G106Bpa	p415 GPD	(Demishtein-Zohary et al., 2017)
Tim17-His <sub>9</sub> W108Bpa	p415 GPD	(Demishtein-Zohary et al., 2017)
prom-Tim44-f R294A	pRS314	This thesis
prom-Tim44-f E300A	pRS314	This thesis
prom-Tim44-f D345A	pRS314	This thesis
prom-Tim44-f Q372A	pRS314	This thesis
prom-Tim44-f I393A	pRS314	This thesis
prom-Tim44-f D345A, Q372A	pRS314	This thesis
prom-Tim44-f D345A, Q372A, I393A	pRS314	This thesis
prom-Tim44-f D345A, Q372A	p414 GPD	This thesis
His <sub>6</sub> -TEV-Tim44 (43-431) D345A, Q372A	pET-Duet1	This thesis
His <sub>6</sub> -TEV-Tim44 (43-431) D345A, Q372A, I393A	pET-Duet1	This thesis
pre-His <sub>9</sub> -Tim44 (43-431)	p415 GPD	This thesis
pre-His <sub>9</sub> -Tim44 (43-431) S271Bpa	p415 GPD	This thesis
pre-His <sub>9</sub> -Tim44 (43-431) L279Bpa	p415 GPD	This thesis
pre-His <sub>9</sub> -Tim44 (43-431) E295Bpa	p415 GPD	This thesis
pre-His <sub>9</sub> -Tim44 (43-431) Y296Bpa	p415 GPD	This thesis
pre-His <sub>9</sub> -Tim44 (43-431) D309Bpa	p415 GPD	This thesis
pre-His <sub>9</sub> -Tim44 (43-431) K311Bpa	p415 GPD	This thesis
pre-His <sub>9</sub> -Tim44 (43-431) A320Bpa	p415 GPD	This thesis
pre-His <sub>9</sub> -Tim44 (43-431) I346Bpa	p415 GPD	This thesis
pre-His <sub>9</sub> -Tim44 (43-431) Q372Bpa	p415 GPD	This thesis
pre-His <sub>9</sub> -Tim44 (43-431) S397Bpa	p415 GPD	This thesis
pre-His <sub>9</sub> -Tim44 (43-431) F422Bpa	p415 GPD	This thesis
prom-Ssc1	pRS314	(Mapa et al., 2010)

prom-Ssc1-His <sub>6</sub>	pRS314	This thesis
prom-Ssc1 D341C, Q448C	pRS314	(Mapa et al., 2010)
prom-Ssc1-His <sub>6</sub> D341C, Q448C	pRS314	This thesis
Ssc1 (23-654) D341C, Q448C+ His <sub>6</sub> -Hep1	pET-Duet1	(Mapa et al., 2010)
Ssc1-His <sub>6</sub> (1-654) D341C, Q448C	pET-Duet1	This thesis

## 2.1.6.2 Cloning strategies

### 2.1.6.2.1 Tim44 constructs in yeast expression vectors

#### a) *Tim44* under endogenous promoter

Tim44 with its endogenous promoter and 3'UTR sequence was cloned into pRS315 vector using BamHI and XhoI restriction sites. The DNA fragment was amplified from yeast gDNA using the following primers:

BamTim44p	fp	5'-CCCGGATCCGAACACCACGACTAATAAAAC-3'
Tim44fXho	rp	5'-CCCCTCGAGGGTACGAAGCCTTTGCACCTG-3'

Here 'fp' refers to forward primer and 'rp' refers to reverse primer.

#### b) *Tim44* under overexpression promoter

Tim44 was overexpressed under GPD promoter and was cloned into p414 GPD and p415 GPD vector using BamHI and XhoI restriction sites. PCR was done by using prom-Tim44-f in pRS314 as template and following primers were used:

BamTim44	fp	5'-CCCGGATCCATGCACAGATCCACTTTTATC-3'
Tim44Xho	rp	5'-GGGCTCGAGTCAGGTGAATTGTCTAGAACC-3'

#### c) *Tim44* (1-262) under endogenous promoter

For cloning Tim44 (1-262) DNA fragment encompassing endogenous Tim44 promoter and 3'-UTR, Tim44 (1-262) was first cloned into pRS315 using BamHI and SalI restriction sites, followed by cloning of 3'-UTR with SalI and XhoI restriction sites. prom-Tim44-f in pRS314 was used as template and primers used for amplification of the respective DNA fragments are listed below.

BamTim44p	fp	5'-CCCGGATCCGAACACCACGACTAATAAAAC-3'
Tim44_263stopSal	rp	5'-CCCGTCGACTCAGCCCACTTTGTTGGTTATTTTC-3'

SalTim44f	fp	5'-CCCGTCTGACTTGGTTTCGATGTACTCTTTTG-3'
Tim44fXho	rp	5'-CCCCTCGAGGGTACGAAGCCTTTGCACCTG-3'

**d) *Tim44 (1-262) under overexpression promoter***

Tim44 (1-262) was cloned into p415 GPD using construct generated above as template and following primers:

BamTim44	fp	5'-CCCGGATCCATGCACAGATCCACTTTTATC-3'
Tim44_263stopSal	rp	5'-CCCGTCTGACTCAGCCCACTTTGTTGGTTATTTTC-3'

**e) *Tim44 (1-209) under overexpression promoter***

For cloning Tim44 (1-209) expressed under overexpression p415 GPD promoter, amplification of Tim44 construct was done using prom-Tim44-f in pRS314 as template and following primers:

BamTim44	fp	5'-CCCGGATCCATGCACAGATCCACTTTTATC-3'
Tim44_209stopSal	rp	5'-CCCGTCTGACTCATGTCTGCAACCACTGCTGTTCC-3'

Cloning was done using BamHI and SalI restriction sites.

**f) *Tim44 (pre-210-431) under overexpression promoter***

Overexpression of Tim44 (pre-210-431) was carried out under GPD promoter by cloning it into p414 GPD vector. prom-Tim44-f (pre-210-431) cloned into pRS314 was used as template (Mapa, 2009) and following primers were used to amplify the DNA for cloning.

BamTim44	fp	5'-CCCGGATCCATGCACAGATCCACTTTTATC-3'
Tim44Xho	rp	5'-GGGCTCGAGTCAGGTGAATTGTCTAGAACC-3'

**g) *Tim44 (pre-264-431) under endogenous promoter***

Tim44 promoter and presequence were amplified and cloned into pRS314 using yeast gDNA as template and following primers:

BamTim44p	fp	5'-CCCGGATCCGAACACCACGACTAATAAAAAC-3'
Tim44preEco	rp	5'-TAAGAATTCCGCACGGGTCGTAGAGGTGG-3'



BamTim44	fp	5'-CCCGGATCCATGCACAGATCCACTTTTATC-3'
Tim44Xho	rp	5'-GGGCTCGAGTCAGGTGAATTGTCTAGAACC-3'

**k) *Tim44 P282Q under endogenous promoter***

P282Q mutation was introduced in Tim44 expressed under endogenous promoter and having 3'-UTR (prom-Tim44-f) in pRS314 by generation of megaprimer. Megaprimer was generated by PCR using prom-Tim44-f in pRS314 as template and the following primers.

BamTim44p	fp	5'-CCCGGATCCGAACACCACGACTAATAAAAC-3'
Tim44_P282Q	rp	5'-CGAAAAGGTCTGGTCCATTAGC-3'

Tim44 P282Q amplicon was generated using megaprimer synthesized above and reverse primer mentioned below, followed by cloning into pRS314 vector using BamHI and XhoI restriction sites.

Megaprimer	fp	Amplicon containing P282Q mutation
Tim44fXho	rp	5'-CCCCTCGAGGGTACGAAGCCTTTGCACCTG-3'

**l) *Tim44 R294A and Tim44 E300A under endogenous promoter***

Specific residues of Tim44 were mutated to alanine in full length Tim44 expressed under the control of its endogenous promoter and 3'-UTR from the plasmid prom-Tim44-f-pRS314. For mutations R294A and E300A, mega reverse primers were generated first using following primers:

Tim44fXho	rp	5'-CCCCTCGAGGGTACGAAGCCTTTGCACCTG-3'
Tim44_R294A	fp	5'-GACTTAGCAGAATACATTGTTC-3'
Tim44_E300A	fp	5'-CATTGTTCCCGCCATTCTCGAAGCG-3'

This was followed by amplification of entire Tim44 construct starting from its promoter using megaprimer as a reverse primer.

BamTim44p	fp	5'-CCCGGATCCGAACACCACGACTAATAAAAC-3'
Megaprimer	rp	Amplicon containing corresponding mutation

Amplified insert was cloned into pRS314 using BamHI and XhoI restriction sites.

**m) Tim44 D345A, Tim44 Q372A and Tim44 I393A under endogenous promoter**

Tim44 D345A, Tim44 Q372A and Tim44 I393A were generated by using 5'-phosphorylated primers that had non-overlapping forward and reverse primers and the mutations were introduced in forward primer sequence.

Tim44_D345A	fp	5' Pho-GGCCGTATCCTAGCCATCAGGGGCGTTG-3'
Tim44_D345A	rp	5' Pho-ATCGGCGTATACATCCTGTTCTTTGAAG-3'
Tim44_Q372A	fp	5' Pho-GGGTGTAGAGCAGCAGAAATCAAC-3'
Tim44_Q372A	rp	5' Pho-GACCACCAGTACTGGGATGTCTTGG-3'
Tim44_I393A	fp	5' Pho-GACGAAGCTAATGCCTTGATGAGCTC-3'
Tim44_D393A	rp	5' Pho-ACCAGCTGCAATCTCGCCAGTTTTC-3'

prom-Tim44-f-pRS314 was used as template.

Entire vector containing Tim44 construct was amplified by PCR that was followed by ligation and transformation into bacteria. Double and triple alanine mutants were generated by using single and double mutant plasmid as template for next round of mutation, respectively.

**n) Tim44 Bpa mutants under overexpression promoter**

To introduce an unnatural amino acid p-benzoyl-L-phenylalanine (Bpa) at different positions of Tim44 *in vivo*, plasmid pre-His<sub>9</sub>-Tim44-p415GPD was mutated in the way that the individual codons were exchanged with amber STOP codon during PCR. To this end, megaprimers were synthesized using a forward primer containing TAG mutation at positions where Bpa was to be subsequently incorporated and a reverse primer of Tim44 containing XhoI restriction site are given below. This method was used for generation of all Bpa mutants except for Tim44 F422Bpa.

Tim44Xho	rp	5'-GGGCTCGAGTCAGGTGAATTGTCTAGAACC-3'
tim44_271BPA	fp	5'-GAAACAGAATCCTAGCGTGTTTACAG-3'
tim44_279BPA	fp	5'-CAATTTAAGTAGATGGACCCAACC-3'
tim44_295BPA	fp	5'-GACACTTAAGATAGTACATTGTTC-3'
tim44_296BPA	fp	5'-CACTTAAGAGAATAGATCGTTCC-3'
tim44_309BPA	fp	5'-GTGAAAGGCTAGGTCAAAGTTC-3'
tim44_311BPA	fp	5'-GAAAGGCGATGTCTAGGTTCTC-3'
tim44_320BPA	fp	5'-GTTTCAGCGAGTAGCCATTCAATG-3'

tim44_346BPA	fp	5'-GTATCCTAGATTAGAGGGGGCGTTG-3'
tim44_372BPA	fp	5'-GTGTAGAGCATAGGAAATCAACC-3'
tim44_397BPA	fp	5'-CTTGATGAGCTAGTATGCCATGGTTTTTC-3'

Subsequently, the DNA fragment encompassing the entire Tim44 construct was amplified from pre-His<sub>9</sub>-Tim44-p415GPD with the megaprimers as reverse primers and a forward primer starting from the presequence of Tim44 with BamHI site.

BamTim44	fp	5'-CCCGGATCCATGCACAGATCCACTTTTATC-3'
Megaprimer	rp	Amplicon containing corresponding Bpa mutation

PCR product generated was cloned into p415 using BamHI and XhoI restriction sites.

#### *o) Tim44 F422Bpa mutant under overexpression promoter*

Amplicon containing TAG mutation at position F422 was generated using pre-His<sub>9</sub>-Tim44-p415GPD as template and primers mentioned below. BamHI and XhoI restriction sites were used to ligate the insert into p415 GPD vector

BamTim44	fp	5'-CCCGGATCCATGCACAGATCCACTTTTATC-3'
tim44_422BPA_xho	rp	5'-CTCGAGTCAGGTGAATTGTCTAGAACCCCGCGCACC TACTCCAAGATCTTCC-3'

### **2.1.6.2.2 Tim44 constructs in bacterial expression vectors**

#### *a) His<sub>6</sub>-TEV-Tim44 truncation constructs*

His<sub>6</sub>-TEV-Tim44 (43-263), His<sub>6</sub>-TEV-Tim44 (43-209) and His<sub>6</sub>-TEV-Tim44 (264-431) were cloned into pETDuet1 using BamHI and EcoRI restriction sites. TEV protease cleavage sites were introduced between His<sub>6</sub>-tag and Tim44 constructs so that the tag could be removed after protein purification using TEV protease. TEV protease cleavage site was introduced during PCR by the forward primer. His<sub>6</sub>-TEV-Tim44 (43-431)-pETDuet-1 was used as template.

Following primers were used for PCR amplification of the His<sub>6</sub>-TEV-Tim44 (43-263).

BamTEVTim44_43	fp	5'-CCCGGATCCGTCAGAGAATCTTTATCAGGGACAAGG TGGAAACCCTCGATC-3'
263stop_Tim44EcoI	rp	5'-CCCGAATTCTCAACCGCCACTTTGTTGGTTATTTTC-3'

Following primers were used for PCR amplification of the His<sub>6</sub>-TEV-Tim44 (43-209).

BamTEVTim44_43	fp	5'-CCCGGATCCGTCAGAGAATCTTTATCAGGGACAAGG TGGAAACCCTCGATC-3'
Tim44_209StopEcoI	rp	5'-CCCGAATTCTCACGCAACCACTGCTGTTCTGC-3'

Following primers were used for PCR amplification of the His<sub>6</sub>-TEV-Tim44 (264-431).

BamTEVTim44_264	fp	5'-CCCGGATCCGTCAGAGAATCTTTATCAGGGATTCTTT GCAGAAACAGAATCC-3'
Tim44Eco	rp	5'-CCCGAATTCTCAGGTGAATTGTCTAGAACC-3'

#### ***b) His<sub>6</sub>-TEV-Tim44 P282Q***

For cloning His<sub>6</sub>-TEV-Tim44 (43-431) P282Q in pETDuet-1, the abovementioned clone generated in 2.1.6.2.1k was used as template DNA and following primers were used to generate PCR product.

BamTEVTim44_43	fp	5'-CCCGGATCCGTCAGAGAATCTTTATCAGGGACAA GGTGGAAACCCTCGATC-3'
Tim44Eco	rp	5'-CCCGAATTCTCAGGTGAATTGTCTAGAACC-3'

This insert was ligated into pETDuet-1 vector using BamHI and EcoRI restriction site.

#### ***c) His<sub>6</sub>-TEV-Tim44 D345A, Q372A and His<sub>6</sub>-TEV-Tim44 D345A, Q372A, I393A***

For cloning His<sub>6</sub>-TEV-Tim44 (43-431) D345A, Q372A and His<sub>6</sub>-TEV-Tim44 (43-431) D345A, Q372A, I393A in pETDuet-1, the abovementioned double and triple mutant clone generated in 2.1.6.2.1m were used as templates and following primers were used to generate PCR product.

BamTEVTim44_43	fp	5'-CCCGGATCCGTCAGAGAATCTTTATCAGGGACAA GGTGGAAACCCTCGATC-3'
Tim44Eco	rp	5'-CCCGAATTCTCAGGTGAATTGTCTAGAACC-3'

This insert was ligated into pETDuet-1 vector using BamHI and EcoRI restriction sites.

### 2.1.6.2.3 Ssc1 constructs in yeast expression vectors

#### a) *Ssc1-His<sub>6</sub> under endogenous promoter*

A DNA fragment encoding Ssc1 fused with His-tag at its C-terminus under endogenous promoter was amplified from yeast gDNA using primers mentioned below and subsequently cloned into pRS314. His-tag was introduced with reverse primer and SacI and XhoI restriction sites were used.

SacI-Ssc1Prom	fp	5'- ATATGAGCTCACAGGCACGCGCAAAACC-3'
Hsp70His6Xho	rp	5'-GGGCTCGAGTTAATGGTGATGGTGATGGTGCTGCTT AGTTTCACCAGATTC-3'

#### b) *Ssc1-His<sub>6</sub> D341C, Q448C under endogenous promoter*

Ssc1-His<sub>6</sub> D341C, Q448C under its endogenous promoter was cloned into pRS314 with SacI and XhoI restriction sites. Amplification of DNA fragment was done using prom-Ssc1 D341C, Q448C as template (Mapa et al., 2010). Primers used to amplify the respective DNA fragment are listed below.

SacI-Ssc1Prom	fp	5'- ATATGAGCTCACAGGCACGCGCAAAACC-3'
Hsp70His6Xho	rp	5'-GGGCTCGAGTTAATGGTGATGGTGATGGTGCTGCTT AGTTTCACCAGATTC-3'

### 2.1.6.2.3 Ssc1 construct in bacterial expression vector

Presequence-containing Ssc1 was cloned into pETDuet1 vector using NdeI and XhoI restriction enzymes. PCR was done using prom-Ssc1-f in pRS314 as template and following primers:

nde_pre_Ssc1	fp	5'-GGAATTGCATATGCTTGCTGCTAAAAACATAC-3'
Hsp70His6Xho	rp	5'-GGGCTCGAGTTAATGGTGATGGTGATGGTGCTGCTT AGTTTCACCAGATTC-3'

## 2.2 Yeast genetics methods

### 2.2.1 *S.cerevisiae* strains used

#### *Yeast strains used*

<i>Strain</i>	<i>Reference</i>
YPH499	(Sikorski and Hieter, 1989)
YPH499 $\Delta$ <i>TIM44::HIS3</i> +pVT-102U-Tim44	(Mapa, 2009)
YPH499 $\Delta$ <i>TIM17::HIS3</i> +pVT-102U-Tim17	(Demishtein-Zohary et al., 2017)
YPH499 $\Delta$ <i>Ssc1::HIS3</i> +pVT-102U-Ssc1	Taken from Mokranjac lab
D273-10B	(Cabral and Schatz, 1978)
<i>mdj1-5</i>	(Westermann et al., 1996)
<i>mge1-3</i>	(Westermann et al., 1995)

#### *Yeast strains generated by transformation*

<i>Strain</i>	<i>Background strain</i>	<i>Reference</i>
prom-Tim44-f	YPH499 $\Delta$ <i>TIM44::HIS3</i>	(Mapa, 2009)
prom-Tim44-f (1-262)	YPH499 $\Delta$ <i>TIM44::HIS3</i>	This thesis
prom-Tim44-f (pre-210-431)	YPH499 $\Delta$ <i>TIM44::HIS3</i>	(Mapa, 2009)
prom-Tim44-f (1-262)+ prom-Tim44-f (pre-210-431) (N+C)	YPH499 $\Delta$ <i>TIM44::HIS3</i>	This thesis
Tim44 (1-262)	YPH499	This thesis
Tim44 (pre-210-431)	YPH499	This thesis
Tim44 (1-209)	YPH499	This thesis
Tim44 (pre-264-431)	YPH499	This thesis
prom-pre-His <sub>9</sub> -Tim44-f (43-431)	YPH499 $\Delta$ <i>TIM44::HIS3</i>	This thesis
prom-Tim44-f P282Q	YPH499 $\Delta$ <i>TIM44::HIS3</i>	This thesis
Tim17-His <sub>9</sub> V104Bpa + pBpa2-PGK1 + 3SUP4-tRNA <sub>CUA</sub>	YPH499 $\Delta$ <i>TIM17::HIS3</i>	(Demishtein-Zohary et al., 2017)

Tim17-His <sub>9</sub> G106Bpa + pBpa2-PGK1 + 3SUP4-tRNA <sub>CUA</sub>	<i>YPH499ΔTIM17::HIS3</i>	(Demishtein-Zohary et al., 2017)
Tim17-His <sub>9</sub> W108Bpa + pBpa2-PGK1 + 3SUP4-tRNA <sub>CUA</sub>	<i>YPH499ΔTIM17::HIS3</i>	(Demishtein-Zohary et al., 2017)
prom-Tim44-f R294A	<i>YPH499ΔTIM44::HIS3</i>	This thesis
prom-Tim44-f E300A	<i>YPH499ΔTIM44::HIS3</i>	This thesis
prom-Tim44-f D345A	<i>YPH499ΔTIM44::HIS3</i>	This thesis
prom-Tim44-f Q372A	<i>YPH499ΔTIM44::HIS3</i>	This thesis
prom-Tim44-f I393A	<i>YPH499ΔTIM44::HIS3</i>	This thesis
prom-Tim44-f D345A, Q372A	<i>YPH499ΔTIM44::HIS3</i>	This thesis
prom-Tim44-f D345A, Q372A, I393A	<i>YPH499ΔTIM44::HIS3</i>	This thesis
prom-Tim44-f D345A, Q372A	<i>YPH499ΔTIM44::HIS3</i>	This thesis
His <sub>9</sub> -Tim44 (pre-His <sub>9</sub> -43-431)	<i>YPH499ΔTIM44::HIS3</i>	This thesis
His <sub>9</sub> -Tim44 (pre-His <sub>9</sub> -43-431) S271Bpa + pBpa2-PGK1 + 3SUP4-tRNA <sub>CUA</sub>	<i>YPH499ΔTIM44::HIS3</i>	This thesis
His <sub>9</sub> -Tim44 (pre-His <sub>9</sub> -43-431) L279Bpa + pBpa2-PGK1 + 3SUP4-tRNA <sub>CUA</sub>	<i>YPH499ΔTIM44::HIS3</i>	This thesis
His <sub>9</sub> -Tim44 (pre-His <sub>9</sub> -43-431) E295Bpa pBpa2-PGK1 + 3SUP4-tRNA <sub>CUA</sub>	<i>YPH499ΔTIM44::HIS3</i>	This thesis
His <sub>9</sub> -Tim44 (pre-His <sub>9</sub> -43-431) Y296Bpa + pBpa2-PGK1 + 3SUP4-tRNA <sub>CUA</sub>	<i>YPH499ΔTIM44::HIS3</i>	This thesis
His <sub>9</sub> -Tim44 (pre-His <sub>9</sub> -43-431) D309Bpa + pBpa2-PGK1 + 3SUP4-tRNA <sub>CUA</sub>	<i>YPH499ΔTIM44::HIS3</i>	This thesis
His <sub>9</sub> -Tim44 (pre-His <sub>9</sub> -43-431) K311Bpa + pBpa2-PGK1 + 3SUP4-tRNA <sub>CUA</sub>	<i>YPH499ΔTIM44::HIS3</i>	This thesis
His <sub>9</sub> -Tim44 (pre-His <sub>9</sub> -43-431) A320Bpa + pBpa2-PGK1 + 3SUP4-tRNA <sub>CUA</sub>	<i>YPH499ΔTIM44::HIS3</i>	This thesis
His <sub>9</sub> -Tim44 (pre-His <sub>9</sub> -43-431) I346Bpa + pBpa2-PGK1 + 3SUP4-tRNA <sub>CUA</sub>	<i>YPH499ΔTIM44::HIS3</i>	This thesis
His <sub>9</sub> -Tim44 (pre-His <sub>9</sub> -43-431) Q372Bpa + pBpa2-PGK1 + 3SUP4-tRNA <sub>CUA</sub>	<i>YPH499ΔTIM44::HIS3</i>	This thesis

His <sub>9</sub> -Tim44 (pre-His <sub>9</sub> -43-431) S397Bpa + pBpa2-PGK1 + 3SUP4-tRNA <sub>CUA</sub>	YPH499Δ <i>TIM44::HIS3</i>	This thesis
His <sub>9</sub> -Tim44 (pre-His <sub>9</sub> -43-431) F422Bpa + pBpa2-PGK1 + 3SUP4-tRNA <sub>CUA</sub>	YPH499Δ <i>TIM44::HIS3</i>	This thesis
prom-Ssc1	YPH499Δ <i>SSC1::HIS3</i>	(Mapa et al., 2010)
prom-Ssc1-His <sub>6</sub>	YPH499Δ <i>SSC1::HIS3</i>	This thesis
prom-Ssc1 D341C, Q448C	YPH499Δ <i>SSC1::HIS3</i>	(Mapa et al., 2010)
prom-Ssc1-His <sub>6</sub> D341C, Q448C	YPH499Δ <i>SSC1::HIS3</i>	This thesis

### 2.2.2 Transformation of yeast cell with plasmid DNA

Cells from required yeast strain were inoculated in 30 mL of YPD medium and were grown overnight at 30°C, 160 rpm. Next day, cells were diluted to OD<sub>600</sub> ~0.1 to in YPD medium to a final volume of 50 mL (for 8 transformations). Cells were allowed to grow at 30°C, 160 rpm until OD<sub>600</sub> reached between 0.5-0.6. Cells were harvested by centrifugation at 3,000 x g, 5 min at RT. Harvested cells were washed with 25 mL of sterile deionized water. Washed cells were resuspended in 1 mL of 100 mM lithium acetate (LiAc) and were transferred to 1.5 mL microcentrifuge tube. Cells were harvested by centrifugation at 16,000 x g for 30 s and resuspended in 400 µL of 100 mM LiAc. Per transformation reaction, 50 µL aliquots of cell suspension were transferred in 1.5 mL microcentrifuge tubes. Cells were re-isolated by centrifugation at 3,000 x g for 5 min, supernatants were removed and the cell pellets carefully overlaid with the following solutions in the given order: 240 µL 50% (w/v) PEG, 36 µL 1 M LiAc, 5 µL 10 mg/mL ssDNA (it was heated at 95°C, 5 min and cooled immediately on ice before use), 60 µL distilled water and 5 µL plasmid DNA (0.1-1 µg). Tubes were vortexed rigorously for 1 min and subsequently incubated at 30°C, 850 rpm for 30 min. The temperature was increased to 42°C for additional 20-25 min. Finally, cells were harvested by centrifugation at 16,000 x g, 1 min, RT, resuspended in 150 µL dH<sub>2</sub>O and cell suspension plated on SD-agar plate with suitable selection markers. The plates were incubated at 30°C for 2 days.

### **2.2.3 5-FOA selection by plasmid shuffling**

The deletion strains of Tim44, Tim17 and Ssc1 were made viable by copy of the respective gene constructs cloned into *URA3* containing vector, pVT-102U. The strains made viable in this way were transformed with the plasmid vector cloned with the gene of interest as described in 2.2.2. pVT-102U vector carrying wild type copy of the gene was removed by plasmid shuffling. Cells were picked from selective medium plates after transformation and were streaked for single colonies. Single colonies were further streaked on selection plate to grow at 30°C. Cells were streaked on selection medium plate supplemented with uracil and 5-fluoroorotic acid (5-FOA) and the plates were incubated at 30°C for 3-5 days.

## **2.3 Cell biology methods**

### **2.3.1 Bacterial culture**

#### **2.3.1.1 Media for *E.coli* growth**

*E. coli* was grown in LB medium.

*LB medium*: 5 g/L yeast extract, 10 g/L bacto-tryptone, 10 g/L NaCl.

*LB-Amp medium*: LB-medium supplemented with 100 µg/mL of ampicillin.

LB medium was sterilized by autoclaving. For plates, 20 g/L bacto-agar was added in LB medium before autoclaving. For preparation of LB-Amp medium, 100 µg/mL of ampicillin was added after the autoclaved medium has cooled down to 50°C.

#### **2.3.1.2 Cultivation of *E.coli***

Single colonies of *E.coli* were picked and inoculated in 3 mL (for minipreps) and 40 mL (for midiprep and primary culture for bacterial protein expression) LB medium. Cells were grown overnight at 37°C, 160 rpm.

### **2.3.2 Yeast culture**

#### **2.3.2.1 Media for *S. cerevisiae* growth**

Non-selective media:

*YP-medium*: 10 g yeast extract, 20 g bacto-peptone, H<sub>2</sub>O to 930 mL, pH 5.0 (adjusted with HCl).

YP-medium was supplemented with different carbon sources given below using following autoclaved stock solutions- 40% Glucose, 30% Galactose and 30% Glycerol

*YPD-medium*: YP-medium supplemented with 2% glucose.

*YPG-medium*: YP-medium supplemented with 3% (v/v) glycerol.

*YPGal-medium*: YP-medium supplemented with 2% galactose.

*Lactate medium*: 3 g yeast extract, 1 g KH<sub>2</sub>PO<sub>4</sub>, 1 g NH<sub>4</sub>Cl, 0.5 g CaCl<sub>2</sub> x 2H<sub>2</sub>O, 0.5 g NaCl, 1.1 g MgSO<sub>4</sub> x 6H<sub>2</sub>O, 0.3 mL 1% FeCl<sub>3</sub>, 22 mL 90% lactic acid, H<sub>2</sub>O to 1 L, pH 5.5 (adjusted with KOH) and supplemented with 0.1% glucose.

Selective media:

*SD medium*: 1.7 g yeast nitrogen base, 5 g (NH<sub>4</sub>)<sub>2</sub>SO<sub>4</sub>, 20 g glucose, H<sub>2</sub>O to 1 L.

*SLac medium*: 1.7 g yeast nitrogen base, 5 g (NH<sub>4</sub>)<sub>2</sub>SO<sub>4</sub>, 22 mL 90% lactic acid, H<sub>2</sub>O to 1 L, pH 5.5 (adjusted with KOH).

These acted as base for selective media. Following stock solutions of selective markers were prepared and sterilized by autoclaving, except tryptophan which was filter-sterilized.

The markers were added into SD or SLac medium for preparation of liquid cultures.

<i>Amino acid</i>	<i>Stock concentration</i>	
Histidine	10 mg/mL	500 X
Leucine	10 mg/mL	333 X
Lysine	10 mg/mL	333 X
Uracil	2 mg/mL	100 X
Adenine	2 mg/mL	100 X
Tryptophan	10 mg/mL	500 X

Following stock solutions were prepared for nitrogen source:

*5X Synthetic minimal medium stock (5X S)*- 8.5 g yeast nitrogen base, 25 g (NH<sub>4</sub>)<sub>2</sub>SO<sub>4</sub>, H<sub>2</sub>O to 1 L followed by autoclave

*5X Synthetic lactate minimal medium stock (5X SLac)*- 8.5 g yeast nitrogen base, 25 g (NH<sub>4</sub>)<sub>2</sub>SO<sub>4</sub>, 110 mL 90% lactic acid, H<sub>2</sub>O to 1 L, pH 5.5 (adjust with KOH), followed by autoclaving

*1 M Bpa*- 270 mg p-benzoyl-L-phenylalanine (Bpa) in 1 mL 1 M NaOH. This was always freshly prepared.

For preparation of 1 L medium for plates, 4% (w/v) bacto-agar in 500 mL H<sub>2</sub>O was autoclaved and allowed to cool at 65°C. 5X S, amino acids and glucose necessary for 1 L of SD medium were diluted in 500 mL of sterile dH<sub>2</sub>O. The two solutions were mixed before pouring medium in Petri dishes. The plates were allowed to solidify and stored at 4°C until use.

For preparation of 5-FOA plates, 1 g of 5-FOA was dissolved in 500 mL of 2-fold concentrated SD medium by shaking at 30°C before mixing it into autoclaved agar. For preparation of Bpa-plates, 1 mM Bpa was added drop by drop from its 1 M stock in NaOH to the 2-fold concentrated SD medium that was pre-heated at 65°C. In case of precipitation of Bpa, the medium was incubated at 65°C until the precipitate was gone. This was followed by addition of autoclaved agar, mixing and pouring into Petri dishes.

### **2.3.2.2 Cultivation of liquid *S. cerevisiae* cultures**

Liquid cultures of yeast cells were normally grown at 30°C with shaking at 160 rpm. All temperature sensitive mutants were grown at 24°C, with shaking. The cultures were diluted with fresh medium when needed, so that they always remained in exponential growth phase. For large-scale isolation of mitochondria, lactate medium or selective lactate medium with 0.1% glucose were used, if not mentioned otherwise. For UV-specific crosslinking, cultures were grown in selective SD medium with 1 mM Bpa and were handled and grown in dark.

## **2.3.3 Assays with yeast cells**

### **2.3.3.1 Drop dilution test**

Yeast cells were inoculated and grown overnight in 10 mL of YPD at 30°C with shaking at 160 rpm, if not mentioned otherwise. The cells were harvested and serially diluted 10-fold in sterile dH<sub>2</sub>O. 2 µL of yeast cell suspension was spotted on to YPD and YPLac or YPG plates. The plates were incubated at three different temperatures, 24°C, 30°C and 37°C, for 2-5 days.

### **2.3.3.2 Bpa-photocrosslinking**

An equivalent of 60-80 OD<sub>600</sub> of cells were collected per sample in case of Ni-NTA pull-down assay and 20 OD<sub>600</sub> of cells were collected for cell lysate preparation. Yeast culture

of cells expressing Bpa-labelled proteins were split in two halves and were harvested by centrifugation at 3,000 x g, 5 min, RT. Cells were resuspended in 5 mL of PBS (10 mM Na-phosphate, 137 mM NaCl, 2.7 mM KCl, pH 7.4 adjusted with HCl). One half was transferred to a small Petri dish (35 X 10 mm) and exposed to UV light (365 nm, 100 Watt, 230 V) for 1 h at 4°C. The other half was kept in dark on ice. Cells were harvested by centrifugation at 3,000 x g, 5 min, 4°C, resuspended in 1 mL of dH<sub>2</sub>O and transferred to 1.5 mL microcentrifuge tubes. Centrifugation at 16,000 x g for 1 min at 4°C was done to pellet down the cells. Cellular pellets were flash-frozen in liquid nitrogen and stored in -20°C until use.

### **2.3.3.3 Preparation of whole cell lysate**

An equivalent of 3 OD<sub>600</sub> of cells was collected by centrifuging yeast culture at 3000 x g, 5 min, RT. Cells were resuspended in 1 mL dH<sub>2</sub>O, transferred to 1.5 mL microcentrifuge tubes and harvested by centrifugation at 16,000 x g, 1 min, RT. Cell pellet was resuspended in 100 µL of dH<sub>2</sub>O and then 100 µL of 0.2 M NaOH was added. Samples were mixed by vortexing and incubated at RT for 5 min. Cells were re-isolated by centrifugation at 16,000 x g at RT for 3 min and supernatant was removed. Pellet was resuspended in 200 µL of 2X Laemmli buffer (120 mM Tris-Cl (pH 6.8), 20% (v/v) glycerol, 4% (w/v) SDS, 0.02% (w/v) bromophenol blue) with β-Mercaptoethanol and was heated at 95°C for 5 min. Sample was centrifuged at 16,000 x g, 3 min, RT, to remove cellular debris. Supernatant was collected and 25 µL of it was loaded on SDS-PAGE. For UV crosslinked cells expressing Bpa-labelled proteins, 200 µL of 0.2 M NaOH was added instead of 100 µL.

### **2.3.3.4 Ni-NTA pulldown of His-tagged proteins from yeast cell**

Ni-NTA pull down was carried out for Bpa mutants to enrich His-tagged proteins along with their crosslinked products. Cells were taken out of the freezer and allowed to thaw at RT for 5 min. They were resuspended in 100 µL of dH<sub>2</sub>O, 200 µL of 0.2 M NaOH was added, the mixture was vortexed and incubated at RT for 5 min. Cells with destabilized cell wall were collected by centrifugation at 16,000 x g, 3 min, RT. Re-isolated cells were resuspended in 300 µL of 50 mM Tris-Cl, pH 8.0, 150 mM NaCl, 1% SDS, 1 mM EDTA and heated at 95°C for 5 min. Lysates were centrifuged at 16,000 rpm, 3 min, RT to remove cell debris. Supernatants were collected in 15 mL centrifuge tubes and diluted to

a final volume of 3 mL with 50 mM Tris, pH 8.0, 300 mM NaCl, 0.5% Triton X-100, 20 mM imidazole, 1 mM PMSF, 1 mM DTT. To this, 50  $\mu$ L of pre-equilibrated Ni-NTA agarose beads were added. Samples were incubated at 4°C on a rotating platform for 30 min. Non-bound material was removed by centrifugation at 4,000 x g, 10 min at 4°C. Beads were resuspended in 500  $\mu$ L of 50 mM Tris-Cl, pH 8.0, 300 mM NaCl, 0.1% Triton X-100, 20 mM imidazole and transferred to 1.5 mL microcentrifuge tubes. Samples were centrifuged at 18,000 x g, 2 min, 4°C and remaining supernatant removed. Beads were washed two more times with 200  $\mu$ L of 50 mM Tris-Cl, pH 8.0, 300 mM NaCl, 0.1% Triton X-100, 20 mM imidazole. Bound proteins were eluted by heating beads at 95°C for 5 min in 70  $\mu$ L of 2X Laemmli buffer containing  $\beta$ -mercaptoethanol with 450 mM imidazole. After heating, samples were centrifuged at 16,000 x g for 3 min and each half of the eluted sample was loaded on a lane of SDS-PA gel and analysed by two different antibodies after western blotting.

### **2.3.3.5 Isolation of crude mitochondria**

5 OD<sub>600</sub> of cells were harvested by centrifugation at 3,000 x g at RT for 5 min, followed by a wash with water. Cells were resuspended in 300  $\mu$ L of SHK buffer (0.6 M Sorbitol, 20 mM HEPES-KOH, pH 7.2, 80 mM KCl) supplemented with 1 mM PMSF. 0.3 g of glass beads (diameter 0.3 mm) were added to resuspended cells and cells were lysed by vigorous intermittent vortexing for 30 s followed by resting of sample on ice for 30 s for four times. Samples were centrifuged at 1,000 x g for 3 min at 4°C to remove glass beads, non-broken cells and nuclei. After centrifugation, supernatant was collected and centrifuged at 18,000 x g, 10 min, 4°C. After centrifugation, the pellet contained crude mitochondria and the supernatant the post-mitochondrial fraction that consists mostly of the cytosol. 50  $\mu$ L of supernatant was collected and subjected to TCA precipitation. TCA precipitation of proteins was carried out by adding 10  $\mu$ L of 72% trichloroacetic acid (TCA) to 50  $\mu$ L supernatant and incubating at -20°C for 10 min. The precipitated proteins were pelleted down by centrifuging at 36,700 x g, 20 min at 4°C. Pellet was washed with 100  $\mu$ L of chilled acetone and centrifuged at 36,700 x g, 10 min at 4°C. Crude mitochondrial and cytosolic fractions were resuspended in Laemmli buffer with  $\beta$ -mercaptoethanol. After 5 min at 95°C, both the cytosolic and mitochondrial fractions were analysed by SDS-PAGE and western blotting.

### **2.3.3.6 Large-scale mitochondria isolation from *S. cerevisiae***

Isolation of mitochondria was done as described previously (Daum et al., 1982a; Daum et al., 1982b). Yeast cells were grown until OD<sub>600</sub> reached 0.7-0.9. Cells were harvested by centrifugation at 4,400 x g for 5 min at RT. Cell pellet was washed once with dH<sub>2</sub>O and the wet weight of cells determined. Cells were resuspended at 0.5 g/mL in DTT buffer (100 mM Tris-SO<sub>4</sub>, 10 mM DTT, pH 9.4). Cell suspension was incubated at 30°C for 10 min on a shaking platform and cells were subsequently re-isolated by centrifugation at 4,400 x g for 5 min, RT. Cells were washed once with 100 mL of 1.2 M sorbitol and resuspended in sorbitol buffer (1.2 M sorbitol, 20 mM potassium phosphate-KOH, pH 7.4) at 6.6 mL/g. Digestion of cell wall was carried out by Zymolase. To this end, 4 mg of Zymolyase per gram wet weight of cells was added to the cell suspension in sorbitol buffer and the suspension incubated for 30-45 min at 30°C on a shaking platform. Formation of sphaeroplast (cells with digested cell wall) was determined by comparison of OD<sub>600</sub> of 50 µl of sample diluted in 2 mL dH<sub>2</sub>O or 1.2 M sorbitol. Sphaeroplasts burst in dH<sub>2</sub>O as it is a hypotonic solution. Therefore, presence of sphaeroplast can be detected by 80-90% reduction in OD<sub>600</sub> measurement in dH<sub>2</sub>O as compared to sorbitol. Sphaeroplasts were harvested by centrifugation at 3,000 x g for 5 min, 4°C and resuspended at 0.15 g/mL in homogenization buffer (0.6 M sorbitol, 10 mM Tris-Cl, 1mM EDTA, 0.2% (w/v) BSA, 1 mM PMSF, pH 7.4). This was followed by homogenization by ten strokes in Dounce-homogeniser. Homogenised sample was centrifuged twice at 1,900 x g at 4°C for 5 min to remove cell debris and nuclei. Supernatant was collected and centrifuged further at 17,400 x g for 12 min at 4°C to pellet mitochondria. Mitochondria containing pellet was resuspended in SH buffer (0.6 M Sorbitol, 20 mM HEPES-KOH, pH 7.4) and centrifuged further at 2,800 x g for 5 min at 4°C to remove remaining debris and nuclei. Mitochondria were re-isolated by centrifugation at 17,400 x g, 12 min, 4°C. Mitochondrial pellet obtained was resuspended in a SH buffer to a final concentration of 10 mg/mL. Resuspended mitochondria were aliquoted, flash frozen in liquid nitrogen and stored in -80°C until use.

## 2.4 Protein biochemistry methods

### 2.4.1 Isolation of recombinant proteins

#### 2.4.1.1 Expression of recombinant proteins in *E.coli*

Recombinant proteins were normally expressed by freshly transforming BL21(DE3) electrocompetent cells with the plasmid clone carrying the protein construct of interest. For expression of mature and presequence form of Ssc1, BL21(DE3) $\Delta$ dnaK::52 strain was used. Transformed cells were diluted in 40 mL of LB-Amp medium and the culture grown overnight at 37°C, 160 rpm. Next day, 40 mL overnight culture was diluted into 2 L fresh LB-Amp medium pre-warmed at 37°C and grown at 37°C, 160 rpm until OD<sub>600</sub> reached ~0.5. Expression of protein was induced by addition of 0.5 mM IPTG and culture was incubated at 37°C for further 3 h with shaking at 160 rpm. Cells were harvested by centrifugation at 3,000 x g, 10 min, 4°C. Cell pellets were stored frozen at -20°C until use.

#### 2.4.1.2 Purification of His<sub>6</sub>-tagged recombinant proteins

All His<sub>6</sub>-tagged proteins, except for presequence-containing Ssc1, were purified as follows. Frozen cell pellet was thawed and resuspended in 50mL of 50 mM Na-phosphate buffer, 300 mM NaCl, 20 mM imidazole, pH 8.0. To this, 1 mg/mL lysozyme and 1mM PMSF were added. Cell suspension was incubated on rotating platform at 4°C for 30 min followed by cell lysis and DNA shearing by sonication (by Branson Sonifier at 80% duty cycle, microtip limit 5, 12 s ON/ 18 s OFF for 10 times). Cell debris was removed by centrifugation at 27,000 x g, 15 min, 4°C. Supernatant was loaded on Ni-NTA agarose column, pre-equilibrated with 20 CV (column volume) of the above buffer. Column was subsequently washed with 10 CV of 50 mM Na-phosphate buffer, 300 mM NaCl, 20 mM imidazole, pH 8.0, followed by 5 CV of 50 mM Na-phosphate buffer, 300 mM NaCl, 20 mM imidazole, pH 8.0, containing 2 mM ATP and 5 mM MgCl<sub>2</sub>. Bound proteins were eluted with 50 mM Na-phosphate buffer, 300 mM NaCl, 300 mM imidazole, pH 8.0. Proteins were further purified by size exclusion chromatography on Superdex 75 10/300 (GE Healthcare) in 20 mM HEPES-KOH, 250 mM KCl, pH 7.4.

For some experiments, the His<sub>6</sub>-tag was removed by cleavage with TEV protease, whose recognition site was genetically engineered between the His-tag and the protein of interest. Imidazole present in the buffer after protein was eluted from Ni-NTA affinity

column was removed by buffer exchange on PD10 column (GE Healthcare) pre-equilibrated with 50 mM Na-phosphate buffer, 300 mM NaCl, 20 mM imidazole, pH 8.0. Recombinantly expressed and purified His<sub>6</sub>-TEV protease was added to the purified protein in 1:75 molar ratio and incubated at 30°C for 1.5 h. His<sub>6</sub>-TEV protease and non-cleaved His-tagged protein, if present, were removed by incubating the sample with 500 µL of pre-equilibrated Ni-NTA agarose beads for 30 min at 4°C on a rotating platform. Sample was centrifuged at 4,000 x g, 10 min, 4°C and supernatant was collected and purified further by size exclusion chromatography on Superdex 75 10/300 column (GE Healthcare), as described above. Proteins were aliquoted, flash frozen in liquid nitrogen and stored in -80°C until use.

#### **2.4.1.3 Purification of mature Ssc1 and its variants**

Mature Ssc1 and its variants were purified upon co-expression with His<sub>6</sub>-Hep1 (Weiss et al., 2002). Briefly, the bacterial cell lysate was first passed through Ni-NTA agarose column to remove His<sub>6</sub>-Hep1 and Ssc1 was then affinity purified from the flow-through on an Mge1 column.

For preparation of Mge1 column, bacterial cell pellet expressing His<sub>6</sub>-Mge1 was resuspended in 50 mL of 50 mM Tris-Cl, 150 mM KCl, 5 mM MgCl<sub>2</sub>, 20 mM imidazole, pH 7.5, containing 1 mg/mL of lysozyme and 1 mM PMSF. Incubation was done at 4°C on a rotating platform for 30 min, followed by cell lysis by sonication. Cell lysate was centrifuged at 27,000 x g for 15 min and passed through pre-equilibrated Ni-NTA column. Column was washed with 5 CV of 50 mM Tris-Cl, 150 mM KCl, 5 mM MgCl<sub>2</sub>, 20 mM imidazole, pH 7.5, followed by 5 CV of 50 mM Tris-Cl, 150 mM KCl, 5 mM MgCl<sub>2</sub>, 20 mM imidazole, pH 7.5 containing 2 mM ATP. Final wash was done with 20 CV of 50 mM Tris-Cl, 150 mM KCl, 5 mM MgCl<sub>2</sub>, 20 mM imidazole, pH 7.5. Mge1 column prepared by this method was stored in 4°C and was used within 2-3 days.

Bacterial cell pellet co-expressing His<sub>6</sub>-Hep1 and Ssc1 was resuspended in 50 mM Tris-Cl, 250 mM KCl, 5 mM MgCl<sub>2</sub>, 10 % glycerol, 1 mM DTT, 20 mM imidazole, pH 7.5. To the cell suspension, 1 mg/mL of lysozyme and 1 mM PMSF were added and it was incubated at 4°C on a rotating platform for 30 min. Cells were lysed by sonication and centrifuged at 27,000 x g, 4°C, 15 min. Supernatant was passed through 3 mL of pre-equilibrated Ni-NTA agarose column to remove His<sub>6</sub>-Hep1. Flow-through from Ni-NTA column was passed through Mge1 column to allow binding of Ssc1 to Mge1. Mge1

column was washed with 20 CV of 50 mM Tris-Cl, 250 mM KCl, 5 mM MgCl<sub>2</sub>, 10% glycerol, 1 mM DTT, 20 mM imidazole, pH 7.5. Bound Ssc1 was eluted with 2 mM ATP in 50 mM Tris-Cl, 250 mM KCl, 5 mM MgCl<sub>2</sub>, 10 % glycerol, 1 mM DTT, 20 mM imidazole, pH 7.5. Removal of ATP in eluted protein fractions was done by buffer exchange using PD10 column equilibrated in 20 mM HEPES-KOH, 200 mM KCl, 5 mM MgCl<sub>2</sub>, 1 mM DTT, pH 7.4. Protein was stored in aliquots at -80°C until use.

#### **2.4.1.4 Purification of presequence-containing Ssc1 and its variants**

Presequence-containing Ssc1 was purified from inclusion bodies. To remove soluble proteins, bacterial pellet was resuspended in 50 mM Na-phosphate buffer, 150 mM NaCl, 2 mM DTT, 1 mM PMSF, pH 7.5. Bacterial cells were lysed by sonication and soluble proteins were separated by centrifuging the lysate at 27,000 x g for 15 min at 4°C. Pellet obtained after centrifugation was resuspended in 50 mL of 50 mM Tris-Cl, 3 M Urea, 2 mM DTT, 20 mM imidazole, pH 8.0 and was incubated at RT on a rotating platform for 1 h. Sample was centrifuged at 27,000 x g, 15 min, 25°C and supernatant, containing Ssc1, was passed through 1.5 mL Ni-NTA column pre-equilibrated in 50 mM Na-phosphate buffer, 150 mM NaCl, 20 mM imidazole, pH 7.5. Column was washed with 30 CV of 50 mM Tris-Cl, 3 M Urea, 2 mM DTT, 20 mM imidazole, pH 8.0. Bound Ssc1 was eluted with 50 mM Tris-Cl, 3 M Urea, 2 mM DTT, 300 mM imidazole, pH 8.0 in 1 mL fractions. To remove imidazole from the buffer, PD MiniTrap G-25 columns (GE Healthcare) were used to exchange the buffer to 50 mM Tris-Cl, 3 M Urea, 2 mM DTT, pH 8.0. Protein aliquots were flash frozen and stored at -80°C until use.

### **2.4.2 Protein detection and analysis**

#### **2.4.2.1 SDS-PAGE**

Analysis of protein samples based on the difference in their molecular weight was done by SDS-PAGE as described previously (Laemmli, 1970). Composition of various buffers was as follows:

Resolving gel	8-16% (w/v) acrylamide, 0.16-0.33% (w/v) bis-acrylamide, 377 mM Tris-Cl (pH 8.8), 0.1% (w/v) SDS, 0.05% (w/v) APS, 0.05% (v/v) TEMED
Stacking gel	5% (w/v) acrylamide, 0.1% (w/v) bis-acrylamide, 60 mM Tris-Cl (pH

	6.8), 0.1% (w/v) SDS, 0.07% (w/v) APS, 0.35% (v/v) TEMED
Running buffer	50 mM Tris-Cl, 384 mM glycine, 0.1% (w/v) SDS, pH 8.3 without adjustment
2X Laemmli Buffer	120 mM Tris-Cl (pH 6.8), 20% (v/v) glycerol, 4% (w/v) SDS, 0.02% (w/v) bromophenol blue

Samples were heated in 2X Laemmli buffer containing 3%  $\beta$ -mercaptoethanol at 95°C for 3-5 min and were loaded on SDS-PA gels prepared using resolving gel and stacking gel composition mentioned above. Chambers, to which SDS-PA gel was clipped on, were filled with running buffer. For large gels (14 cm x 9 cm x 0.1 cm), electrophoresis was done at constant current of 35 mA for 100 min and for small gels (10 cm x 5.5 cm x 0.075 cm), at constant current of 25 mA for 45 min. When the bromophenol blue dye reached the bottom of the resolving gel, proteins were detected by either staining SDS-PA gels with coomassie brilliant blue (CBB) or were transferred to nitrocellulose membrane or were scanned for fluorescence.

#### 2.4.2.2 CBB staining

Coomassie Brilliant Blue (CBB) staining was typically done to analyse the purification of recombinant proteins. Following are the composition of staining and destaining solutions used:

CBB staining solution	0.1% (w/v) CBB R-250, 40% methanol, 10% glacial acetic acid
CBB destaining solution	40% methanol, 10% glacial acetic acid

SDS-PA gel was transferred to CBB staining solution and incubated on a shaking platform at RT for 30 min. Gel was briefly rinsed in deionized water and then incubated with destaining solution on a shaking platform until protein bands were clearly visible.

#### 2.4.2.3 Transfer of proteins to nitrocellulose membrane

Transfer of proteins from SDS PA gel to nitrocellulose membranes was done by semi-dry western blot transfer method. Proteins were transferred at constant current of 250 mA for 1 h. For crosslinking experiments, transfer was done at constant current of 250 mA for

1.25 h. Composition of transfer buffer used was as follows: 20 mM Tris, 150 mM glycine, 20% (v/v) methanol and 0.02% SDS.

#### **2.4.2.4 Fluorescence scanning**

Analysis of proteins labelled with fluorophores was done by fluorescence scanning using Typhoon FLA 9500 (GE Healthcare). For detection of proteins labelled with ATTO 532 dye, 532 nm laser and LPG filter were used. For detection of proteins labelled with ATTO 647N, Alexa 647, CF640R and ATTO 647, 635 nm laser and LPR filter were used. Scanning was done at 700-1000 V exposure and at 25 or 50  $\mu\text{m}$  pixel size.

#### **2.4.2.5 Estimation of protein concentration**

For estimation of protein concentration, Bradford assay was done (Bradford, 1976). Standard plot for Bradford assay was made using bovine IgG (Bio-Rad) and was prepared simultaneously with protein samples of unknown concentration. Protein samples used for concentration estimation were either used directly or were diluted 5-10 fold. The final volume of protein sample was made up to 34  $\mu\text{L}$  and 1 mL of 1:5 diluted Bradford reagent (Bio-Rad) was added. Samples were subsequently incubated at RT for 10 min. Absorbance was measured at 595 nm wavelength and concentration was determined by comparison with standard curve.

### **2.4.3 Assays with purified proteins**

#### **2.4.3.1 Ni-NTA pull down**

Purified His<sub>6</sub>-tagged Tim44 N-terminal domain was incubated with purified Tim44 C-terminal domain in equimolar ratio in 1.5 mL microcentrifuge tube for 5 min at RT. For high salt condition, 20 mM Tris-Cl, 300 mM NaCl, 10 mM imidazole, pH 8.0 was used and for low salt condition, 20 mM Tris-Cl, 50 mM NaCl, 10 mM imidazole, pH 8.0 was used. At least 60  $\mu\text{g}$  of each the proteins were present in a reaction volume of 300  $\mu\text{L}$ . 100  $\mu\text{L}$  of reaction mixture was taken out, subjected to TCA precipitation, as described below, and used as 'input'. To the remaining 200  $\mu\text{L}$  of reaction mixture, 50  $\mu\text{L}$  of pre-equilibrated Ni-NTA agarose beads were added and the samples were incubated on a rotating platform at 4°C for 30 min. Ni-NTA agarose beads were separated from the solution by centrifuging at 18,000 x g, 2 min, 4°C. Non-bound material was subjected to TCA precipitation. Ni-NTA agarose beads with bound proteins were washed three times

with 1 mL buffer. Bound proteins were eluted by two successive incubations with 250  $\mu$ L of 20 mM Tris-Cl, 50 mM NaCl, 300 mM imidazole, pH 8.0. Elution fractions were pooled and TCA-precipitated.

TCA precipitation was carried out by addition of 12% TCA to protein solution. Samples were mixed thoroughly and incubated at  $-20^{\circ}\text{C}$  for 10 min. Precipitated proteins were collected by centrifugation at  $36,700 \times g$  for 20 min at  $4^{\circ}\text{C}$ . Protein precipitate was washed with 500  $\mu$ L of pre-cooled acetone and centrifuged at  $36,700 \times g$  for 10 min at  $4^{\circ}\text{C}$ . Protein pellet was dissolved in 25  $\mu$ L 2X Laemmli buffer containing  $\beta$ -mercaptoethanol by shaking for 10 min at RT, followed by boiling at  $95^{\circ}\text{C}$  for 5 min. Samples were then loaded on SDS-PA gel.

### **2.4.3.2 Pull-down with proteins immobilized to CNBr-Sepharose beads**

#### ***a) Immobilization of proteins to CNBr-Sepharose beads***

CNBr-Sepharose 4B (GE Healthcare) beads were allowed to swell and were later washed in 1 mM HCl. 0.8 mL of washed beads were packed in a Poly-Prep Chromatography column (Bio-Rad). Buffer in which protein samples were stored was exchanged with the column buffer (0.1 M  $\text{NaHCO}_3$ , 0.5 M NaCl, pH 8.3) using a PD10 column. 3.5-8.0 mg (222  $\mu$ mol) of protein was added per 0.8 mL of CNBr-Sepharose beads, the column was closed on both sides and incubated on a rotating platform for 1 h at RT to allow proteins to react with the CNBr groups. Non-bound proteins were removed by gravity flow and column was subsequently washed with 12.5 CV of Column buffer. To block remaining reactive sites, 6 mL of 1M ethanolamine, pH 8.0 was loaded on the column. After 4 mL passed through, the column was closed and left at RT for 2 h. Ethanolamine was allowed to pass through and column was washed with 30 mL of column buffer. 10 mL of 0.05%  $\text{NaN}_3$  was allowed to pass through column and column was stored at  $4^{\circ}\text{C}$  until use.

Beads were taken and washed in 20 mM Tris-Cl, 80 mM KCl, 10% glycerol, pH 8.0, followed by sequential washing of beads in above buffer with 0.1% and 0.5% Triton X-100 just before use.

#### ***b) Pull-down of interacting proteins***

Isolated mitochondria were resuspended at 1 mg/mL in 20 mM Tris-Cl, 80 mM KCl, 10% glycerol, pH 8.0 supplemented with 2 mM PMSF and 0.5% Triton X-100 and solubilized at  $4^{\circ}\text{C}$  for 30 min. Insoluble material was removed by ultracentrifugation step at  $124,500 \times g$  for 20 min at  $4^{\circ}\text{C}$ . 900  $\mu$ L of supernatant was added to 100  $\mu$ L of pre-equilibrated

CNBr-sepharose beads with immobilized protein and the mixture incubated on a rotating platform for 30 min at 4°C. Beads were centrifuged at 18,000 x g for 2 min at 4°C for removal of unbound material and washed three times in 200 µL of 20 mM Tris-Cl, 80 mM KCl, 10% glycerol, pH 8.0 supplemented with 0.1% Triton X-100. Bound material was eluted by heating the beads in 2X Laemmli buffer with β-mercaptoethanol at 95°C for 3 min. Beads were removed by a brief centrifugation step and supernatant was split into three parts and was loaded in three different wells on SDS-PA gel.

#### **2.4.3.3 Thermal Shift Assay**

Stability of purified proteins were analysed by thermal shift assay. Reaction mixture comprised of 6.2 µM protein and 5X SYPRO Orange in six different buffers. Compositions of buffers used are given in table 3.1 of section 3.2.3. Unfolding of proteins was estimated by measurement of fluorescence (excitation wavelength of 485 nm and emission wavelength of 530 nm) in qPCR machine with a temperature gradient from 5°C to 95°C. Assay was done with two different batches of purified proteins and in three technical replicates.

#### **2.4.3.4 Labelling of proteins with fluorophores**

Site-specific fluorophore labelling of purified cysteine versions of proteins was done by reaction between sulfhydryl group of cysteine and maleimide group of fluorophore dye. Frozen proteins were thawed and incubated with 2 mM DTT for 10 min on ice just prior to labelling so as to reduce all of the sulfhydryl groups. DTT was removed by buffer exchange using NAP-5 column (GE Healthcare).

For labelling mature Ssc1 with donor (ATTO 532) and acceptor (ATTO 647N, Alexa 647 or CF640R) dyes- protein, donor and acceptor fluorophores were incubated in 1:2:2 molar ratios in 50 mM Tris-Cl, 250 mM KCl, 5 mM MgCl<sub>2</sub>, pH 7.0 at 4°C for 3 h. For labelling protein with ATTO 647 as an acceptor dye, the dye was incubated with protein in 5-fold molar excess over protein. Free dye was removed by buffer exchange on NAP-5 column and protein was stored in 20 mM HEPES-KOH, 200 mM KCl, 5 mM MgCl<sub>2</sub>, pH 7.2 in aliquots at -80°C until use.

For labelling purified precursor Ssc1, purified protein, donor (ATTO 532) and acceptor (ATTO 647N, Alexa 647 or CF640R) dye, were incubated in 1:2:2 ratio in 50 mM Tris-Cl, 3M Urea, pH 7.0 at 4°C for 3 h. For labelling with ATTO 647, acceptor dye was added in 10-fold molar excess over protein. Free dye was removed by buffer exchange by

NAP-5 or PD MiniTrap G25 column. Protein was stored in 50 mM Tris-Cl, 3M Urea, pH 7.0 in aliquots at -80°C until use.

For rough estimation of concentration of labelled protein, absorbance of 1.5  $\mu$ L of protein sample was measured using NanoDrop. Total protein concentration was estimated by measuring absorbance at 280 nm. For measuring amount of bound donor and acceptor fluorophore, absorbance at absorption maxima wavelength of dye as recommended by manufacturer was measured ( $\lambda_{\text{abs}}$ : ATTO 532- 532 nm, ATTO 647N- 646 nm, ATTO 647- 647 nm and CF640R- 642 nm). Concentration of dye labelled to protein was calculated using Beer-Lambert Law equation (molar extinction co-efficient  $\epsilon_{\text{max}}$ : ATTO 532-  $1.15 \times 10^5$  L/mol cm, ATTO 647N-  $1.5 \times 10^5$  L/mol cm, ATTO 647-  $1.2 \times 10^5$  L/mol cm, CF640R-  $1.05 \times 10^5$  L/mol cm).

## **2.4.4 Assays with isolated mitochondria**

### **2.4.4.1 Chemical crosslinking**

To study protein-protein interactions within the TIM23 complex in intact mitochondria, following chemical crosslinkers were used: disuccinimidyl glutarate (DSG) and disuccinimidyl suberate (DSS). Mitochondria were diluted in SI buffer (50 mM HEPES-KOH, 0.6 M Sorbitol, 75 mM KCl, 10 mM Mg(Ac)<sub>2</sub>, 2 mM KH<sub>2</sub>PO<sub>4</sub>, 2.5 mM EDTA, 2.5 mM MnCl<sub>2</sub>, pH 7.2) in 100  $\mu$ L reaction volume. Where indicated, samples were incubated at 37°C for 30 min. ATP depletion of mitochondria was done by addition of 1 U of apyrase and 10  $\mu$ M oligomycin followed by incubation at 25°C for 10 min. ATP charging of mitochondria was done by addition of 4 mM ATP, 4 mM NADH, 10  $\mu$ M Phosphocreatine (CP) and 10  $\mu$ g creatine kinase (CK), followed by incubation at 25°C for 3 min. Samples were transferred to ice and 75  $\mu$ M DSS or DSG from stock solutions prepared in DMSO were added and crosslinking was done on ice for 30 min. Crosslinking reaction was stopped by treatment with 100 mM glycine (pH 8.8) for 10 min on ice. Samples were diluted with 500  $\mu$ L of SH buffer (20 mM HEPES-KOH, 0.6 M sorbitol, pH 7.2) and mitochondria re-isolated by centrifugation at 18,900 x g for 10 min at 4°C. Mitochondria were solubilized in 2X Laemmli buffer with  $\beta$ -mercaptoethanol and analyzed by SDS-PAGE followed by western blotting.

#### **2.4.4.2 Crosslinking of arrested precursor**

<sup>35</sup>S-labelled precursor protein, pcytb<sub>2</sub>(1–167)ΔDHFR, was arrested by incubating with energized mitochondria for 15 min at 25°C as described in 2.4.4.4 for protein import. Difference here is that in order to arrest the precursor protein, the buffer used in import process was supplemented with 2 μM methotrexate and 5 mM NADPH. Mitochondria with arrested precursor that spanned through the TOM and TIM23 complex were subject to crosslinking with DSS followed by quenching with glycine as described in 2.4.4.1. Re-isolation of mitochondria was done by centrifugation at 17,400 x g, 10 min at 4°C. Mitochondria in pellet were subject to lysis in harsh condition followed by immunoprecipitation as described in 2.4.4.3.

#### **2.4.4.3 Immunoprecipitation**

##### *a) Co-immunoprecipitation of protein complexes in mitochondria*

For co-immunoprecipitation experiments, antibodies were first immobilized on Protein A Sepharose CL-4B (PAS) beads. Beads were washed with dH<sub>2</sub>O and were equilibrated in TBS buffer (50 mM Tris-Cl, 150 mM NaCl, pH 7.5). Purified antibody of interest was added to the beads and incubated on a rotating platform for 1 h at 4°C. Unbound antibody was removed by washing the beads with TBS buffer and beads were equilibrated in 20 mM Tris-Cl, 80 mM KCl, 10 % glycerol, 5 mM EDTA, pH 8.0, containing 0.05% (w/v) digitonin.

Lysis of mitochondria was done by resuspending in 1 mL of 20 mM Tris-Cl, 80 mM KCl, 10% glycerol, 5 mM EDTA, pH 8.0 containing 1% digitonin and 2 mM PMSF, followed by incubation at 4°C on a rotating platform for 15 min. In case of temperature sensitive mutants, 1 mg of mitochondria was diluted in SH buffer and was incubated at 37°C for 30 min. Mitochondria were re-isolated by centrifugation at 18,900 x g, 10 min, 4°C. This was followed by lysis of mitochondria as mentioned above. Clarification of the lysate was done by centrifugation at 124,500 x g for 25 min at 4°C and 300 μL of supernatant was added to the Protein A-Sepharose beads with pre-bound antibodies. Mitochondrial lysate was incubated with the beads on a rotating platform at 4°C for 45 min. Beads were washed with 200 μL of 20 mM Tris-Cl, 80 mM KCl, 10% glycerol, 5 mM EDTA, pH 8.0 containing 0.05% digitonin three times. Bound fractions were eluted with 90 μL of 2X Laemmli buffer, split into 3 equal aliquots and loaded on SDS-PA gels.

***b) Immunoprecipitation in harsh condition***

Mitochondria crosslinked with arrested precursor was resuspended in 50  $\mu$ L of 50 mM Na-phosphate, 100 mM NaCl, 10% glycerol, 5 mM EDTA, pH 8.0 supplemented with 1% SDS and 2 mM PMSF and was lysed by shaking for 5 min at RT. Lysate was diluted with 950  $\mu$ L of 50 mM Na-phosphate, 100 mM NaCl, 10% glycerol, 5 mM EDTA, pH 8.0 containing 0.2% Triton X-100 and soluble fraction was separated by centrifuging at 124,500 x g for 20 min at 2°C. Binding of the proteins to PAS beads and washing of the beads was carried out as described in 2.4.4.3a. Elute was subjected to SDS-PAGE followed by analysis by autoradiography.

**2.4.4.4 Import of precursor proteins into isolated mitochondria**

For import of fluorophore-labelled presequence containing Ssc1 into isolated mitochondria, 200  $\mu$ g of isolated mitochondria were incubated at 25°C for 10 min in SI buffer (50 mM HEPES-KOH, 0.6 M sorbitol, 75 mM KCl, 10 mM Mg(Ac)<sub>2</sub>, 2 mM KH<sub>2</sub>PO<sub>4</sub>, 2.5 mM EDTA, 2.5 mM MnCl<sub>2</sub>, pH 7.2) with 0.5 mg/mL of BSA. This was followed by addition of 2.5 mM ATP, 3.3 mM NADH, 10 mM phosphocreatine, 0.1  $\mu$ g/ $\mu$ L creatine kinase and incubation at 25°C for 3 min. To this, 4  $\mu$ L of 3-15 nM fluorophore labelled Ssc1 diluted in 30 mM HEPES-KOH, pH 7.3, 7 M urea was added and import of protein was allowed to take place at 25°C for 10 min. For different batches of isolated mitochondria, different dilutions of labelled protein were tested such that single dually-labelled protein enters single mitochondria. To stop import, sample was diluted in 1 mL of ice cold SH buffer (20 mM HEPES-KOH, 0.6 M sorbitol, pH 7.2) and 35  $\mu$ g/mL of proteinase K (PK) was added to digest the non-imported material. PK digestion was carried out for 5 min on ice. Inhibition of PK was done by incubating samples in 0.67 mM PMSF for 5 min on ice. Mitochondria were centrifuged at 13,600 x g, 10 min, 4°C. Mitochondrial pellet was washed in 1 mL of SH buffer containing 3 mg/mL BSA. Mitochondria were resuspended in 20  $\mu$ L of SH buffer and were stored on ice until use. After importing protein into mitochondria in this way, mitochondria were used within 2-3 h for single molecule fluorescence analysis.

Import of <sup>35</sup>S-labelled precursor proteins into isolated mitochondria was done as described above with following modifications. Import reactions contained 1  $\mu$ L of radiolabelled lysate per 50  $\mu$ g mitochondria. Import was stopped by diluting the reactions into SH buffer containing 1  $\mu$ M valinomycin, followed by incubation with 45  $\mu$ g/mL PK

for 15 min on ice. PK was inhibited by addition of 0.9 mM PMSF and incubation for 5 min on ice. Re-isolated mitochondria were solubilized in 20  $\mu$ L of 2X Laemmli buffer, heated at 95°C for 5 min and loaded on SDS-PA gel.

#### **2.4.4.5 Blue Native PAGE (BN-PAGE)**

Mitochondria were lysed at 2 mg/mL in 20 mM Tris-Cl, 80 mM KCl, 10% glycerol, 2 mM PMSF, pH 8.0, with 1% digitonin for 15 min at 4°C on a rotating platform. Centrifugation was done at 124,500 x g for 25 min at 4°C to clarify the lysate. Supernatant was collected and to 40  $\mu$ L of supernatant, 2  $\mu$ L of 5% Coomassie Brilliant Blue-G was added. Samples were loaded on 4–16% Native PAGE Bis-Tris Gel (Life Technologies). Proteins from gel were transferred to PVDF membrane and were analysed by immunostaining.

#### **2.4.4.6 Estimation of membrane potential**

For estimation of membrane potential generation across inner membrane of isolated mitochondria, fluorescence of membrane potentiometric dye, DiSC<sub>3</sub>(5), was analysed. In a cuvette, 2 mM ATP, 2 mM NADH and 0.5  $\mu$ M DiSC<sub>3</sub>(5) in 2 mL of SI buffer (50 mM HEPES-KOH, 0.6 M sorbitol, 75 mM KCl, 10 mM Mg(Ac)<sub>2</sub>, 2 mM KH<sub>2</sub>PO<sub>4</sub>, 2.5 mM EDTA, 2.5 mM MnCl<sub>2</sub>, pH 7.2) was added. This was followed by addition of 90  $\mu$ g of isolated mitochondria. Membrane potential was dissipated by addition of 5  $\mu$ M valinomycin. Fluorescence was analysed in Fluorolog-3 (Horiba Scientific, Jobin Yvon Technologies). Measurements were carried out at excitation and emission wavelengths of 622 nm and 670 nm, respectively.

#### **2.4.4.7 Immobilization of mitochondria on cover slides**

For cleaning, cover slides were sonicated in HPLC-grade acetone for 20 min in a closed slide holder put into a sonication bath. Washing of the slides was done with dH<sub>2</sub>O. Slides were immersed in absolute ethanol for 20 min, washed with dH<sub>2</sub>O and dried. Slides were finally cleaned in Plasma Cleaner (Diener electronic) for 15 min. The clean slides were immersed in PEG-silane (6-9 PEG units) and biotin-PEG-silane (6 mg) in 50 mL toluene solution at 55°C, overnight. Next day, a rubber with hole was glued to the slide and the hole with slide at its bottom formed a chamber for adding samples. 0.2 mg/mL solution of streptavidin in PBS was added into the chamber and incubated for 15 min at RT. Non-

bound streptavidin was removed by three washes with PBS. About 20-200 nM biotinylated  $\alpha$ Tom22 or  $\alpha$ Porin in PBS was added and incubated for 15 min at RT. After removal of antibody solution, the surface was washed three times with PBS, followed by one wash with SI buffer. 200  $\mu$ g of mitochondria having labelled-Ssc1 resuspended in 20  $\mu$ L SH buffer was diluted in 100  $\mu$ L of SI buffer and was added into the well followed by incubation for 5 min at RT. Mitochondrial resuspension was pipetted out and the surface was washed with SI buffer thrice. Finally, 100  $\mu$ L of SI buffer was added and slide was immediately used for single molecule HiLo measurement. To energize mitochondria, SI buffer was supplemented with 8 mM ATP, 8 mM NADH, 20 mM phosphocreatine and 0.02  $\mu$ g/ $\mu$ L of creatine kinase. To deplete mitochondria of ATP, SI buffer was supplemented with 0.03 U/ $\mu$ L of apyrase and 20  $\mu$ M oligomycin.

#### **2.4.4.8 Single molecule HiLo measurements**

Single molecule HiLo measurement was done in a total internal reflection fluorescence (TIRF) microscopy setup as described previously (Heiss, 2011). Lasers of following wavelength were used to excite the sample: 491 nm, 532 nm and 647 nm. Detection of emitted light was carried out by two different cameras: green region camera and red region camera. Emission in green region by excitation from 491 nm was used for detection of mitochondria. Emission in green region and red region by excitation from 532 nm and 647 nm laser were used for detection of donor and acceptor, respectively. Analysis of the data was done using a MATLAB based program.

## **2.5 Methods in immunology**

### **2.5.1 Affinity purification of antibodies**

Purified proteins against which specific antibodies were to be isolated were coupled to CNBr-Sepharose beads as described in 2.4.3.2, with a modification that 5 mg of antigen protein were coupled per mL of beads. CNBr-Sepharose column with bound protein that was stored in 0.05%  $\text{NaN}_3$  solution at 4°C, was left at RT for 30 min and equilibrated with 10 mL of 10 mM Tris-Cl, pH 7.5. 6 mL antiserum was diluted in 24 mL of 10 mM Tris-Cl, pH 7.5 and was loaded on CNBr-Sepharose column under gravity flow. After binding, column was washed with 10 mL of 10 mM Tris-Cl, pH 7.5, followed by 10 mL of 10 mM Tris-Cl, 0.5 M NaCl, pH 7.5. Elution was done by passing 10 mL of solutions with different pH: 10 mM Na-citrate, pH 4.0, followed by 100 mM glycine-HCl, pH 2.5

and then by 100 mM Na<sub>2</sub>HPO<sub>4</sub>, pH 11.5. Elute was collected in 1 mL fractions. Neutralization was done immediately by addition of 200 µL of 1M Tris-Cl, pH 8.8, in case of Na-citrate and glycine-HCl and by 100 µL glycine, pH 2.2, in case of Na<sub>2</sub>HPO<sub>4</sub> solution. Eluted fractions were analysed for specificity by immunodecoration of mitochondrial lysate fractions run on SDS-PA gel followed by transfer on nitrocellulose membrane. Specific fractions were pooled, aliquoted and stored in -20°C until use.

### **2.5.2 Immunodecoration with specific antibodies**

Nitrocellulose membrane with protein transferred from SDS-PA gel, were incubated with 5% (w/v) solution of milk in TBS on a shaking platform for 30 min at RT. Membrane was incubated with primary antibody diluted 100-1000 fold in 5% milk in TBS for 3 h at RT or 16 h at 4°C on a shaking platform. Washing was done by shaking for 10 min each in TBS buffer, followed by TBS buffer containing 0.05% Triton X-100 and once again in TBS buffer, at RT. HRP labelled secondary antibody was diluted 1:10000 fold in 5% milk in TBS and membrane was incubated in it for 1-3 h at RT on a shaker. Membrane was washed sequentially in TBS buffer, TBS buffer with 0.05% Triton X-100 and TBS buffer, as described above. Washed membrane was treated with chemiluminescent peroxidase substrate prepared by mixing equal volumes of ECL1 (100 mM Tris-Cl, pH 8.5, 440 µg/mL luminol, 65 µg/mL p-coumaric acid) and ECL2 solutions (100 mM Tris-Cl, pH 8.5, 0.6% hydrogen peroxide) and the signals were detected by exposure to X-ray films.

### **2.5.3 Biotinylation of antibodies**

Buffer in which affinity purified antibodies were stored was exchanged to PBS using PD MiniTrap G-25. The antibody concentration was determined using by Nanodrop. 60-fold molar excess of N-Hydroxysuccinimidobiotin (EZ-Link NHS-Biotin from Thermo Scientific) solution in DMSO was added to the antibodies and the mixture was incubated on ice for 3 h. Removal of free biotin was done by passing the samples through PD MiniTrap G-25 column pre-equilibrated with PBS. Biotinylated antibody solution was stored in aliquots at -20°C until use.

## 3. Results

### 3.1 Role of Tim44 in communication of the translocation channel and the import motor of the TIM23 complex

Tim44 is one of the central subunits of the TIM23 complex that binds both the translocation channel and the import motor of the complex. All the protein-protein interactions of Tim44 have previously been mapped to its N-terminal domain (residues



**Figure 3.1: Schematic representation of domain structure of Tim44.** See text for details.

43-210) (Figure 3.1) (Schilke et al., 2012; Schiller et al., 2008). The only function assigned to the C-terminal domain (residues 211-431) has been an interaction with cardiolipin-containing membranes through helices A1 and A2 (residues 235-263) (Marom et al., 2009). Interestingly, on the level of primary sequence, the remaining part of the C-terminal domain (264-431), here referred to as C-core domain (Cc), is more highly conserved across eukaryotes than the N-terminal domain. Accordingly, here an assessment of the importance of the two domains of Tim44 for its function *in vivo* was carried out.

#### 3.1.1 The N-terminal domain of Tim44 extended to include the membrane-recruitment helices of the C-terminal domain is not sufficient to support the function of Tim44

If the N-terminal domain of Tim44 is responsible for all interactions of Tim44 with protein subunits of the TIM23 complex and the only function of the C-terminal domain is to recruit Tim44 to the inner membrane of mitochondria, then a version of Tim44 encompassing its N-terminal domain extended to include the A1 and A2 helices of the C-terminal domain should be sufficient to support the function of the full length Tim44. Tim44 (1-262) comprised the N-terminal domain and A1 and A2 helices from the C-terminal domain (Figure 3.1). Since Tim44 is an essential protein, rescue of the function

of full length Tim44 was assessed by determining the viability of yeast when Tim44 (1-262) was expressed as the only version of Tim44. To this end, Tim44 (1-262) was expressed under its endogenous promoter in a Tim44 shuffling strain. Tim44 shuffling strain is a haploid strain which has the chromosomal copy of *TIM44* replaced with a *HIS3*



**Figure 3.2: Lack of rescue of Tim44 function by Tim44 (1-262).** Tim44 (1-262) was expressed in Tim44 shuffling strain and its ability to support Tim44 function was analysed by plasmid shuffling on 5-FOA medium. Full length Tim44 and empty vector were used as controls.

cassette and the strain is made viable by expressing full length Tim44 from a *URA3* plasmid. *URA3* vector can be removed by selecting cells on 5-Fluoroorotic acid (5-FOA) containing plates.

Cells expressing Tim44 (1-262) were not viable on a medium containing 5-FOA (Figure 3.2). As expected, cells transformed with an empty vector were also not able to grow and the ones transformed with a plasmid encoding full length Tim44 under its endogenous promoter were viable. This suggests that Tim44 (1-262) cannot rescue the function of the full length Tim44. In addition, this result suggests that the Cc-domain of Tim44 has an essential function.

### **3.1.2. Two domains of Tim44 co-expressed *in trans* can support function of Tim44**

Could the two domains of Tim44 expressed *in trans* support the function of the full length protein? To test this possibility, Tim44 shuffling strain was co-transformed with a plasmid coding for the extended N-terminal domain of Tim44, Tim44(1-262), and a plasmid coding the C-terminal domain of Tim44, Tim44 (pre-210-431) (Figure 3.3). In addition, plasmids coding for each of the two domains were individually used for transformation. The empty vector and the one encoding for the full length Tim44 were used as negative and positive controls, respectively. When growth was analysed on

medium containing 5-FOA, neither of the two individual domains could rescue the function of the full length protein. Surprisingly, however, when the extended N-terminal

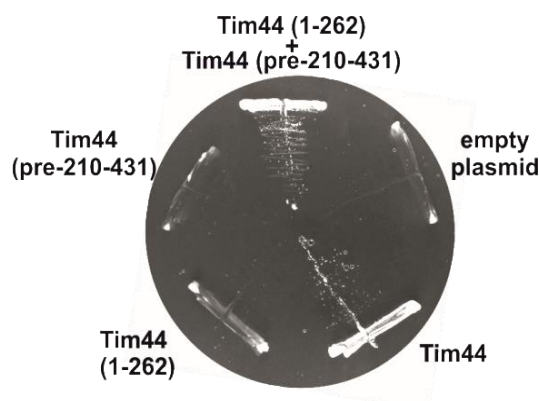


**Figure 3.3: Rescue of Tim44 function by its two domains expressed *in trans*.** Tim44 shuffling strain was co-transformed with Tim44 (1-262) and Tim44 (pre-210-431) and the viability of cells was analysed on 5-FOA. Individual Tim44 constructs, full length construct and empty vector were used as controls.

(1-262) and the C-terminal domain (pre-210-431) were co-expressed as separate polypeptides in yeast, cells were viable. This suggests that when two domains of Tim44

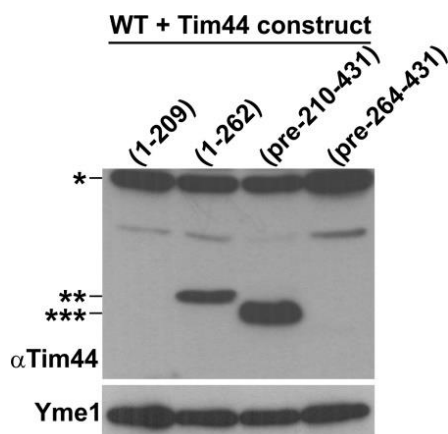


**Figure 3.4: Expression of individual domains of Tim44 in yeast.** Tim44 domain constructs with and without A1 and A2 helices were transformed in YPH499 wild type yeast strain. Cell lysates of transformed cells were analysed for expression of Tim44 domains by immunostaining. Protein bands were detected with antibody against full length Tim44, \*-full length, \*\*-N-terminal domain with A1 and A2 helices, \*\*\*-C-terminal domain

are expressed *in trans*, the function of the full length protein can be reconstituted. This strain will be referred to as N+C in the following text.

The rescue was dependent on the presence of A1 and A2 helices on both domains as their absence from either of the two domains, made the rescue not possible (data not shown). This could be due to the fact that only constructs that contain the two helices could be stably expressed in yeast (Figure 3.4).

To exclude the trivial possibility that N+C cells are viable due to a stable interaction

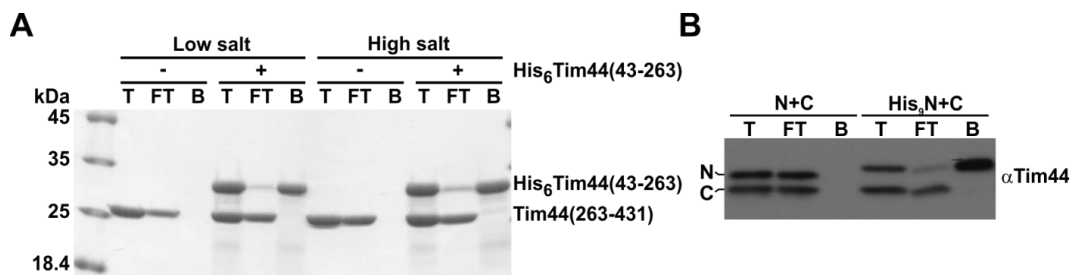


**Figure 3.5. Interaction between N-terminal and C-terminal domains of Tim44.** A) Recombinantly expressed and purified His<sub>6</sub>-Tim44(43-263) was preincubated with Tim44(263-431) in either high (300 mM NaCl) or low salt (50 mM NaCl) buffer, before Ni-NTA agarose beads were added. After washing steps, bound proteins were eluted and all the samples were analysed by SDS-PAGE and CBB staining. B) Isolated mitochondria from indicated cells were lysed in digitonin and incubated with Ni-NTA agarose beads. After washing steps, bound proteins were eluted and the samples analysed by SDS-PAGE and immunostaining. T-total, FT-flowthrough, B-bound.

between N and C domains, direct interaction between N-terminal and C-terminal domains was analysed. To this end, Ni-NTA pull down assays were performed with N-terminally His-tagged N-terminal domain and the non-tagged C-terminal domain expressed both in bacteria and in yeast (Figure 3.5). The recombinantly expressed and purified C core domain, Tim44 (263-431), was not co-isolated on Ni-NTA beads upon pre-incubation with the recombinantly expressed and purified His-tagged N-terminal domain, His<sub>6</sub>-Tim44 (43-263). Same observation was made irrespective whether the interaction was assayed in buffer with low or high salt concentration (Figure 3.5 A). Furthermore, mitochondria were isolated from N+C and His<sub>9</sub>-N+C cells. The latter expresses a His<sub>9</sub>-tagged version of the extended N-terminal domain. Mitochondria were solubilized with digitonin and the lysates incubated with Ni-NTA agarose beads (Figure 3.5 B). His<sub>9</sub>-tagged N-terminal domain bound efficiently to the beads, however, the C-terminal domain remained in flow-through fraction. Taken together, these results suggest that the two domains do not interact stably with each other.

Overall, the function of the full length Tim44 can be reconstituted from its two domains expressed *in trans* and the N+C strain can be used to obtain further insight into the function of Tim44 and its domains.

### 3.1.3 N+C strain is severely sick

Growth of N+C strain was tested and compared to the strain carrying the full length copy of Tim44 under its endogenous promoter (FL). The growth of FL and N+C strains were

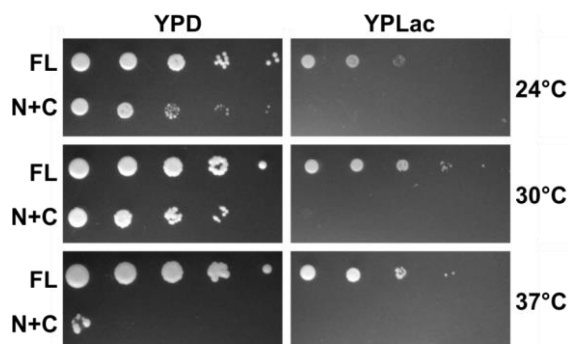


**Figure 3.6. Growth of N+C strain.** FL and N+C cells were grown overnight and serially diluted 10-fold. Growth was analysed on YPD and YPLac plates at indicated temperatures. YPD plates were incubated for 2 days and YPLac plates were kept for 3-4 days.

compared by serially diluting the cells and spotting them on plates containing fermentable (YPD) and non-fermentable (YPLac) carbon sources. The growth was assessed at three different temperatures: 24°C, 30°C and 37°C. N+C strain grew slowly, in comparison to FL, at 24°C and 30°C on YPD plates (Figure 3.6). It showed barely any growth at 37°C on YPD and none at all on YPLac plates at any of the temperatures tested. The severe growth defect of N+C cells at higher temperature and no growth on non-fermentable medium show that the strain has a severely impaired mitochondrial function. This further suggests that the function of Tim44 can be reconstituted from its individual domains only very poorly.

In order to check whether the co-expression of the two domains of Tim44 *in trans* affected expression of other proteins in mitochondria, a comparison between the protein profiles of mitochondria isolated from FL and N+C cells was done. To this end, mitochondrial lysates were separated by SDS-PAGE and analysed by immunostaining (Figure 3.7). Tim44 was immunostained with an antibody raised against the full length protein. In case of mitochondria isolated from N+C cells, no full length Tim44 was observed. Instead, two faster migrating bands were detected. When compared to the

migration pattern of individual domains (see Figure 3.4), the faster migrating band, of the two seen in N+C mitochondria, corresponded to the C-terminal domain and the slower corresponded to the extended N-terminal domain. Analysis of the expression of proteins

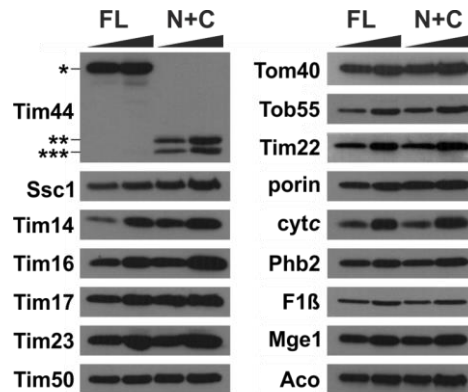


**Figure 3.7. Expression of mitochondrial proteins in N+C cells.** Mitochondria were isolated from FL and N+C cells that were grown in fermentable medium. Isolated mitochondria were lysed in 2X Laemmli buffer with  $\beta$ -mercaptoethanol, separated by SDS-PAGE and analysed by immunodecoration. \*-full length, \*\*-N-terminal domain with A1 and A2 helices, \*\*\*-C-terminal domain

localized in various subcompartments of mitochondria, such as outer membrane (Tom40, Tob55, porin), inner membrane (Tim14, Tim16, Tim17, Tim23, Tim50, Tim22, Phb2, F1 $\beta$ ), intermembrane space (cyt c) and matrix (Ssc1, Mge1, aconitase) revealed no major differences between FL and N+C mitochondria (Figure 3.7). Only Tim14, Tim16 and Ssc1, subunits of the import motor of the TIM complex, were slightly upregulated. This is likely a compensatory mechanism for a poorly functional Tim44.

### 3.1.4 Protein import in N+C strain is impaired

As Tim44 plays a crucial role in protein import, investigation of *in vivo* and *in vitro* protein import in N+C strain was carried out. *In vivo* protein import efficiency was assessed by analysing the cell lysates for accumulation of the precursor form of mitochondrial matrix targeted protein, Mdj1, which is imported by the TIM23 complex (Figure 3.8). In cells with impaired import via the TOM and TIM23 complexes, a precursor form of Mdj1, that is normally not detectable, accumulates (Waegemann et al., 2015). In FL cells grown at 24 or 30°C, only the mature form of Mdj1 was observed, demonstrating efficient import into mitochondrial matrix. In contrast, in N+C cells a slower migrating band corresponding to unprocessed precursor form of Mdj1 was

additionally detected. This accumulation of precursor suggests that import of proteins via TIM23 complex is defective in N+C cells.

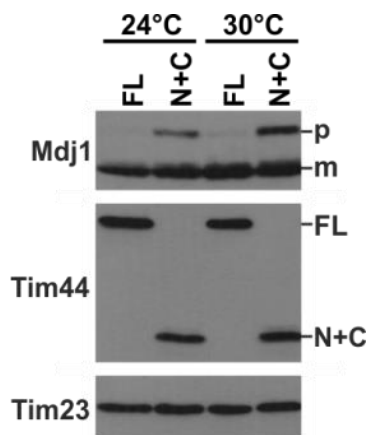


**Figure 3.8. Mdj1 precursor accumulation in N+C.** Indicated cells were grown in fermentable medium at 24°C and 30°C and cell lysates were separated by SDS-PAGE and analysed for the presence of Mdj1 precursor form by immunodecoration. p-precursor form, m-mature form.

The nature of mitochondrial protein import defect in N+C cells was analysed by *in vitro* import assays, which were carried out by importing <sup>35</sup>S-labelled precursor proteins into isolated mitochondria. The precursor proteins that were used in this study were targeted to different compartments of mitochondria and used different protein translocases for their import (Figure 3.9). Matrix-targeted precursors that require TIM23 complex, such as pF1 $\beta$ , pcytb<sub>2</sub>(1–167) $\Delta$ DHFR, and pSu9(1–69)DHFR, showed remarkably slower and less efficient import into mitochondria isolated from N+C cells when compared to FL. Similarly, import of a presequence-containing inner membrane protein Oxa1 was also reduced. Laterally inserted inner membrane proteins that require TIM23 complex, pDLD1 and pcytb<sub>2</sub>, were likewise imported less efficiently into N+C mitochondria. However, precursor whose insertion into the inner membrane is not dependent on the TIM23 complex, AAC, was imported with comparable efficiencies in N+C mitochondria as in FL. This suggests that the severe growth defect of N+C cells is due to the impaired protein import by the TIM23 complex.

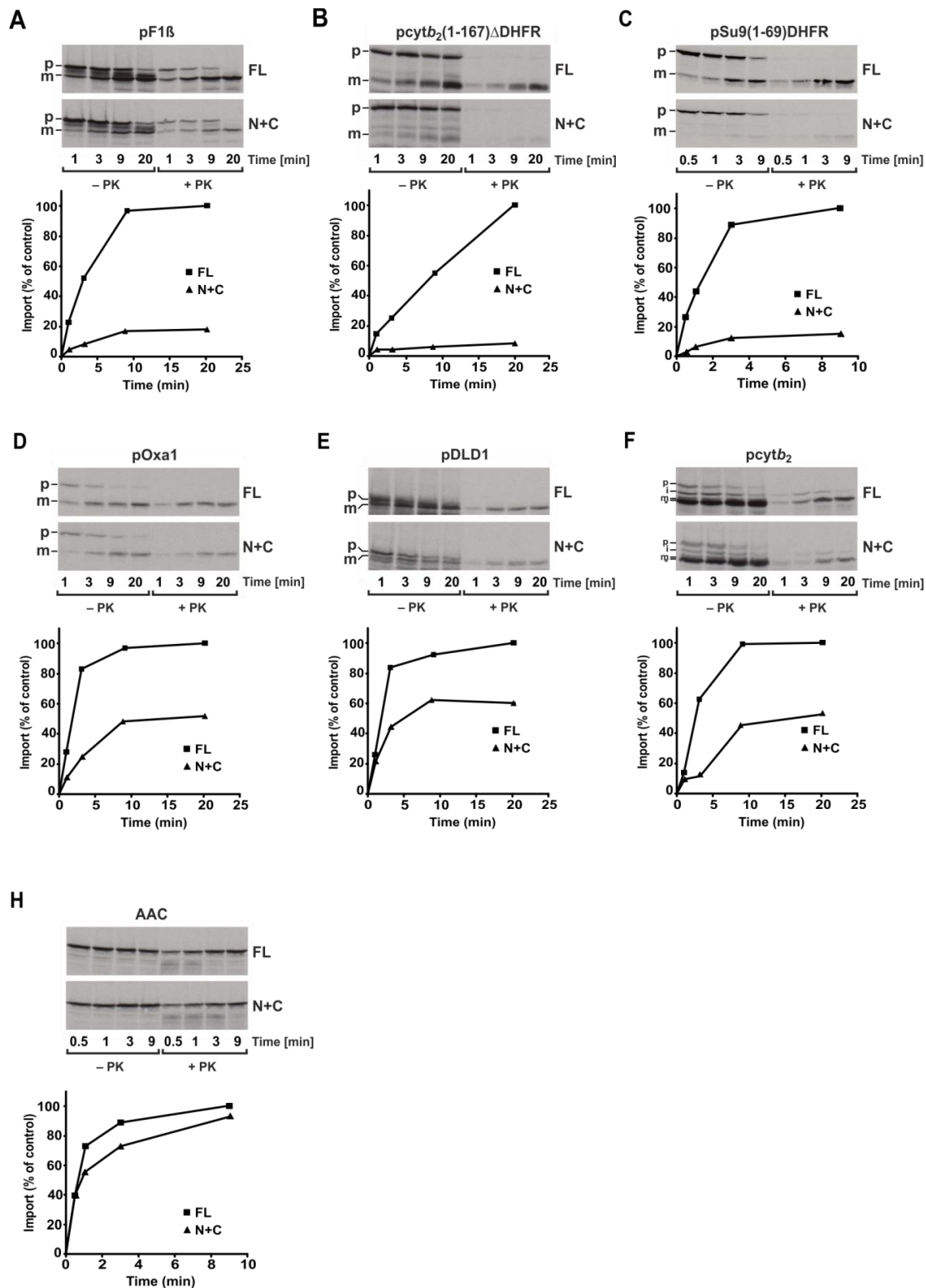


**Figure 3.9. *In vitro* protein import in N+C.** Isolated mitochondria were incubated with various types of <sup>35</sup>S-labelled precursor proteins in the presence of ATP. At the indicated time points, samples were taken out. Half of the samples were treated with proteinase K (PK) to remove excess precursor protein that was not imported and then PK is inhibited by addition of PMSF. Mitochondrial lysates were analysed by autoradiography. p-precursor form, i-intermediate form, m-mature form

A possibility of a general defect in mitochondrial function was tested by analyzing the ability of isolated mitochondria to generate membrane potential. To this end, a

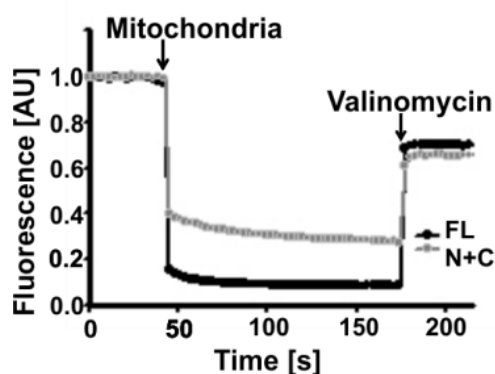


**Figure 3.10. Membrane potential in N+C and FL mitochondria.** Mitochondria were added to buffer containing ATP, NADH and membrane potentiometric dye, DiSC<sub>3</sub>(5). Mitochondria take up the dye in a membrane potential-dependent manner. To dissipate membrane potential, a K<sup>+</sup> transporter, valinomycin was added. Fluorescence was analysed at an excitation wavelength of 622 nm and emission wavelength of 670 nm.

potentiometric dye, DiSC<sub>3</sub>(5) (3,3'-dipropylthiadicarbocyanine iodide), was used and analysed for change in its fluorescence due to presence of mitochondrial membrane potential across inner membrane (Figure 3.10). The membrane potential in N+C mitochondria was slightly reduced compared to full length. This is in agreement with the involvement of Tim44 in import of a number of subunits of the respiratory chain complexes. However, N+C mitochondria are still able to generate membrane potential.

### 3.1.5 Assembly of TIM23 complex in N+C strain is normal

To investigate a possible cause of defective protein import by the TIM23 complex in N+C cells, the assembly of the TIM23 complex was analysed. To this end, digitonin-solubilized mitochondria isolated from FL and N+C were subjected to coimmunoprecipitation with affinity purified antibodies against channel subunits, Tim17 and Tim23, and import motor subunit, Tim16 (Figure 3.11). The immunoprecipitation with pre-immune serum was used as a negative control. Comparable co-immunoprecipitation profiles were obtained with mitochondria isolated from FL and N+C cells, suggesting that the assembly of the TIM23 complex is not affected in N+C cells. In addition, both N-terminal and C-terminal domain of Tim44 were recruited to the TIM23 complex in N+C cells.

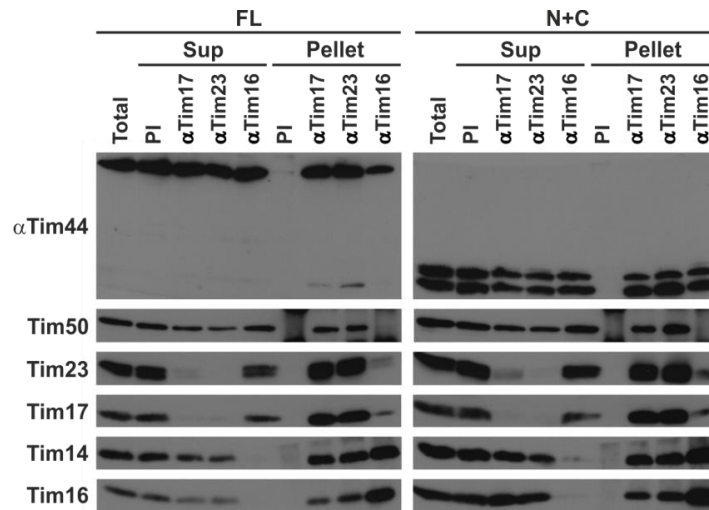


**Figure 3.11. Assembly of the TIM23 complex in N+C cells.** Mitochondria, solubilized in buffer containing digitonin, were subjected to co-immunoprecipitation with antibodies to Tim17, Tim23 and Tim16. Total (20%), supernatant (Sup, 20%) and bound (Pellet, 100%) fractions were analysed by SDS-PAGE followed by immunodecoration with the indicated antibodies. Immunoprecipitation with antibodies from preimmune serum (PI) was used as a negative control.

### 3.1.6 Conformation of TIM23 complex in N+C strain is altered

Despite the apparently proper assembly of the TIM23 complex in N+C cells, there is a possibility that the assembled complex is not in a proper conformation necessary for its function. The molecular environment of the various TIM23 subunits and thereby the conformation of the complex was analysed by chemical crosslinking in intact isolated mitochondria. The crosslinker-treated mitochondria were lysed and analysed by immunostaining (Figure 3.12). Tim14 and Tim16 crosslinking patterns looked comparable between N+C and FL mitochondria (Figure 3.12 A, B). The notable exceptions were the crosslinks of Tim14 and Tim16 to Tim44. As expected, they were not found in the corresponding region in case of N+C mitochondria. N- and C- domains are smaller in molecular weight compared to the full length protein and their crosslinks would migrate faster than those of the full length protein. In agreement with this, lower molecular weight crosslinks in N+C mitochondria were observed that were absent in FL. These new crosslinks may correspond to the crosslinks of Tim14 and Tim16 with N- or C-domains of Tim44. When crosslinking pattern of Tim23 was analysed, a stronger band

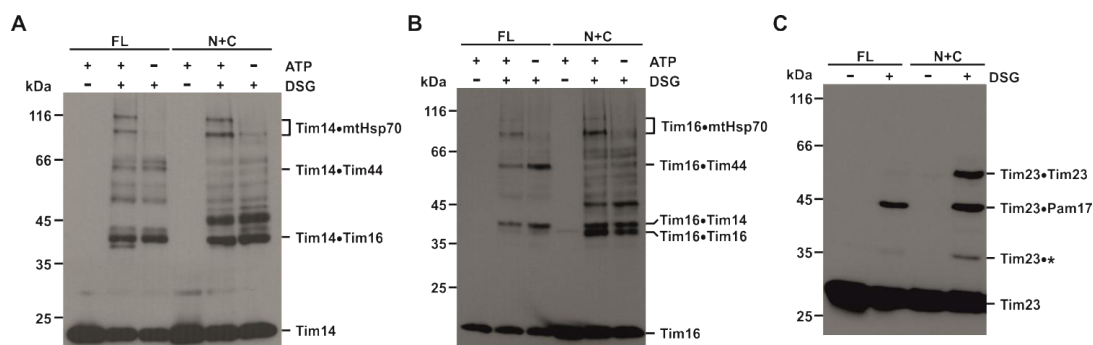


**Figure 3.12. Crosslinking patterns of TIM23 subunits in N+C mitochondria.** Isolated mitochondria were treated with a membrane permeable, primary amine specific chemical crosslinker, disuccinimidyl glutarate (DSG), in presence and absence of ATP. Mitochondria were lysed and run on SDS-PA gel. Crosslinks were analysed by immunostaining with antibodies for A) Tim14; B) Tim16; and C) Tim23.

corresponding to Tim23 dimer was observed in N+C mitochondria (Figure 3.12 C). This latter result is suggestive of a conformational alteration of the TIM23 complex.

For further confirmation of conformational alteration of the TIM23 complex, blue native PAGE analysis of digitonin-solubilized mitochondria was done (Figure 3.13). Tim14 and Tim16 were found in comparable complexes in FL and N+C mitochondria. However, in

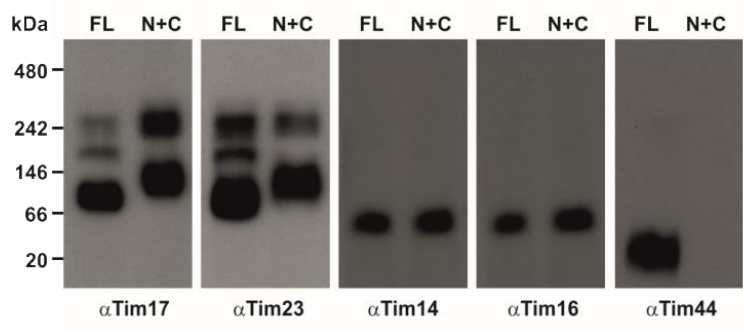


**Figure 3.13. Altered conformation of the TIM23 complex.** Mitochondria were solubilized in digitonin. Protein complexes were separated by BN-PAGE and analysed by immunostaining with the indicated antibodies.

case of Tim17 and Tim23, the 90 kDa complex migrated slower in N+C than in FL. Also, the higher molecular weight complexes, which contain additional subunits, were different in N+C and FL mitochondria. Since the only known subunits of the 90 kDa complex are Tim17 and Tim23, this suggests that the conformation of TIM23 translocation channel in N+C mitochondria is altered compared to FL.

Taken together, N+C strain shows poor growth compared to FL. This is due to the defect in TIM23 complex dependent protein import into mitochondria. Defect in protein import is likely caused by altered conformational flexibility of the TIM23 complex.

### 3.1.7 C-terminal domain of Tim44 interacts with precursor protein

Following the characterization of N+C, this strain was used to determine the domain of

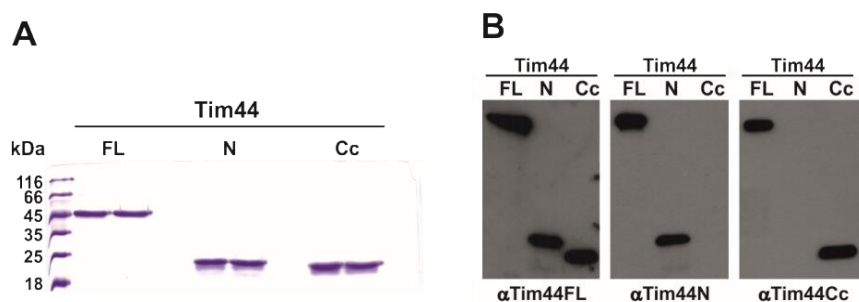


**Figure 3.14: Purification of specific antibodies against Tim44 domains.** A) Recombinantly expressed and purified Tim44 protein and its individual domains were run on SDS-PA gel and were detected by CBB staining. B) Purified Tim44 FL, N and Cc proteins were immobilized on CNBr-Sepharose beads. Rabbit serum having antibodies against full length Tim44 was passed through the CNBr-Sepharose columns and antibodies specific for Tim44 FL, N and Cc, were purified. Specificity of the purified antibodies was analysed by immunostaining each of the recombinantly expressed and purified protein with each of the purified antibodies. Tim44 FL (43-431), Tim44 N(43-209) and Tim44 Cc (264-431).

Tim44 interacting with the entering precursor. To this end, the full length, the N-terminal and the core of the C-terminal domain of Tim44 were recombinantly expressed and purified from bacteria [Tim44 (43-431), N (43-209) and Cc (264-431)] (Figure 3.14 A). The purified proteins were used for affinity purification of antibodies that specifically recognize the N- and Cc- domain of Tim44. The specificity of these affinity purified antibodies were analysed by immunostaining of the recombinant full length, N-terminal and Cc proteins with the purified antibodies (Figure 3.14 B). As a result, domain-specific Tim44 antibodies that do not cross-react with the other domain were obtained and were used for the experiment described below.

Previous studies showed that Tim44 is in close vicinity of precursors arrested across both TOM and TIM23 complexes (Berthold et al., 1995; Miyata et al., 2017; Schneider et al., 1994). To analyse which domain of Tim44 interacts with an entering precursor, N+C mitochondria were employed. To this end,  $^{35}\text{S}$ -labelled matrix targeted precursor protein pcytb<sub>2</sub>(1-167) $\Delta$ DHFR was arrested to form an intermediate complex spanning both TOM and TIM23 complexes in FL and N+C mitochondria (Figure 3.15). The mitochondria with the arrested precursor intermediate were then crosslinked with primary amine-specific crosslinker, disuccinimidyl suberate (DSS). After solubilisation of the samples in SDS-containing buffer to dissociate all noncovalent protein-protein interactions, the

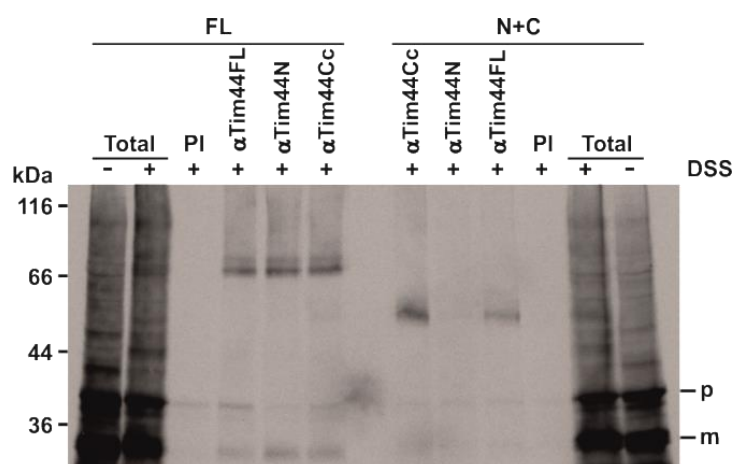


**Figure 3.15: Interaction of arrested precursor with Tim44 C-terminal domain.**  $^{35}\text{S}$ -labelled matrix targeted precursor protein pcytb<sub>2</sub>(1-167) $\Delta$ DHFR was arrested in mitochondria to form an intermediate spanning TOM and TIM23 complexes. Samples were crosslinked with disuccinimidyl suberate (DSS), non-covalent interactions were subsequently destroyed by solubilizing mitochondria in buffer containing SDS and immunoprecipitations with antibodies specific for FL (43-431), N (43-209) and Cc (264-431)-domain of Tim44 were done. The detection of the crosslinks between the arrested protein and Tim44 and its domains was done by autoradiography. p-precursor form; m-mature form.

crosslinking of the arrested precursor to Tim44 and its domains was analysed by immunoprecipitation with antibodies specific for each domain. Autoradiography of samples obtained from FL mitochondria showed that the crosslinks to the precursor can be immunoprecipitated with antibodies specific for each of the domains. Interestingly, with N+C mitochondria crosslinks of the precursor were only observed in case the immunoprecipitation was done with antibodies specific for full length Tim44 and with the

one to its Cc domain. This suggests that the entering precursor is in close proximity to the C-terminal domain of Tim44.

### 3.1.8 Interaction partners of N- and Cc- domain of Tim44 in the TIM23 complex

Previous studies have shown Tim44 interacts with Ssc1, Tim14/Tim16 and Tim23 (Schilke et al., 2012; Schiller et al., 2008; Ting et al., 2014). To evaluate the direct interaction partners of individual domains, recombinantly expressed and purified full

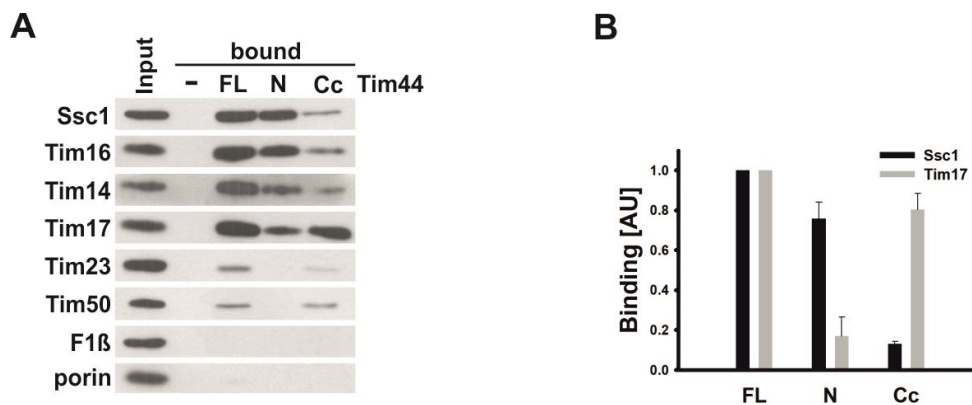


**Figure 3.16. Interaction between Tim44 and Tim17 through Cc-domain of Tim44.** A) Recombinantly expressed and purified Tim44 protein constructs were immobilized on CNBr-Sephrose beads. Mitochondria were solubilized in buffer containing Triton X-100 and incubated with the beads. Samples were analysed by SDS-PAGE and immunostaining. B) Quantification of band intensities of bound Ssc1 and Tim17 for comparison.

length, N-terminal and Cc domain of Tim44 were covalently linked to CNBr-Sephrose beads and incubated with mitochondrial lysates (Figure 3.16). Mitochondria were solubilized with Triton X-100 as it dissociates the TIM23 complex into individual subunits, except for the Tim14-Tim16 complex that remains stable, so that direct interactions of Tim44 and its domains could be assessed. In agreement with the previously published data, both full length and N-terminal domain of Tim44 showed interaction with Ssc1 and Tim14/Tim16 complex (Schilke et al., 2012; Schiller et al., 2008). Interestingly, the full length and the Cc domain showed a prominent binding with Tim17, suggesting that Tim44 also interacts with Tim17 and it does so through its Cc domain.

In conclusion, novel interacting partners of Tim44 Cc domain, precursor protein and Tim17, were determined in this study.

## 3.2 Characterization of yeast Tim44 P282Q mutation associated with cancer in humans

Findings described in section 3.1 suggest that the core of the C-terminal domain of Tim44 interacts with entering precursor and with Tim17. Previously, it has been reported that a point mutation P308Q in the Cc-domain of human Tim44 is associated with oncogenic thyroid carcinoma (Bonora et al., 2006). This residue is highly conserved in Tim44 found across various species (Handa et al., 2007). Therefore, to decipher whether this mutation affects the interplay of Tim44 with its interactors, corresponding mutant version Tim44 P282Q in yeast was analysed.

### 3.2.1 Tim44 P282Q mutation does not affect growth in yeast

First whether yeast cells expressing Tim44 P282Q in *TIM44* deletion background are viable or not was tested. Tim44 shuffling strain was transformed with Tim44 P282Q

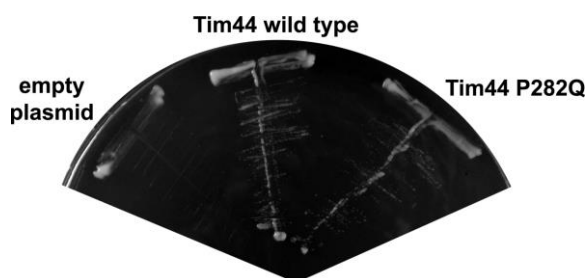


**Figure 3.17. Rescue of Tim44 function by P282Q mutant.** Tim44 shuffling strain was transformed with Tim44 constructs in pRS314 vector. Selection was done by plasmid shuffling on selective medium containing 5-FOA. Plate was incubated at 30°C for 3 days.

expressed under endogenous promoter and the functionality of the mutant Tim44 was assessed on a 5-FOA plate (Figure 3.17). Cells transformed with empty vector did not grow on 5-FOA plate whereas those transformed with a wild type copy of Tim44 did. Interestingly, cells expressing Tim44 P282Q were also viable suggesting that the mutant version is able to support the function of Tim44.

To analyse its functionality in more detail, mutant and wild type cells were grown at three different temperatures on plates containing fermentable and non-fermentable medium

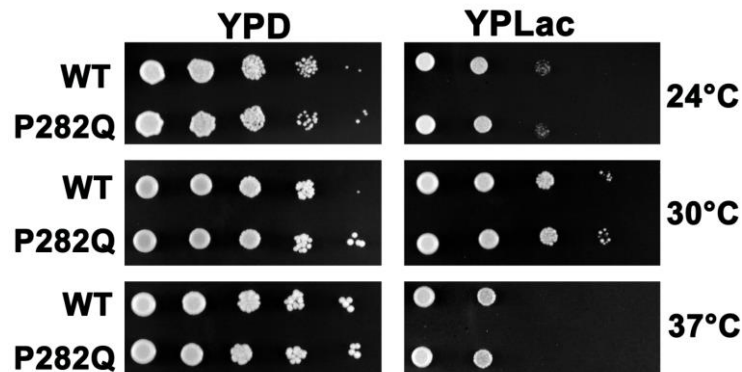


**Figure 3.18. Growth of Tim44 P282Q.** Yeast cells were grown on YPD medium overnight at 30°C. On the next day, cells were harvested, a serial dilution of 10-fold was made and cells were spotted on plates with either fermentable (YPD) or non-fermentable (YPLac) carbon source. Plates were incubated at 24°C, 30°C and 37°C. YPD plates were incubated for 2 days and YPLac for 3-4 days.

(Figure 3.18). Cells expressing Tim44 P282Q did not show any obvious difference in growth at any of the temperatures tested when compared to the wild type. This indicates that the mutation does not have any major effect on Tim44 function.

### 3.2.2 TIM23 complex function in Tim44 P282Q mutants is not compromised

The effect of P282Q mutation in Tim44 on TIM23 complex was investigated by analysis of the expression of TIM23 complex subunits. To this end, isolated mitochondria from mutant and wild type strains were lysed and immunostained with antibodies specific for TIM23 complex subunits (Figure 3.19). Protein levels of TIM23 complex subunits were indistinguishable between the wild type and P282Q mutant.

Further, assembly of TIM23 complex in Tim44 P282Q mutant was analysed by co-immunoprecipitation. To this end, digitonin-solubilized mitochondria were subjected to coimmunoprecipitation with antibodies specific for channel subunit, Tim17, and for import motor subunit, Tim16 (Figure 3.20). No obvious difference was found in coimmunoprecipitation profiles of TIM23 complex in wild type and Tim44 P282Q mitochondria. This suggests that P282Q mutation in Tim44 do not have any major effect on the assembly of the TIM23 complex.

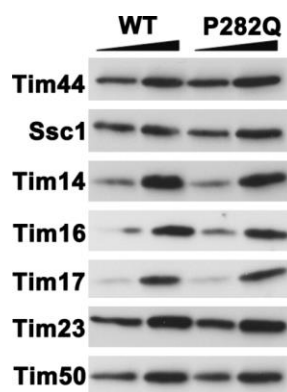


**Figure 3.19. Expression of TIM23 complex subunits in Tim44 P282Q mutant.** Mitochondria were isolated from yeast strains that were grown in lactate medium at 30°C. 25 µg and 50 µg of isolated mitochondria were lysed in Laemmli buffer and analysed by immunostaining.

To analyse if the mutation has an effect on the protein import carried out by TIM23 complex, *in vivo* protein import in the mutant and wild type strain was analysed. Cells

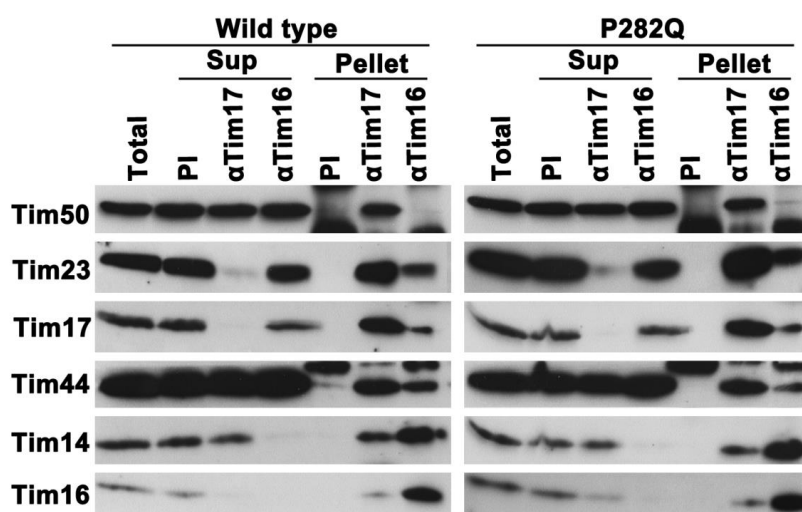


**Figure 3.20. Assembly of TIM23 complex in Tim44 P282Q mutant.** Isolated mitochondria were solubilized with digitonin and subjected to precipitation with Tim17 and Tim16 antibodies prebound to Protein A-Sepharose. Preimmune serum (PI) was used as negative control. Total (20%), bound (Pellet, 100%) and unbound (Sup, 20%) fractions were analysed by SDS-PAGE and immunodecoration.

were grown in fermenting medium at different temperatures and their lysates were

analysed for accumulation of the precursor form of Mdj1 and of the long isoform of Mgm1. Mdj1 is imported into mitochondrial matrix in a presequence-dependent manner through the TIM23 complex (Waegemann et al., 2015). Defects in the TIM23 complex lead to accumulation of a slower migrating precursor form of Mdj1. Mgm1, on the other hand, exists as a long and a short isoform. The two isoforms are present within mitochondria in a certain ratio. Formation of the short isoform depends on the ATP-dependent activity of the import motor of the TIM23 complex and the defects in this process lead to accumulation of the long isoform (Herlan et al., 2003). No apparent difference in accumulation of the precursor form of Mdj1 or the long isoform of Mgm1

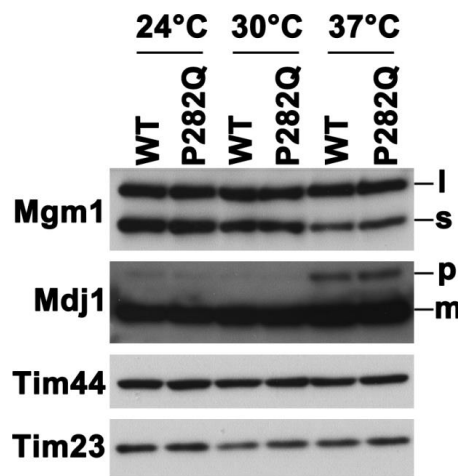


**Figure 3.21. *In vivo* import of TIM23 complex dependent proteins in Tim44 P282Q mutant.** Yeast cells were grown in YPD medium overnight at 24°C, 30°C and 37°C. Cells were lysed and cell lysate was analysed by immunodecoration.

was found between Tim44 P282Q and wild type cells (Figure 3.21). This is in agreement with the observation that no growth defect was observed in mutant strain. Taken together, this mutation does not affect the mitochondrial function in any major way, at least in yeast.

### 3.2.3 Stability of Tim44 with P282Q mutation

Though no obvious effect of the P282Q mutation in Tim44 was observed in yeast, the corresponding P308Q mutation predisposes human carriers to oncocytic thyroid carcinoma (Bonora et al., 2006). Hence, to further analyse the effect of this mutation on Tim44, thermal shift assay was employed to determine stability of the wild type and mutant proteins. Thermal shift assay with recombinantly expressed and purified wild type

and P282Q mutant version of Tim44 was carried out in buffers with varying pH and salt concentrations (Figure 3.22 and Table 3.1). In general, Tim44 was more stable at higher salt concentrations as melting temperatures ( $T_m$ ) of unfolding of the protein increased with increasing salt concentration in the buffer.

**Table 3.1. Melting temperature of Tim44 and Tim44 P282Q by thermal shift assay**

	Buffer composition	Tim44		Tim44 P282Q	
		avg	std dev	avg	std dev
		$T_m$ (°C)		$T_m$ (°C)	
A	20mM HEPES/NaOH, 50mM NaCl, pH 7.1	51.4	0.409447	47.4	0.459226
B	20mM HEPES/NaOH, 150mM NaCl, pH 7.1	54.2	0.192325	50.3	0.468808
C	20mM HEPES/NaOH, 450mM NaCl, pH 7.1	58.9	0.603453	55.0	0.494627
D	20mM NaH <sub>2</sub> PO <sub>4</sub> /Na <sub>2</sub> HPO <sub>4</sub> , 50mM NaCl, pH 8.0	50.0	0.237253	46.5	0.316776
E	20mM NaH <sub>2</sub> PO <sub>4</sub> /Na <sub>2</sub> HPO <sub>4</sub> , 150mM NaCl, pH 8.0	52.4	0.314854	49.2	0.491415
F	20mM NaH <sub>2</sub> PO <sub>4</sub> /Na <sub>2</sub> HPO <sub>4</sub> , 450mM NaCl, pH 8.0	56.0	0.134257	52.5	0.518612

Interestingly, the melting temperature of the wild type protein was higher, in every condition tested, than that of the mutant. The difference between the two was ranging

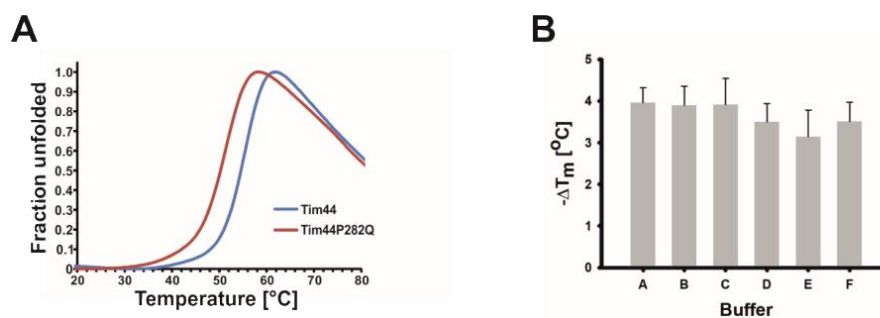


**Figure 3.22. Stability of Tim44 P282Q mutant by thermal shift assay.** A) Representative melting curves in buffer A (described in table 3.1). 6.2  $\mu$ g of recombinantly expressed and purified proteins were mixed with 5X SYPRO Orange dye in different buffers in a 96 well plate and fluorescence of the dye was measured while heating sample from 5°C to 95°C. Excitation was done at 485 nm and emission was measured at 530 nm. B) Plot showing differences in temperature of melting ( $\Delta T_m$ ) between purified Tim44 and Tim44 P282Q in different buffers (see Table 3.1 for buffer composition). Negative symbol denotes that the  $T_m$  of mutant protein is decreased compared to wild type.

from 3.5 to 4°C (Figure 3.22 and Table 3.1). This suggests that the P282Q mutation affects stability of Tim44.

Taken together, P282Q mutation in Tim44 does not have any major effect on yeast growth or function of the TIM23 complex. However, the recombinantly expressed and purified mutant protein is less stable than the wild type protein. This lower stability of the protein may be the reason behind a tissue-specific clinical manifestation of the corresponding mutation in human Tim44, P308Q, in thyroid cancer.

### **3.3 Residues that are involved in interaction of Tim44 C-terminal domain with TIM23 complex subunits**

Results presented here so far show that the core of the C-terminal domain of Tim44 interacts with entering precursor and Tim17. In this part of the project, the focus was to identify residues that play a role in interaction between Tim44 and Tim17. In addition, mapping of the surface of C-terminal domain of Tim44 was done to identify residues that are involved in interaction with Tim17 and other subunits of TIM23 complex.

#### **3.3.1 Site-specific photocrosslinking between Tim44 and Tim17**

Tim17 contains four predicted transmembrane helices spanning the inner membrane of mitochondria. Loops facing the matrix side of mitochondrial inner membrane connect TM1 with TM2 and TM3 with TM4. Previous studies found no indication for an interaction of the loop between TM1 and TM2 with Tim44 (Ting et al., 2014). Therefore, analysis of the loop between TM3 and TM4 for a potential interaction with Tim44 was done here. In this loop, a mutation of a highly conserved R105 led to severe growth defect in yeast (Demishtein-Zohary et al., 2017). This suggests that R105 is crucial for functioning of TIM23 complex and may have a role in interaction between Tim17 and Tim44.

To decipher the role of R105 in Tim17 and Tim44 interaction, previously established method of site-specific photocrosslinking using Bpa (p-benzoyl-L-phenylalanine) was employed (Chen et al., 2007). Bpa is an unnatural amino acid that can be incorporated at specific sites on protein of interest by suppressing the TAG STOP codon, introduced at that position, with a tRNA optimized to deliver Bpa that is then incorporated into the polypeptide chain at TAG sites. Bpa incorporated in protein of interest reacts with neighbouring C-H bond upon illumination with UV light. To investigate Tim44-Tim17

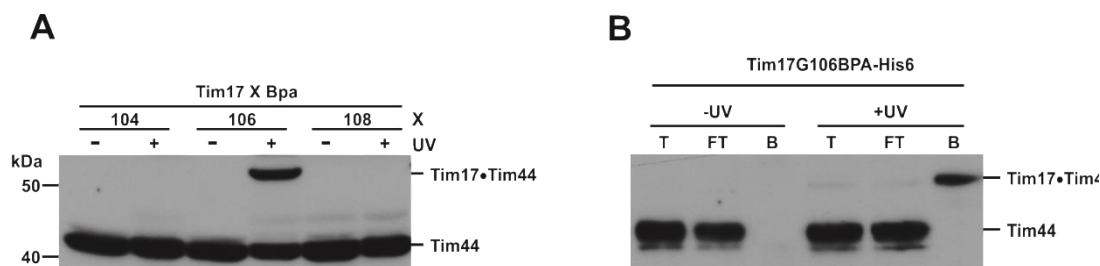


**Figure 3.23. Tim44 binds to loop between TM3 and TM4 of Tim17.** A) Yeast cells expressing a His-tagged version of Tim17-His<sub>6</sub> and Bpa introduced in the loop between TM3 and TM4 were grown in SD medium with 1 mM Bpa at 30°C. Cells were harvested and illuminated with UV light for 1 h, where indicated. Cell lysates were analysed by SDS-PAGE and immunostaining. B) Indicated cells were treated as in A, but were additionally incubated with Ni-NTA agarose beads before analysis. Total, bound and unbound fractions were analysed by SDS-PAGE and immunostaining. T-total (3.5%), FT-flow through (3.5%), B-bound (100%)

interaction, Bpa was introduced at various positions near R105 in Tim17 and cells were exposed to UV light. The lysates of cells having Bpa in positions near R105, V104Bpa, G106Bpa and W108Bpa, were analysed for crosslinking with Tim44 (Figure 3.23 A). Upon immunostaining with antibodies to Tim44, position 106Bpa gave an additional slower migrating band in a UV exposure dependent manner. Positions 104Bpa and 108Bpa, on the other hand, showed no additional bands. When lysates of cells expressing Tim17-His<sub>6</sub> 106Bpa were incubated with Ni-NTA agarose beads prior to the SDS-PAGE analysis, the higher molecular weight band was specifically retained on the beads showing that it corresponds to a crosslink between Tim44 and Tim17 (Figure 3.23 B). This confirms that the interaction between Tim44 and Tim17 occurs also *in vivo* and that the loop between TM3 and TM4 of Tim17 and residue R105 in particular play an important role in the process.

### 3.3.2 Functional analysis of conserved residues on the surface of C-terminal domain of Tim44

In order to determine the residues of Cc domain that are important for the function of Tim44 and may play a role in its interaction with Tim17, the previously determined structure of the C-terminal domain of Tim44 was used to identify surface exposed conserved residues on Tim44 Cc domain. The conserved residues in the core of protein

structure are involved in maintenance of the overall structure of the protein. On the other hand, surface exposed residues are typically conserved only if they are involved in interaction with other proteins or molecules (Dickerson, 1971). As positively charged R105 was shown to be involved in the interaction from the Tim17 side, a particular focus was given to the conserved negatively charged residues in Tim44. A surface conservation model of the C-terminal domain of Tim44 (Josyula et al., 2006) was generated using an online tool, ConSurf (Glaser et al., 2003; Landau et al., 2005). Based on the result obtained from ConSurf web tool, following residues were chosen for further analysis and were mutated to alanine- R294, E300, D345, Q372 and I393 (Figure 3.24). In addition, due to spatial proximity of D345, Q372 and I393 with each other in Tim44 C-terminal

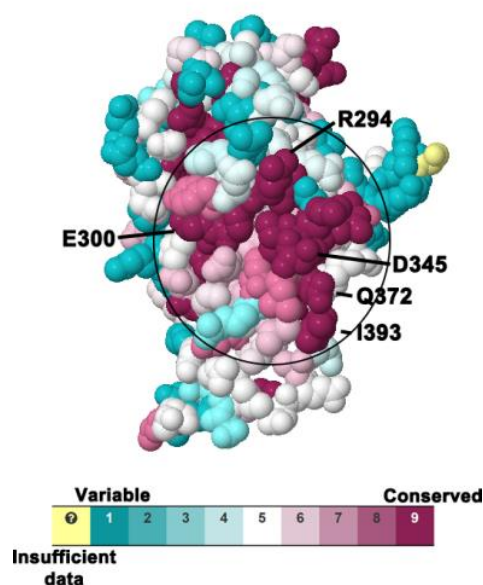


**Figure 3.24. Surface exposed conserved residues of Tim44 C-terminal domain.**

Conservation of Tim44 C-terminal domain (PDB ID: 2FXT) residues as given by ConSurf webtool. Encircled patch of conserved residues shows potential interaction surface where residues that were mutated for the study are shown.

domain crystal structure, these residues were also analysed in combination to give double (D345, Q372) and triple (D345, Q372, I393) alanine mutants.

Plasmids encoding the mutant versions of Tim44 were transformed into the Tim44 shuffling strain and the ability of the respective mutants to support function of Tim44 was assayed on 5-FOA plates upon removal of the wild type copy of Tim44 (Figure 3.25 A). The double mutant (D345A, Q372A) and the triple mutant (D345A, Q372A, I393A) were not viable, suggesting that they could not rescue the function of the wild type Tim44. The

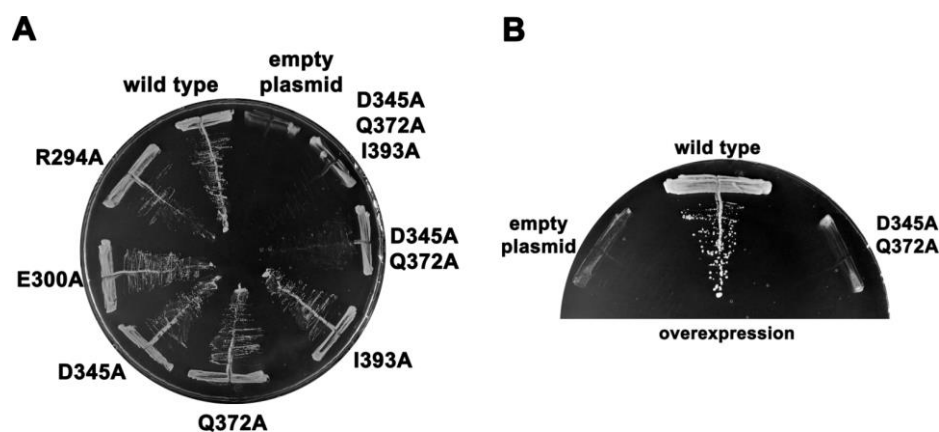


**Figure 3.25. Mutational analysis of surface exposed conserved residues of Tim44 C-terminal domain.** A) Tim44 shuffling strain was transformed with pRS314 plasmids encoding Tim44 mutants under endogenous promoter. Selection was done on 5-FOA plate incubated at 30°C for 3 days. B) Tim44 mutant under overexpression GPD promoter was analysed as in A.

ability of Tim44 (D345A, Q372A) to support growth of yeast cells was additionally analysed under overexpression conditions as these two positions are close to each other in the structure. However, even when expressed under an overexpression promoter, Tim44 (D345A, Q372A) could not rescue the function of wild type Tim44 (Figure 3.25 B). This indicates that residues D345 and Q372 play an important role in Tim44 function.

Growth of single Tim44 mutants that were viable (Figure 3.25 A) was further analysed on fermentable (YPD) and non-fermentable (YPLac) media at different temperatures (Figure 3.26). On fermentable medium, none of the mutants showed obvious growth defects at any of the temperatures tested, except for *tim44*<sup>D345A</sup>, which grew slightly slower than wild type at 37°C. On non-fermentable medium, *tim44*<sup>D345A</sup> showed slower growth at 30°C and was severely affected in growth at higher temperature, 37°C. *tim44*<sup>Q372A</sup> and *tim44*<sup>I393A</sup> also showed severe growth defects at 37°C. Taken together, these results show that residues D345 and Q372 are important for proper function of Tim44 and the corresponding mutants were analysed further.

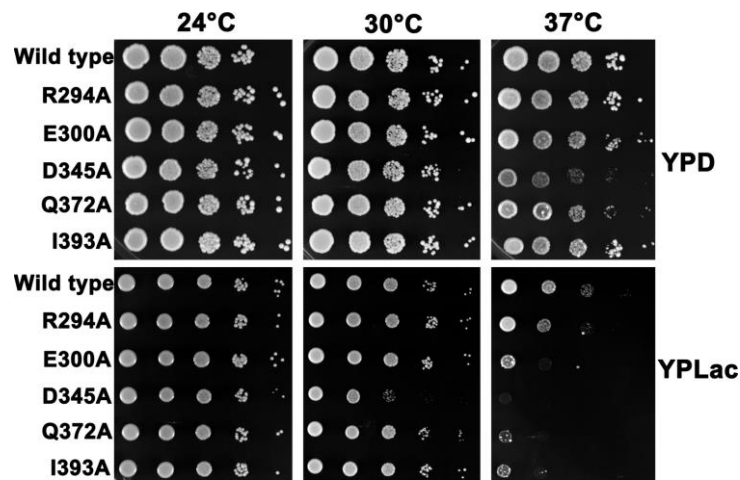


**Figure 3.26. Growth of Tim44 mutants.** Yeast cells were grown in YPD medium overnight at 30°C, serial 10-fold dilutions were prepared and spotted on YPD and YPLac plates. The plates were incubated at 24°C, 30°C and 37°C. YPD plates were incubated for 2 days and YPLac were kept at respective temperatures for 3-5 days.

**a) Functional analysis of *tim44*<sup>D345A</sup>**

To determine whether the growth defect of *tim44*<sup>D345A</sup> could be explained by an impaired function of the TIM23 complex, *in vivo* TIM23-dependent protein import was analysed. Wild type and *tim44*<sup>D345A</sup> cells were grown at three different temperatures, cell lysates were prepared and analysed for accumulation of the long isoform of Mgm1 (Figure 3.27). In *tim44*<sup>D345A</sup> cells, an increased accumulation of the long form of Mgm1 was observed, especially at 37°C, suggesting that the activity of the import motor of the TIM23 complex

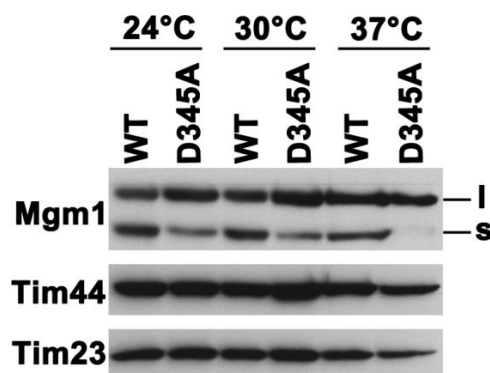


**Figure 3.27. In vivo import in *tim44*<sup>D345A</sup>.** Yeast cells were grown in YPD at 24°C, 30°C and 37°C. Cell lysates were analysed by SDS-PAGE and immunodecoration. l- long isoform, s- short isoform

is indeed affected and providing a possible explanation for the growth defect.

The impaired import was not due to the instability of mutant Tim44 or any other subunit of the TIM23 complex, as their levels were indistinguishable between mitochondria isolated from wild type and *tim44<sup>D345A</sup>* cells (Figure 3.28).

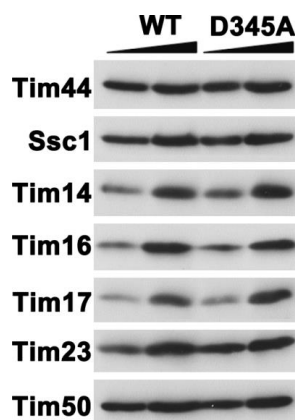


**Figure 3.28. Levels of TIM23 complex subunits in *tim44<sup>D345A</sup>*.** Yeast cells were grown in lactate medium at 24°C and mitochondria were isolated. Mitochondrial lysates were analysed by SDS-PAGE and immunodecoration.

In order to determine if the assembly of TIM23 complex is affected in *tim44<sup>D345A</sup>*, isolated mitochondria were solubilized and co-immunoprecipitated with antibodies specific for a

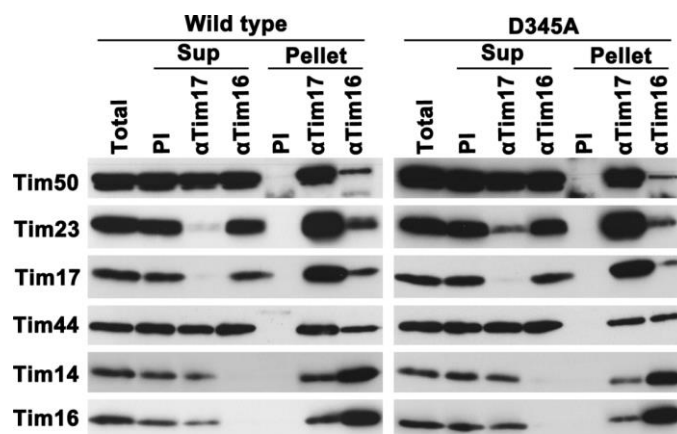


**Figure 3.29. Assembly of the TIM23 complex in *tim44<sup>D345A</sup>*.** Isolated mitochondria were pre-incubated at 37°C, solubilized with 1% digitonin and co-immunoprecipitated with Tim17 and Tim16 antibodies prebound to Protein A-Sepharose beads. Antibodies from preimmune serum (PI) were used as a negative control. Total (20%), supernatant (Sup, 20%) and bound (Pellet, 100%) fractions were analysed by SDS-PAGE and immunostaining with indicated antibodies.

channel subunit, Tim17, and for an import motor subunit, Tim16. Since *tim44<sup>D345A</sup>*

showed a stronger growth defect at 37°C, isolated mitochondria were pre-incubated at 37°C prior to the solubilisation. Comparison of the bound fractions revealed reduced co-precipitation of Tim44, Tim14 and Tim16 with Tim17 antibodies in *tim44<sup>D345A</sup>* mitochondria (Figure 3.29). Similarly, lower levels of Tim17, Tim23 and Tim50 were observed in coimmunoprecipitates of Tim16 antibody. Hence, introduction of D345A mutation in Tim44 impairs the interaction between Tim44 and the channel subunits of TIM23 complex and affects the proper assembly of the complex.

In summary, D345 residue in Tim44 plays an important role in TIM23 complex function and affects the interaction between the channel and import motor subunits.

**b) Functional analysis of *tim44<sup>Q372A</sup>***

A similar analysis was done with *tim44<sup>Q372A</sup>*. Mitochondria were isolated and levels of the

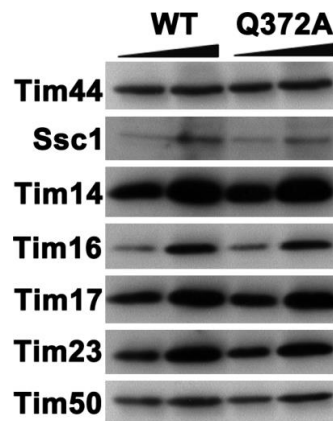


**Figure 3.30. Levels of TIM23 complex subunits in *tim44<sup>Q372A</sup>*.** Mitochondria were isolated from yeast cells grown in lactate medium at 24°C. Isolated mitochondria were lysed in Laemmli buffer and analysed by SDS-PAGE and immunodecoration.

TIM23 complex subunits were analysed (Figure 3.30). The levels of Tim44 and other subunits of the TIM23 complex were comparable in wild type and *tim44<sup>Q372A</sup>*.

Assembly of the TIM23 complex was further analysed by co-immunoprecipitation (Figure 3.31). As with mitochondria isolated from *tim44<sup>D345A</sup>* cells, interaction between the translocation channel and the import motor was reduced in *tim44<sup>Q372A</sup>*. This suggests that Q372 residue is important for Tim44-mediated assembly of the TIM23 complex.

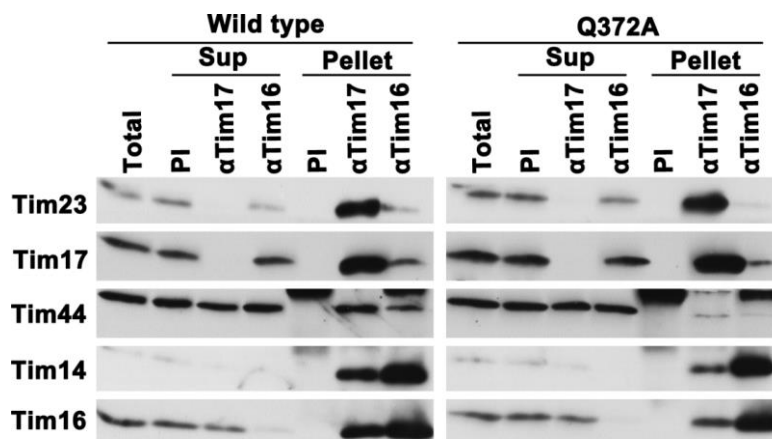


**Figure 3.31. Assembly of the TIM23 complex in *tim44*<sup>Q372A</sup>.** Mitochondria were pre-incubated at 37°C and lysates prepared in 1% digitonin. Samples were analysed as in Figure 3.29.

To summarize, both D345 and Q372 in C-terminal domain of Tim44 are highly conserved surface exposed residues and are important for assembly of the TIM23 complex. However, whether these residues represent a direct binding site for Tim17 or some other TIM23 complex subunit or have a role in maintenance of the structural integrity of Tim44 remains unclear.

### *c) Functional analysis of Tim44 double and triple alanine mutants*

Since the double and triple mutants of Tim44- *tim44*<sup>D345A, Q372A</sup> and *tim44*<sup>D345A, Q372A, I393A</sup> were non-viable, determination of whether these residues form the direct binding site for interaction between Tim44 and Tim17 was done by *in vitro* pull down assay (Figure 3.32). To this end, mitochondrial lysate prepared in Triton X-100 was allowed to pass through the beads that had purified Tim44 (D345A, Q372A) and Tim44 (D345A, Q372A, I393A) immobilized on it. TIM23 complex dissociates into individual subunits upon solubilisation of mitochondria with Triton X-100 and as a result direct one-on-one interactions between Tim44 mutant and TIM23 complex subunits can be analysed in this way. When bound fractions from wild type and mutant proteins were compared, no apparent difference in binding of any subunit including Tim17 was observed. This suggests that even though D345 and Q372 are crucial for interaction of Tim44 with the channel components of TIM23 complex, these residues do not appear to play a direct role in Tim44-Tim17 interaction.

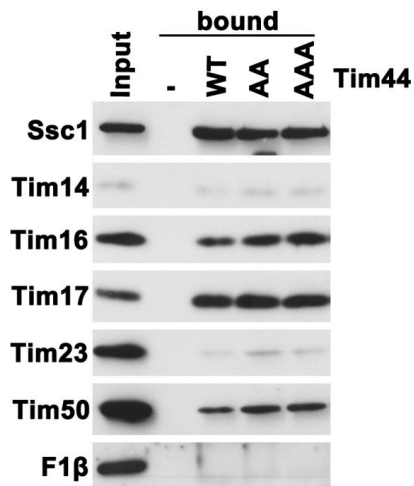


**Figure 3.32. Interaction of Tim44 double and triple mutant with Tim17 through *in vitro* pull-down assay.** Recombinantly expressed and purified Tim44 mutant proteins were immobilized on CNBr-Sepharose beads. D273-10B mitochondria solubilized in buffer containing Triton X-100 as described for Figure 3.16. Tim44 constructs used were as follows: WT- Tim44 (43-431); AA- Tim44 (43-431) (D345A, Q372A); AAA- Tim44 (43-431) (D345A, Q372A, I393A)

### 3.3.3 Site-specific photocrosslinking of C-terminal domain of Tim44

As the region on the C-terminal domain of Tim44 that was initially chosen for the

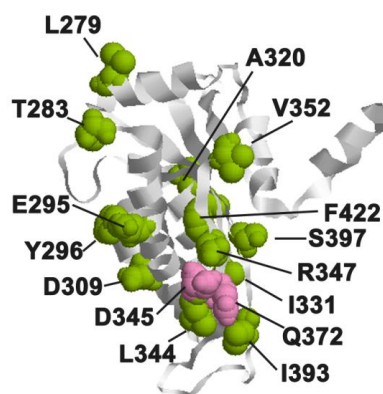


**Figure 3.33. Tim44 C-terminal domain surface positions analysed for Bpa-crosslinking with Tim17.** D345 and Q372 are shown in pink. Remaining residues in green were analysed for Bpa-photocrosslinks between Tim44 and Tim17.

analysis did not give any positive evidence for a direct interaction with Tim17, a broader mapping of the surface of the C-terminal domain was done. To this end, Bpa was introduced at various positions (Figure 3.33) on the conserved interfaces of Tim44 *in vivo*, cells were exposed to UV light and samples were analysed for slower migrating crosslinked products. Amongst the positions that were analysed for Tim44 crosslinks, some are shown here and these gave high molecular weight crosslinked product in presence of UV illumination (Figure 3.34 A, B). However, none of those corresponded to Tim44-Tim17 crosslink. As a result, no positive evidence for D345 and Q372 in Tim44 to have a role in direct binding with Tim17 could be obtained.

In addition, during the course of this work a report suggested that Tim44 Cc-domain

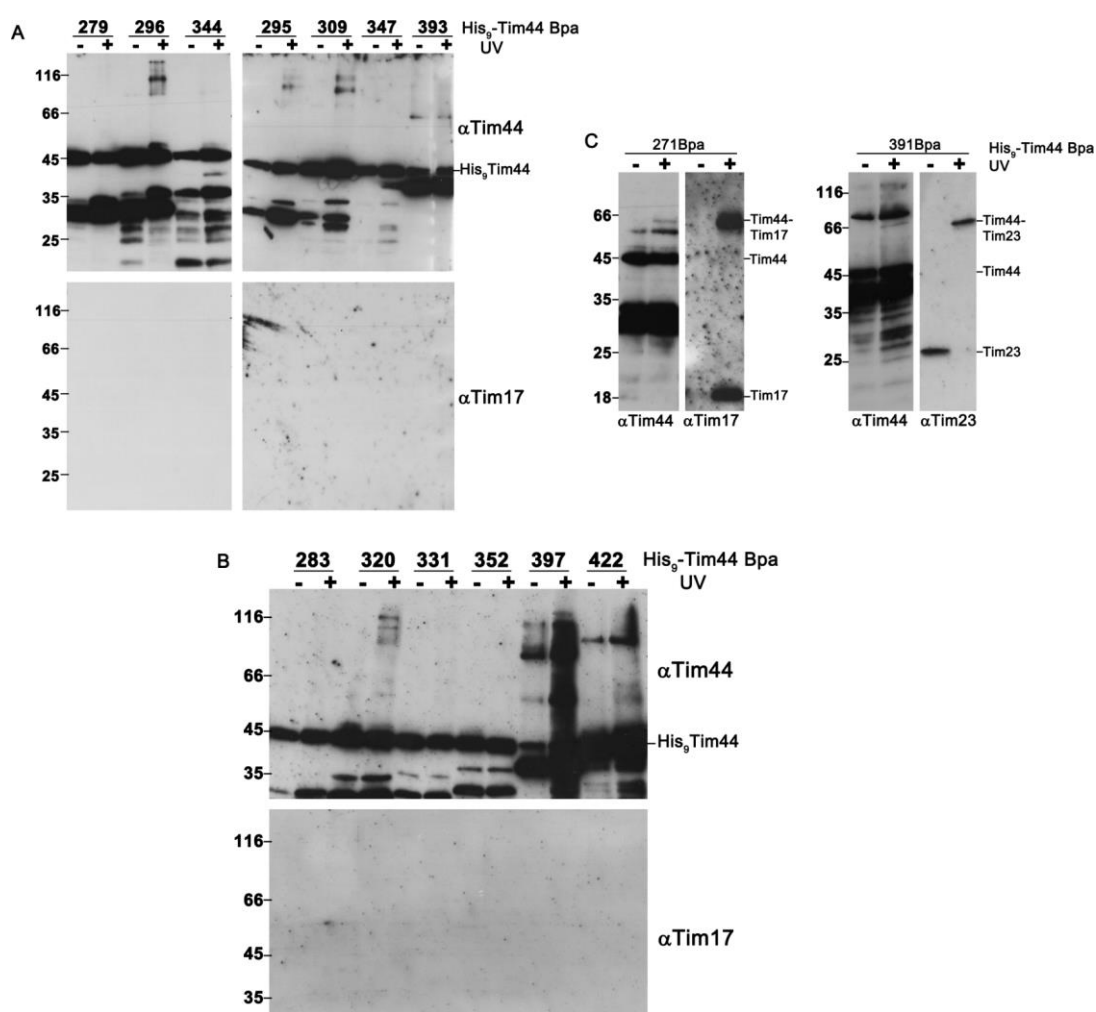


**Figure 3.34. Bpa-crosslinking of Tim44 C-terminal domain surface positions.** Yeast cells expressing His<sub>9</sub>-Tim44 with Bpa incorporated at various positions were illuminated under UV light for 1 h. His-tagged Tim44 was enriched with Ni-NTA pull-down and crosslinked product was analysed as described in Figure 3.23B. A and B shows positions analysed in this study and C shows positions used by (Ting et al., 2017).

gives Bpa-photocrosslinks at certain positions (Ting et al., 2017). These positions were tested and confirmed to give crosslinks as given in previously published report (Figure 3.34 C).

The residues that were analysed for Tim44-Tim17 crosslinking products but did not give positive crosslinking with Tim17, were then further analysed. There are two possible explanations for these products, either these are intramolecular Tim44 crosslinks or Tim44 Cc-domain has another binding partner. Based on the size of the crosslinked products for positions in Tim44 that gave high molecular weight crosslinking band, Ssc1 was analysed as a potential binding partner (Figure 3.35). Indeed, when Bpa was introduced at position 279 of Tim44, a crosslink with Ssc1 was observed. This suggests that, in cells, Ssc1 is present within the crosslinking distance of the Tim44 Cc-domain.

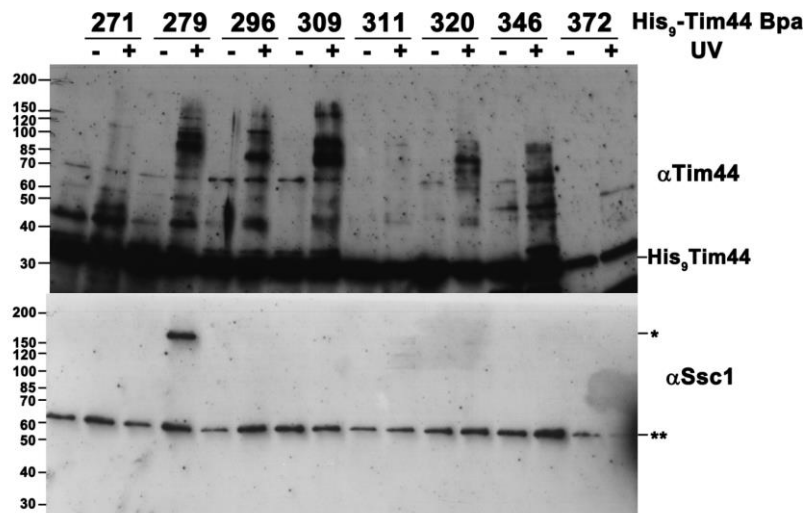


**Figure 3.35. Interaction between C-terminal domain of Tim44 and Ssc1.** Cells expressing His-tagged versions of Tim44 with Bpa introduced at indicated positions were grown in SD medium with 1 mM Bpa. Half of the samples were exposed to UV light for 1 h and the other halves were kept in the dark as a control. Cells were lysed in buffer containing 1% SDS, diluted in buffer containing 0.5% Triton X-100 and subsequently incubated with Ni-NTA agarose beads to bind His-tagged Tim44 and its crosslinking partners. Bound fractions were analysed by SDS-PAGE and immunostaining. \*-crosslink between Tim44-Ssc1, \*\*-background binding of mtHsp70 to Ni-NTA agarose beads

Taken together, Tim44 C-terminal domain surface was mapped for various interaction partners.

### **3.4 Conformation of Ssc1 in mitochondria**

The study so far revealed novel molecular insight into how Tim44 organizes the TIM23 complex by connecting the translocation channel and the import motor. By recruiting mtHsp70 to the translocation channel, Tim44 enables the chaperone to convert the energy of ATP hydrolysis into unidirectional translocation of proteins across the inner membrane. The key to understanding the latter process lies in understanding of the ATP-hydrolysis driven conformational changes of mtHsp70 (Ssc1 in yeast). Conformational dynamics of Ssc1 were previously analysed *in vitro* by single molecule FRET in a collaboration of our group with the group of Prof. Don Lamb at LMU Munich (Mapa et al., 2010; Sikor et al., 2013). This part of the study was set out to adopt the previously reported *in vitro* approach for a more physiologically relevant environment, namely intact mitochondria. To this end, a method was developed to import fluorescently labelled Ssc1 into isolated mitochondria, confirm that mitochondria remain functional after import and then, in collaboration with the Lamb group, to develop methods to immobilize mitochondria with imported labelled Ssc1 and finally measure FRET at single molecule level.

#### **3.4.1 Generation of Ssc1 construct for *in organello* FRET measurements and its functionality *in vivo***

For analysis of *in organello* Ssc1 conformation, previously established domain sensor of Ssc1 was used (Mapa et al., 2010; Sikor et al., 2013). This sensor contains cysteine residues introduced at positions 341 and 448 in the ATPase and SBD domains, respectively. After labelling of cysteine residues with FRET-pair fluorophores, this sensor was successfully used to analyse the ATP-dependent interaction of the two domains of Ssc1 *in vitro* (Mapa et al., 2010; Sikor et al., 2013). To be able to import such a sensor into isolated mitochondria, presence of the presequence in purified Ssc1 was a prerequisite. However, despite the fact that the recombinant mature Ssc1 was easily soluble upon co-expression with Hep1, addition of the presequence, interestingly, rendered Ssc1 insoluble even in the presence of Hep1 (data not shown). To make the purification of the presequence-containing Ssc1 from the inclusion bodies easier, a His<sub>6</sub>-tag was introduced at the C-terminus of the protein (Figure 3.36 A). As a result, presequence-containing Ssc1 (D341C, I448C) that has C-terminal His<sub>6</sub>-tag, was recombinantly expressed in bacteria and purified from inclusion bodies using a buffer

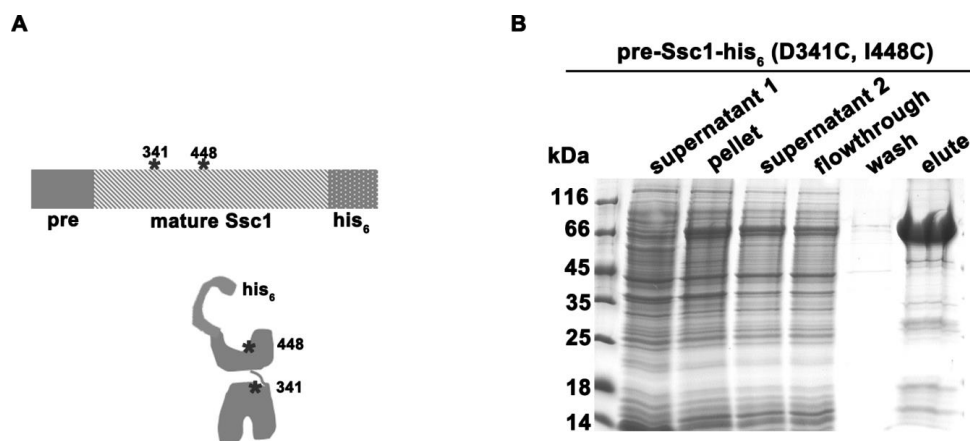


**Figure 3.36. pre-Ssc1-his<sub>6</sub> (D341C, I448C) purification.** A) Schematic representation of presequence containing Ssc1 used in study with cysteine positions used for labelling with donor-acceptor dye pair. B) Recombinantly expressed pre-Ssc1-his<sub>6</sub> (D341C, I448C) was purified from inclusion bodies by solubilizing them in buffer containing 3 M urea followed by Ni-NTA affinity chromatography.

containing 3 M urea (Figure 3.36 B). This protein construct will be referred to as pre-Ssc1-his<sub>6</sub> (341C, 448C) in the following text.

In order to confirm that the C-terminal His<sub>6</sub>-tag and cysteine double mutation do not

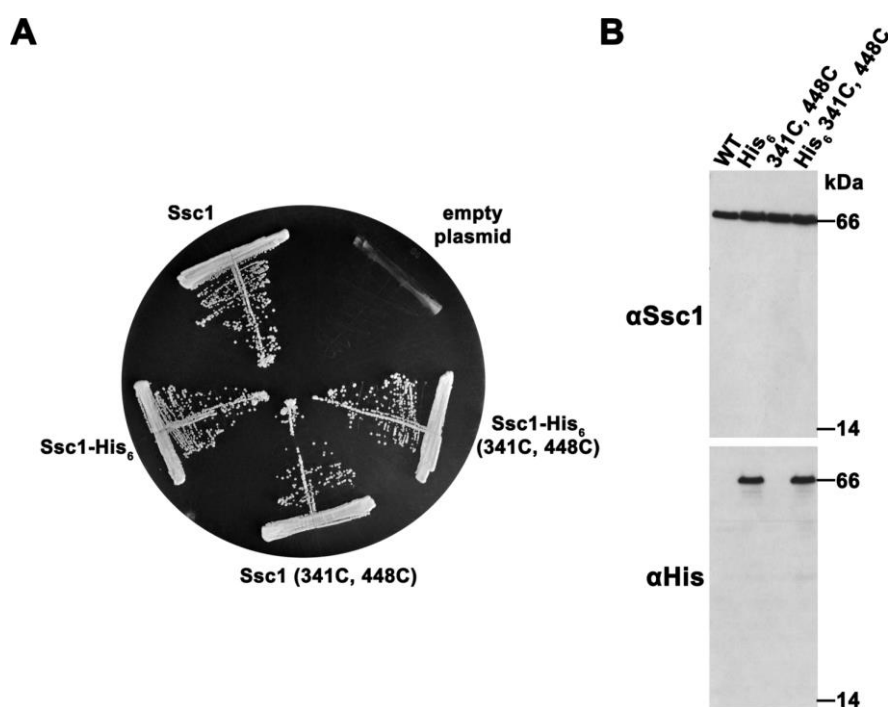


**Figure 3.37. Rescue of Ssc1 function by C-terminal His<sub>6</sub>-tagged double cysteine Ssc1 mutant.** A) Ssc1 shuffling strain was transformed with indicated Ssc1 constructs under endogenous promoter and their ability to rescue the function of Ssc1 was analysed on medium containing 5-FOA. Plates were kept at 30°C for 3 days. B) Cell lysates were analysed for expression of His<sub>6</sub>-tagged protein by immunostaining.

interfere with Ssc1 function, the ability of this construct to support viability of yeast cells was tested (Figure 3.37 A). In agreement with previously published data, both the strain expressing Ssc1 with the C-terminal His<sub>6</sub>-tag and the strain expressing two cysteines-version of Ssc1, Ssc1 (D341C, I448C) were viable (Liu et al., 2001; Mapa et al., 2010). This suggests that the His<sub>6</sub>-tag and cysteine mutations individually do not interfere with Ssc1 function. Also the strain expressing C-terminally His<sub>6</sub>-tagged Ssc1 with cysteine mutations, Ssc1-His<sub>6</sub> (341C, 448C), was viable, suggesting that it is functional as well and can rescue the function of wild type Ssc1. Expression of the constructs was confirmed by analysis of cell lysates by immunostaining (Figure 3.37 B). All of the strains showed expression of Ssc1, however, only Ssc1-His<sub>6</sub> and Ssc1-His<sub>6</sub> (D341C, I448C) showed signals when analysed for expression of His-tagged protein.

To analyse possibly more subtle effects of the His<sub>6</sub>-tag and cysteine mutations on Ssc1 function, yeast strains were serially diluted and grown on fermentable (YPD) and non-fermentable medium (YPG) at 24°C, 30°C and 37°C (Figure 3.38). No apparent difference was observed in growth of wild type and C-terminally His<sub>6</sub>-tagged double cysteine mutants, confirming that neither the His-tag nor the two cysteine exchanges interfere with the function of Ssc1 *in vivo*.

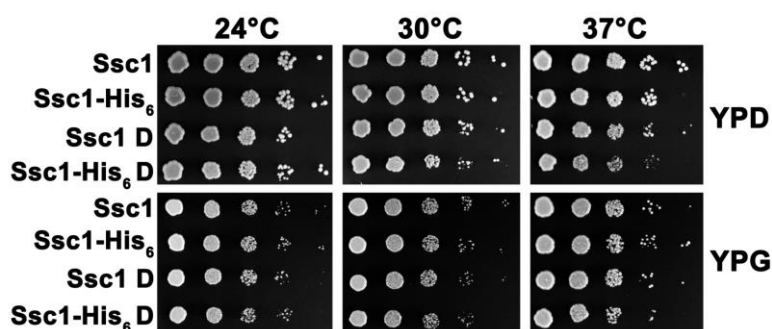


**Figure 3.38. Growth assay of yeast strains expressing Ssc1 constructs.** Yeast cells were grown on YPGal medium overnight at 30°C. Cells were serially diluted 10-fold and were grown on fermentable (YPD) and non-fermentable (YPG) media at 24°C, 30°C and 37°C. YPD plates were incubated for 2 days and YPG plates were incubated for 3-4 days. ‘D’ denotes domain sensor (D341C, I448C)

### 3.4.2 Import of donor-acceptor dye pair labelled Ssc1 into isolated mitochondria

The purified pre-Ssc1-his<sub>6</sub> (D341C, I448C) protein was labelled with commercially available donor fluorophore, ATTO 532 maleimide, and acceptor fluorophore, ATTO 647N maleimide. The above mentioned dyes were chosen as they were used in previous *in vitro* studies of Ssc1 conformation (Mapa et al., 2010; Sikor et al., 2013). The labelled protein was incubated with isolated mitochondria. Import reactions were analysed by immunostaining with  $\alpha$ His to check whether His-tagged protein was imported into mitochondria (Figure 3.39). In the absence of membrane potential across inner membrane, no import took place. However, increasing amounts of His<sub>6</sub>-tagged protein accumulated in mitochondria over time in the presence of membrane potential, indicative of efficient import.

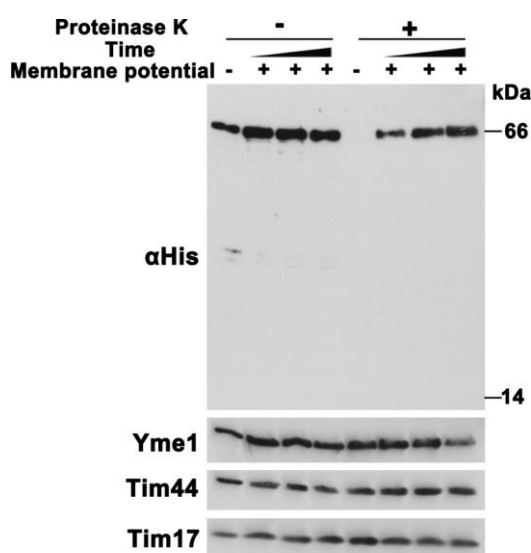


**Figure 3.39. Import of pre-Ssc1-his<sub>6</sub> (ATTO 532, ATTO 647N) into isolated mitochondria.** Isolated mitochondria were incubated with pre-Ssc1-his<sub>6</sub> (ATTO 532, ATTO 647N). After 3, 10 and 30 min, aliquots were removed and import was stopped. In half of the samples, non-imported protein was degraded by treating the samples with proteinase K. Mitochondria were reisolated and the samples were analysed by SDS-PAGE and immunostaining. No membrane potential controls had mitochondria pretreated with valinomycin so as to prevent any import.

It has been reported that the acceptor dye used, ATTO 647N, may not be suitable for *in vivo* studies as it can non-specifically bind to membranes (Kolmakov et al., 2010). Therefore, a number of other acceptor dyes, based on their excitation and emission

wavelengths, were considered. In the end, Alexa 647, CF640R and ATTO 647 were chosen for further analysis. Purified pre-Ssc1-his<sub>6</sub> (D341C, I448C) was labelled with ATTO 532 as a donor and one of the four acceptor dyes. As a result, four different samples of dually labelled pre-Ssc1-his<sub>6</sub> (341C, 448C) were analysed for their import into isolated mitochondria (Figure 3.40). Import reactions were analysed by fluorescence scanning of SDS-PA gels for both donor and acceptor dyes. In case of all four samples, PK-protected, processed form of Ssc1 was detected when import was done in the presence of membrane potential. This shows that recombinant Ssc1 can be efficiently imported into mitochondria and that the mitochondrial protein import channels are able to

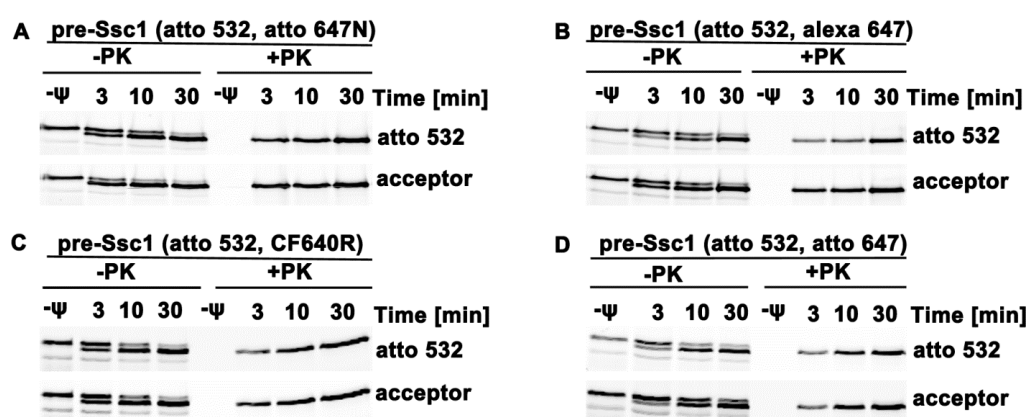


**Figure 3.40. Import of dually labelled Ssc1 with different acceptor dyes.** pre-Ssc1-his<sub>6</sub>, labelled with ATTO 532 as donor and different acceptor dyes, was imported into isolated mitochondria. At indicated time points samples were taken out, import was stopped and non-imported material was digested with proteinase K (PK) in half of the samples. Mitochondria were reisolated and analysed by SDS-PAGE followed by fluorescence scanning at 532 nm for donor and 635 nm for acceptor. No membrane potential sample (-ψ) was mitochondria treated with valinomycin before import. Different acceptor dyes used were as follows: A) ATTO 647N; B) Alexa 647; C) CF640R; and D)

accommodate fluorescently labelled proteins.

To verify the specificity of the import reactions, mature and presequence containing Ssc1, both labelled with ATTO 532 and ATTO 647, were imported into isolated mitochondria. Import reactions were analysed by fluorescence scanning of SDS-PA gels (Figure 3.41). When mature Ssc1 was incubated with isolated mitochondria, no protein was protected from proteinase K, suggesting that labelled mature Ssc1 was not imported into mitochondria. However, with presequence containing Ssc1, an additional, faster running

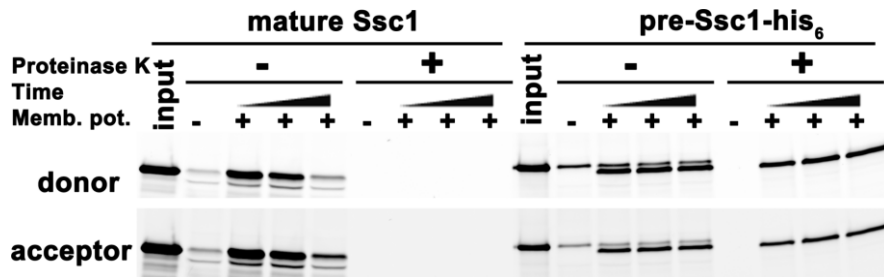


**Figure 3.41. Presequence and membrane potential dependent import of Ssc1 (ATTO 532, ATTO 647) in isolated mitochondria.** Mature Ssc1 and presequence containing Ssc1 were unfolded in buffer containing 7 M urea and were imported into isolated mitochondria. Non-imported proteins were digested by proteinase K treatment. Mitochondrial lysates were analysed for imported proteins by SDS-PAGE followed by fluorescence scanning at 532 nm and 635 nm. In case of no membrane potential control, mitochondria pretreated with valinomycin were used.

protein band appeared upon incubation with energised mitochondria. The same band also remained intact after PK treatment. This indicates that only the precursor form of Ssc1 can be imported into mitochondria and that the presequence is removed upon import. In conclusion, recombinant and dually labelled Ssc1 constructs can be imported in a presequence- and a membrane potential-dependent manner into isolated mitochondria.

### 3.4.3 Characterization of mitochondria after import of pre-Ssc1-his<sub>6</sub> (ATTO 532, ATTO 647)

Before moving to the FRET measurements, it was important to confirm that the functionality of isolated mitochondria was not affected by import of labelled Ssc1. To this end, several assays were performed. First, the ability of mitochondria to generate membrane potential after import of Ssc1 was analysed and compared to mitochondria that were freshly taken out of -80°C freezer and were used as an untreated control (Figure 3.42 A). Both the sample and control mitochondria could generate membrane potential to a similar extent, as judged from fluorescence measurements with DiSC<sub>3</sub>(5). As expected, if mitochondria were treated with valinomycin before import of Ssc1, no membrane potential could be generated. To confirm that the same amounts of mitochondria were used in measurements, mitochondrial lysates were analysed by immunostaining (Figure 3.42 B). Both untreated control and samples were comparable in amounts, showing that several reisolation and resuspension steps performed during the import reaction do not

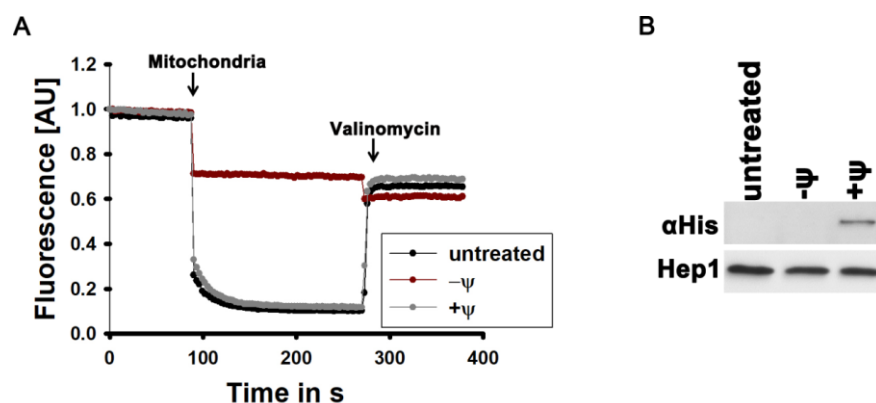


**Figure 3.42. Generation of membrane potential in mitochondria after import of labelled Ssc1.** A) Fluorescence quenching of DiSC<sub>3</sub>(5) dye was used to determine generation of membrane potential in untreated mitochondria, mitochondria that had undergone import with no membrane potential (-ψ) and mitochondria that had undergone import with membrane potential (+ψ) for 10 min. B) Analysis of lysate of mitochondria used in membrane potential study by immunostaining.

lead to an obvious loss of the material and the mitochondrial functionality is retained, at least when judged by their ability to generate membrane potential.

Next, how long mitochondria could maintain the membrane potential after import was determined by analysing the recovery of fluorescence by DiSC<sub>3</sub>(5) over time (Figure

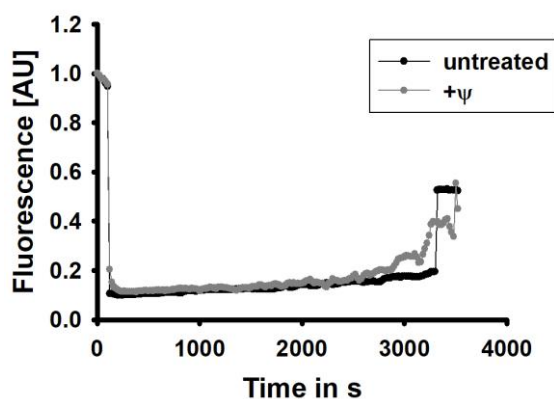


**Figure 3.43. Maintenance of membrane potential in mitochondria after import of labelled Ssc1.** Untreated mitochondria and mitochondria after import of labelled Ssc1 (+ψ), were added to import buffer containing DiSC<sub>3</sub>(5). Fluorescence quenching of the dye was analysed over time to determine the time period over which membrane potential is maintained. In case of untreated mitochondria, valinomycin was added to dissipate membrane potential and recover fluorescence.

3.43). Mitochondria, after import of labelled Ssc1, maintained the membrane potential for about 40 min and later started to lose it on their own. To rule out the possibility that the loss in membrane potential across inner membrane was not due to the depletion of added ATP and NADH during the measurement, additional amounts of ATP and NADH were added into the reaction (data not shown). Further addition of ATP and NADH also did not show any improvement in the time mitochondria could maintain potential across inner membrane. Mitochondria, freshly taken out of the freezer, appeared functional even longer. Still, mitochondria remain healthy for a considerable time after import and single molecule FRET measurements could be carried out within 40 min after import of labelled Ssc1.

To obtain a deeper insight into functionality of mitochondria after import of labelled Ssc1, their ability to import further proteins was analysed. A matrix targeted  $^{35}\text{S}$ -labelled precursor protein, pSu9-DHFR, was imported into mitochondria that had already undergone import of pre-Ssc1-his<sub>6</sub> (ATTO 532, ATTO 647) and in mitochondria freshly taken out of the  $-80^{\circ}\text{C}$  freezer (Figure 3.44). The import efficiency in mitochondria which

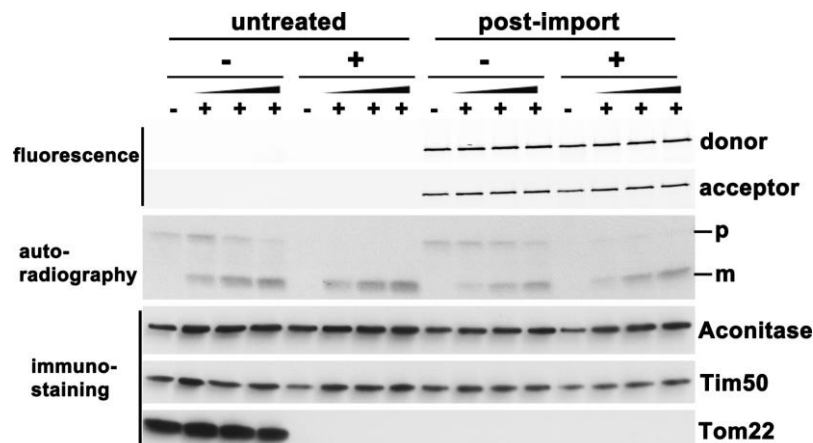


**Figure 3.44. Import of matrix targeted precursor in mitochondria after import of labelled Ssc1.**  $^{35}\text{S}$ -labelled matrix targeted precursor protein was imported into untreated mitochondria and mitochondria in which pre-Ssc1-his<sub>6</sub> (ATTO 532, ATTO 647) was imported. Analysis of mitochondrial lysate was done by fluorescence scanning of SDS-PA gel to detect labelled Ssc1 that got imported, autoradiography after the transfer of protein into nitrocellulose membrane was done to detect  $^{35}\text{S}$ -labelled pSu9-DHFR and immunodecoration using nitrocellulose membrane was done to detect mitochondrial proteins of different compartments. p-precursor form, m-mature form

had labelled Ssc1 previously imported was slightly less compared to import in

mitochondria that were freshly taken out of  $-80^{\circ}\text{C}$ . This is likely due to the absence of surface exposed receptors of the TOM complex in mitochondria that have imported labelled Ssc1. These are removed during PK treatment after import of Ssc1 performed to degrade non-imported material. The integrities of the outer and inner membranes were, however, not compromised, as judged by immunostaining of an inner membrane protein with a large IMS-exposed domain (Tim50) and a matrix protein (aconitase).

Overall, after import of labelled Ssc1 into isolated mitochondria, the mitochondria could generate membrane potential and import matrix targeted precursor proteins. This suggests that mitochondria remain functional and can be used for single molecule measurements to analyse conformation of labelled Ssc1 *in organello*.

### 3.4.4 Immobilization of mitochondria

To perform single molecule FRET studies on labelled Ssc1 imported into mitochondria, HiLo measurements using TIRF setup were planned. Therefore, immobilization of mitochondria with imported labelled Ssc1 on glass surface of cover slides was prerequisite for measurements. Previous reports have shown that mitochondria can be immobilized on a glass surface with polylysine coating (Kuzmenko et al., 2011).

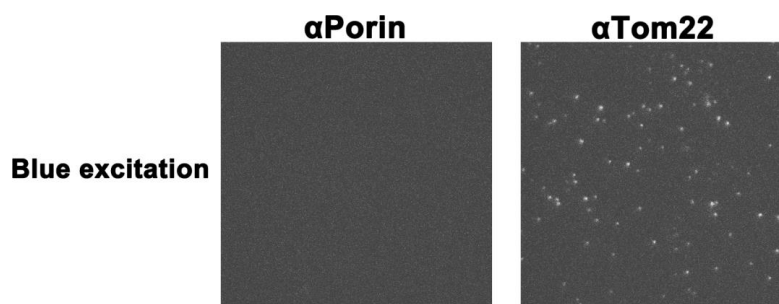


**Figure 3.45. Immobilization of isolated mitochondria after import of Ssc1.** Labelled Ssc1 was imported into isolated mitochondria. Non-imported labelled protein was removed by proteinase K digestion followed by its inhibition by PMSF. Streptavidin was immobilized on cover slides coated with PEG/biotinylated PEG. 10 nM biotinylated  $\alpha$ Porin and  $\alpha$ Tom22 were immobilized on streptavidin. To this, mitochondria obtained after import were immobilized by incubating at RT for 10 min. Visualization of bound mitochondria was done by exciting the sample with 491 nm laser and detecting the fluorescence in green region on a TIRF setup.

However, polylysine was unsuitable for our measurements as it gave a high background over the sample. Hence, a more specific, antibody-dependent system was tested for

immobilization of mitochondria. The major challenge associated with immobilizing the mitochondria using antibodies was to choose the correct antibody, especially since the proteinase K treatment, used to degrade non-imported Ssc1, also digests the proteins that are exposed on the outer surface of mitochondria. As a result, immobilization based on antibody would heavily rely on the efficiency of proteinase K digestion or abundance of protein that will be digested. To this end, antibodies against two outer membrane proteins-  $\alpha$ Porin and  $\alpha$ Tom22, were tested (Figure 3.45). The cover slides were first coated with a mixture of PEG and biotinylated-PEG. Coating of the glass surface with PEG is essential to prevent non-specific binding. Streptavidin was then immobilized on the glass through an interaction with biotinylated PEG, followed by binding of biotinylated antibodies to streptavidin. Finally, mitochondria obtained after import were added. Immobilization of mitochondria worked with  $\alpha$ Tom22 but not with  $\alpha$ Porin. It could be due to efficiency of biotinylation was better with  $\alpha$ Tom22. Alternatively, the epitope recognized by  $\alpha$ Porin was degraded by PK more efficiently or it is not accessible to the antibody in intact mitochondria. Overall, biotinylated  $\alpha$ Tom22 were used for immobilization of mitochondria for further studies.

### **3.4.5 *In organello* conformation of Ssc1 at single molecule resolution**

After successful establishment of protocols for import of labelled Ssc1 and immobilization of mitochondria, conformation of labelled Ssc1 imported into isolated mitochondria was analysed by HiLo measurement at single molecule resolution. For this, the import reactions had to be optimized so that one molecule of dually labelled Ssc1 was imported per mitochondrion. Analysis of FRET efficiencies of particle in wild type suggests that, in the presence of ATP, the majority of Ssc1 molecules show low FRET efficiency (Figure 3.46). This means that the two domains of Ssc1 are, surprisingly, undocked in the presence of ATP inside mitochondria. On the other hand, upon ATP depletion, two distinct populations with low and high FRET were observed. This suggests that upon ATP depletion the two domains exist in both docked and undocked state. Interestingly, the low FRET state observed both in the presence and absence of ATP is reminiscent of the substrate bound state observed *in vitro* (Mapa et al., 2010; Sikor et al., 2013). Further analysis of Ssc1 conformation inside mitochondria derived from temperature sensitive mutant strains of its co-chaperones, *mdj1-5* and *mge1-3*, was

carried out (Figure 3.46) (Westermann et al., 1996; Westermann et al., 1995). Mitochondria lacking functional cochaperones of Ssc1 would lock the Ssc1 conformation at a specific state of Hsp70 cycle. Indeed, in case of *mdj1-5* in which stimulation of ATP hydrolysis by Ssc1 is impaired, a prominent high FRET population reminiscent of *in vitro*

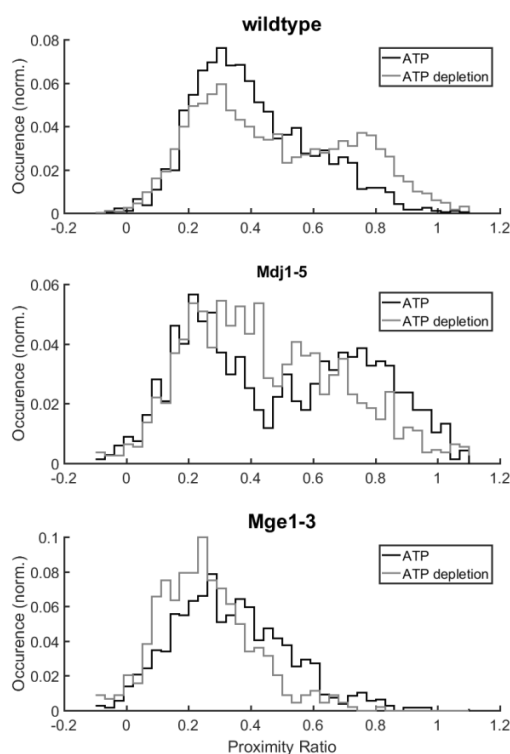


**Figure 3.46. Conformation of Ssc1 by single molecule HiLo measurement.**

Mitochondria from the mentioned strain after import of dually-labelled Ssc1 were immobilized on glass cover slide and HiLo measurement was carried out on a TIRF setup. Detection of mitochondria was done by excitation with blue laser and emission was analysed in green region. Donor and acceptor fluorophores excitations were done at 532 nm and 647 nm, respectively. In ATP sample, ATP was added exogenously into buffer and ATP depletion was achieved by addition of apyrase and oligomycin.

ATP-bound docked state along with a low FRET population in both ATP and ATP-depleted conditions was observed. In contrast, in case of mitochondria where slow exchange of ADP with ATP in Ssc1 takes place, *mge1-3*, only a prominent low FRET peak in presence and absence of ATP suggestive of Ssc1 locked in substrate bound ADP state was found. Taken together, an assay to analyse the conformation of Ssc1 *in organello* was developed in this study.

## 4. Discussion

### 4.1 Tim44 as the organizer of the TIM23 complex

The TIM23 complex is major protein translocase of the mitochondrial inner membrane. Over 50% of mitochondrial proteins use this complex for their translocation into the organelle. Though a considerable progress has been made towards identifying the complete set of the components of the TIM23 complex, our understanding of molecular mechanisms of its function are still rather fragmentary. In this thesis, I provide novel and unexpected molecular insight into the function of one of its subunits –Tim44. Tim44 is a peripheral membrane protein that resides at the matrix side of the inner mitochondrial membrane. It has been proposed that Tim44 serves as an anchor for recruitment of channel and import motor subunits of the TIM23 complex and thereby, organizes the entire complex. However, how Tim44 does this remained unclear. My work here demonstrated that the two-domain structure of Tim44 has a crucial role in the process and revealed a previously unappreciated essential function of the core of the C-terminal domain (Cc domain).

Yeast cells expressing a truncated version of Tim44 lacking Cc-domain were not viable, suggesting an essential function of this domain. The importance of Cc domain is also supported by the finding that a mutation in the C-core domain of human Tim44, P308Q, is associated with familial oncocyctic thyroid carcinoma (Bonora et al., 2006). An analysis I performed with the corresponding mutation in yeast Tim44, P282Q, showed no apparent growth or *in vivo* protein import defect, suggesting that yeast is a more robust system. This finding also shows that the mutation does not cause a major impairment of the Tim44 function, in agreement with previously established idea that deleterious mutations in Tim44 would be embryonically lethal in humans. However, the association of the mutation with cancer suggests that it does have some implications for Tim44 function. Indeed, analysis of recombinant Tim44, wild type and mutant, in this study revealed that the P282Q mutation renders protein less stable, in comparison to the wild type protein. Using the crystal structure of Tim44 C-terminal domain, the position of the Pro282 residue was mapped to a short loop between A3 and A4 helices (Josyula et al., 2006). Interestingly, proline and glycine residues are often found in short loops where they play an important role in the formation of native protein structure (Krieger et al., 2005).

Pro282 in Tim44 may thus play a role in attaining proper conformation of Tim44. In addition, it was previously proposed that this position may have an influence on the flexibility of A1 and A2 helices, which also rendered previous crystallization attempts of the mutant human Tim44 unsuccessful (Handa et al., 2007). As a result, P282Q mutation in Tim44 C-core domain could compromise the structural integrity and/or conformational flexibility of Tim44, which could, in adverse conditions, lead to a tissue-specific destabilization of Tim44 and to development of cancer in carrier patients.

One of the major findings presented here is that the two domain structure of Tim44 plays an essential role in the communication of the translocation channel and the import motor of the TIM23 complex. It has been shown before that the Tim44 N-terminal domain interacts with mtHsp70, Tim16 and presequences (Marom et al., 2011b; Schilke et al., 2012; Schiller et al., 2008). Recently, it has also been reported that the N-terminal domain of Tim44 interacts with Tim23 (Ting et al., 2014). The C-terminal domain of Tim44, on the other hand, was found to interact with cardiolipin-containing membranes via its A1 and A2 helices (234-263) (Marom et al., 2011b; Weiss et al., 1999). However, binding partners, if any, of the remaining part of Tim44 C-terminal domain (264-431), C-core domain, remained unknown. I elucidated the different interaction partners of the two domains of Tim44. Recombinant N-terminal domain of Tim44 bound to mtHsp70 and Tim14-Tim16 subcomplex from the mitochondrial lysate, in agreement with previous reports (D'Silva et al., 2004; Schilke et al., 2012; Schiller et al., 2008). Since Triton X-100, the detergent used to prepare the mitochondrial lysate in this assay, does not dissociate the Tim14-Tim16 complex, it was not possible to confirm that Tim44 N-domain interacts directly with Tim16 (Schilke et al., 2012). Nevertheless, the interaction with Tim14-Tim16 subcomplex is in accordance with previous reports. Surprisingly, the same *in vitro* pull-down assay revealed an interaction between the recombinant Cc-domain of Tim44 with Tim17, a channel subunit of TIM23 complex. Therefore, Tim44 C-terminal domain not only interacts with the inner membrane of mitochondria but is also involved in protein-protein interactions within the TIM23 complex. Based on these findings, I searched for a potential Tim44-binding site in the loop of Tim17 that connects TM3 and TM4 at the matrix side of the inner membrane. Indeed, when Bpa was introduced at position 106 of Tim17, a specific crosslink between Tim17 and Tim44 was observed, revealing the site of attachment of Tim44 on Tim17. A combination of a mutational analysis and Bpa-photocrosslinking of this loop suggested that R105 is involved in interaction with Tim44 (Demishtein-Zohary et al., 2017). This confirms the

presence of Tim44-Tim17 interaction *in vivo* and indicates that binding of Tim44 by Tim17 is critical for TIM23 complex function.

To map the binding site for Tim17 on the C-terminal domain of Tim44, I used the available crystal structure of the C-terminal domain of Tim44 to identify conserved, surface exposed residues. Since R105 in Tim17 was identified to be important for Tim17 interaction with Tim44 (Demishtein-Zohary et al., 2017), I initially analysed only conserved negatively charged residues on Tim44 C-terminal domain surface. Conserved residue D345 and its direct neighbour Q372 were found to be important for Tim44 function, however no positive evidence was found for their direct role in Tim44-Tim17 interaction. In agreement with these findings, a recent study from the Craig group revealed that a different surface exposed region of the C-terminal domain of Tim44 can be crosslinked to Tim17 (Ting et al., 2017), the result which I could also reproduce. However, the importance of this region of Tim44 for its function and the interaction with Tim17 has not been investigated further. The same study from the Craig group revealed that D345 can actually be crosslinked to Tim23, suggesting that D345 may be involved in an interaction of Tim44 C-domain with Tim23 (Ting et al., 2017). As crosslinks between with the N-terminal domain of Tim44 and the matrix-exposed loop between TM1 and TM2 of Tim23 were previously shown (Ting et al., 2014), Tim23 appears to interact or at least is in close vicinity of both N- and C-terminal domains of Tim44. Intriguingly, I could not observe any stable interaction between full length Tim44 and either of its domains with Tim23 using the pull-down assay that revealed the other interactions. Site-specific photocrosslinking *in vivo* may catch a weak and/or a transient interaction between Tim44 and Tim23 (Ting et al., 2014; Ting et al., 2017) which may not prevail in a detergent-solubilized *in vitro* system. It is also possible that the conformation of Tim23 and/or Tim44 necessary for their interaction may only exist when the entire complex is assembled in the inner membrane. Either way, it appears that the interaction between Tim44 and Tim17 is more robust than the Tim44 interaction with Tim23. It is thus tempting to speculate that Tim17 acts as a recruitment site for Tim44, which is then followed by binding of Tim44 to Tim23. It would be also interesting to decipher whether binding of Tim44 to Tim17 induces conformational alterations within TIM23 complex causing the Tim44 interaction with Tim23. Understanding the sequence of events that lead to binding of Tim44 to Tim23 and Tim17 will demonstrate how these interactions lead to the organization of the TIM23 complex. Further investigation of the dynamics of the interplay of Tim44, Tim17 and Tim23 would allow us to delineate whether the

different Tim44 molecules bind different subunits of TIM23 complex or one single Tim44 molecule interacts dynamically with both Tim17 and Tim23 by undergoing conformational changes that may underlie the transport of precursor proteins into mitochondria.

In addition to previously shown interaction partners of Tim44 C-domain to Tim23 and Tim17, the Bpa-photocrosslinking carried out in this study suggests that Tim44 C-domain is also in close vicinity of Ssc1. Tim44 that had Bpa incorporated at position Leu279 gave a slow migrating crosslink with Ssc1. This position can be mapped to a region in Tim44 C-terminal domain that is distinct from both Tim23 and Tim17 binding sites (Figure 4.1).

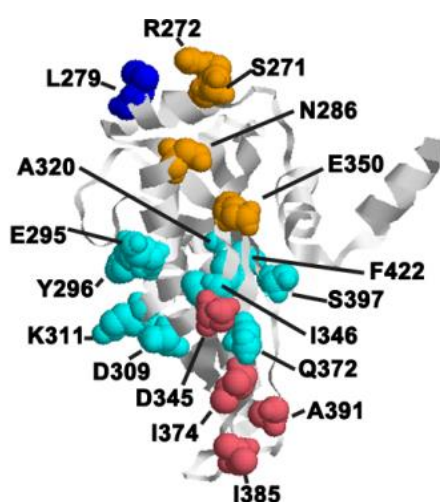


**Figure 4.1. Representation of positions giving Bpa-photocrosslinks in Tim44 C-terminal domain.** Positions depicted in the crystal structure of Tim44 C-terminal domain (Josyula et al., 2006) that gave high molecular weight site-specific Bpa-crosslinks with different TIM23 complex subunits. Different colors represent different subunits that crosslinked to Tim44 and are as follows: Orange- Tim17 (Ting et al., 2017); Pink- Tim23 (Ting et al., 2017); Blue- Ssc1 (this thesis); Cyan- not known (this thesis). Note that position Q372 was also analysed by (Ting et al., 2017).

Analysis of the conserved residues in the vicinity of Leu279 in Tim44, such as Thr403, Arg404, Pro363, Asp281, Trp417 and Phe289, could reveal the residue(s) crucial for Tim44-Ssc1 interaction and evaluate the importance of this interaction for the overall process of protein translocation.

A further unexpected finding of my work was that the C-terminal domain of Tim44 also interacts with the entering precursor protein, providing further explanation for the essential nature of this domain. The interaction of Tim44 C-domain with channel

subunits, Tim23 and Tim17, positions Tim44 C-domain in the vicinity of the entering precursor protein. It has also been reported that purified Tim44 N-domain crosslinks with presequences (Ting et al., 2017) suggesting that both domains of Tim44 interact with precursor protein - presequence interacts with the N-domain and the mature part of precursor with the C-domain. Considering that Tim44 C-terminal domain has also been found to interact with Ssc1 in this study, it is tempting to speculate that the SBD of Ssc1 may play a role in interaction of Ssc1 with the Tim44 C-terminal domain. It can be further postulated that, during protein import, the interaction between N-domain and the entering presequence induces conformational changes within Tim44 that lead to an interaction of the Tim44 C-domain with the entering precursor allowing a cross-talk among different subunits of the TIM23 complex. It is tempting to speculate that the proposed conformational changes are mediated through A1 and A2 helices. The crystal structures of Tim44 derived from yeast and human provide support for this hypothesis as the two structures have A1 and A2 helices in different orientation (Handa et al., 2007; Josyula et al., 2006). In the structure of yeast Tim44, the A1 and A2 helices protrude away from the core domain whereas in the structure of the human Tim44 they are wrapped around the C-terminal domain core of Tim44(Handa et al., 2007). Further support for this hypothesis comes from the fact that the N- and C-domains of Tim44 co-expressed *in trans* can support the function of Tim44 only very poorly. When the two domains are not covalently linked to each other, rearrangements within the molecule are expected to be severely impaired.

Taken together, the interplay of Tim23, Tim17, entering precursor and Ssc1 with Tim44 C-terminal domain and interaction of Tim23, Tim14-Tim16 and Ssc1 with Tim44 N-domain makes it obvious that Tim44 has an important role not only in organization of the TIM23 complex but also in mediating cross-talk between different subunits of TIM23 complex during protein translocation.

Based on these results and previously available data, we proposed the following model for translocation of proteins by the TIM23 complex (Figure 4.2). Tim44 is anchored to inner membrane via the A1 and A2 helices on the C-terminal domain such that the N-domain and C-core domain are exposed to the matrix side (Figure 4.2 inset). The N-domain interacts with mtHsp70, Tim14-Tim16 subcomplex and Tim23 and C-domain interacts with Tim17 in the resting state of TIM23 complex (Figure 4.2). As the precursor protein enters, its presequence first interacts with the N-domain of Tim44, followed by conformational changes in Tim44 domains such that its C-domain comes in contact with

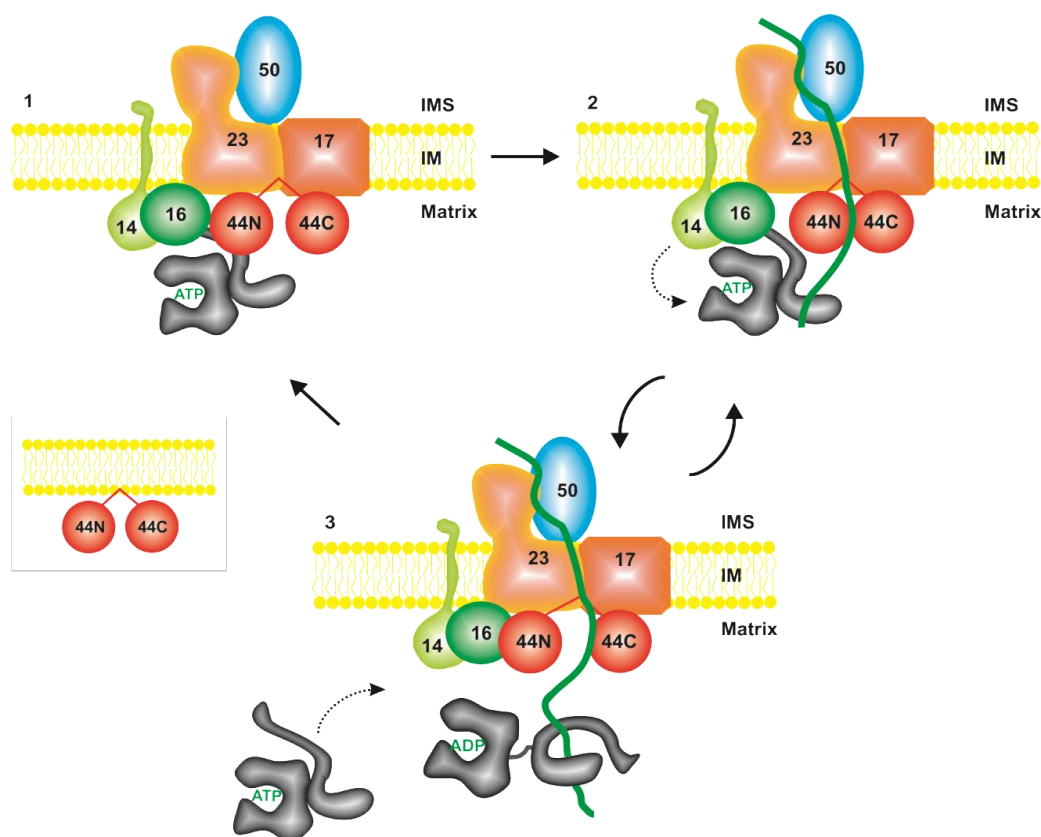


**Figure 4.1. Schematic representation of the proposed model.** Detailed description of the model is given in text.

Tim23 and the entering precursor protein. This rearrangement in Tim44 domains primes the import motor for activation. The entering precursor binds to mtHsp70 of the import motor and as a result, mtHsp70 undergoes conformational changes with the help of its co-chaperones Tim14-Tim16 and is released from the TIM23 complex. During this process, ATP bound to mtHsp70 is hydrolysed and energy from ATP hydrolysis is converted into unidirectional transport of precursor into matrix. As mtHsp70 takes a segment of the precursor protein away from the inner membrane and into the matrix, a place is freed for a new molecule of mtHsp70 to be recruited to the TIM23 complex. The cycle continues until the entire protein is translocated across the inner membrane and the rearrangements in Tim44 domains likely occur in each cycle. Once the precursor is completely inside the matrix, the TIM23 complex reverts back to the resting state (Banerjee et al., 2015).

## 4.2 Conformation of Ssc1 in intact mitochondria

The subunit of the import motor of the TIM23 complex that hydrolyses ATP and thus directly converts the energy of ATP-hydrolysis into translocation of proteins is mtHsp70 or Ssc1. Ssc1 also carries out folding of proteins in the mitochondrial matrix. Both

functions of Ssc1 depend on its ability to undergo regulated conformational changes that are driven by hydrolysis of ATP. Previous studies with different members of the Hsp70 family revealed that ATP-bound Hsp70s have their two domains in close proximity to each other, whereas in ADP and/or substrate bound state the two domains can be in close proximity or separated from each other (Bertelsen et al., 2009; Kityk et al., 2012; Mapa et al., 2010; Sikor et al., 2013). However, all the studies on conformations of Hsp70s have only been carried out in *in vitro* systems with purified proteins. The conformational dynamics of an Hsp70 in an *in vivo* system has not yet been demonstrated.

Study of conformational changes of proteins *in vitro* and *in vivo* is frequently carried out by FRET imaging microscopy. To perform this, proteins are often tagged with fluorescent proteins that constitute FRET pairs, such as GFP and RFP, to analyse *in vivo* intra- and inter-molecular FRET (Bajar et al., 2016). However, this can only be done for proteins that are stable and functional with fluorescent protein tags. Alternately, small molecule fluorophores that form donor-acceptor pair can be attached to the proteins of interest for intra- and inter-molecular FRET analysis. Due to their small size, such fluorophores are less likely to destroy the structural and functional integrity of proteins. Transfer of the fluorophore-labelled proteins into cells is carried out by microinjection. To analyse the conformation of Ssc1 in a more physiologically relevant condition, use of microinjection to transfer fluorophore-labelled Ssc1 into mitochondria of cells, however, would be disadvantageous. This is because the amount of protein that goes inside cell or any organelle after microinjection is difficult to control (Abbaci et al., 2008). In addition, manipulation of nucleotide concentrations is much more difficult in a whole yeast cell in comparison to isolated mitochondria.

Hence, a non-invasive method to analyse the conformation of donor-acceptor fluorophore labelled Ssc1 inside isolated mitochondria was developed. Fluorophore-labelled presequence-containing Ssc1 could not only be imported into and subsequently folded inside mitochondria but also its nucleotide state could be manipulated inside mitochondria. The analysis of the inter-domain communication in Ssc1 inside mitochondria revealed that the two domains of Ssc1 can exist in both docked and undocked state upon ATP depletion. In contrast, in the presence of ATP, two domains of Ssc1 were exclusively undocked. The *in organello* conformation of Ssc1 upon ATP depletion is comparable to previously reported *in vitro* conformation of Ssc1 in the presence of ADP (Mapa et al., 2010; Sikor et al., 2013). On the contrary, the conformation of Ssc1 in presence of ATP *in organello* is opposite to the docked state that

was found *in vitro*. Instead, the *in organello* conformation of Ssc1 in ATP state is comparable to that of peptide substrate-bound state of Ssc1 *in vitro*. This suggests that, in the presence of ATP, Ssc1 readily binds to substrates present inside mitochondria. It is tempting to speculate that Ssc1 inside mitochondria is completely engaged in chaperoning activity and even little disturbances would be sufficient to collapse the mitochondrial proteostasis.

I also analysed the conformation of Ssc1 inside mitochondria that lacked one of Ssc1 cochaperones. Mdj1 assists Ssc1 in recognition of substrate and stimulates the ATPase activity of Ssc1 upon substrate binding. Inactive Mdj1 will, therefore, reduce substrate binding and/or ATP hydrolysis in Ssc1, which would result in increased levels of ATP-bound form of Ssc1. Indeed, in mitochondria containing inactivated Mdj1, increased levels of Ssc1 molecules in high FRET population, corresponding to the *in vitro* ATP-bound form, were found. A low FRET population, corresponding to substrate-bound state was also present, in agreement with the notion that Hsp70s possess a basal ATP hydrolysis rate and are able to bind substrates also in the absence of J proteins. On the other hand, in the absence of an active nucleotide exchange factor, an increase in substrate bound form of Ssc1 is expected as exchange of ADP to ATP in Ssc1 will be impaired and thereby also release of bound substrates. As postulated, in mitochondria containing inactive Mge1, essentially only the substrate bound form of Ssc1 was detected. Overall, a non-invasive tool to analyse the conformation of Ssc1 in intact mitochondria was developed. This tool can be further used to study the dynamics of the lid in substrate binding domain of Ssc1 and can also be extended to study the conformational dynamics of other proteins that are targeted to mitochondrial matrix.

## 5. Summary

Mitochondria contain their own genome and a complete apparatus for its expression. However, mitochondrial DNA codes for a very limited number of proteins so that about 99% of the proteins that are found in mitochondria are encoded by nuclear genome, translated in cytosol as precursor proteins and transported into different subcompartments of mitochondria with the help of several protein complexes known as protein translocases. Over 50% of mitochondrial proteins are translocated by the TIM23 complex. The TIM23 complex is the major protein translocase of mitochondrial inner membrane that uses the energy of membrane potential across the inner membrane and ATP in the matrix to transport proteins across and insert them into the inner membrane. It is comprised of at least 11 protein subunits that can be functionally classified into the receptors, translocation channel and the import motor of the complex. This study provides novel insights into the molecular mechanisms of protein translocation into mitochondrial matrix by the TIM23 complex.

Tim44 is a component of the TIM23 complex found at the matrix side of the inner membrane where it is ideally positioned to connect the translocation channel in inner membrane with the matrix-exposed import motor. The study carried out here demonstrates that the two-domain structure of Tim44 has an essential role in communication between the translocation channel and the import motor. The N-terminal domain interacts with the components of the import motor whereas the C-terminal domain of Tim44 interacts with entering precursor and with the channel subunit, Tim17. The importance of the C-terminal domain of Tim44 is further supported by the finding that carriers of a mutation P308Q in C-terminal domain of human Tim44 develop familial thyroid cancer. The corresponding mutation in yeast, P282Q, showed no obvious growth or import defects, however, the recombinantly expressed and purified protein was less stable than the wild type protein providing potential hints into the molecular mechanisms of the disease. To map the binding site of Tim17 on Tim44, the available crystal structure of C-terminal domain of Tim44 was used to identify conserved, surface-exposed residues. Mutation of D345 and Q372 showed growth defect in yeast and impaired interaction between the channel and import motor of TIM23 complex. However, no positive evidence was found for their direct involvement in Tim17-Tim44 interaction. From the Tim17 side, a loop between transmembrane segments TM3 and TM4 of Tim17 was found

to be the binding site of Tim44. Further mapping of the surface of the C-terminal domain of Tim44 identified a surface that is in close vicinity of the mitochondrial Hsp70 (mtHsp70 or Ssc1) *in vivo*.

Overall, the study here establishes that the two domains of Tim44 have different interaction partners within the TIM23 complex. Based on these findings, a model was proposed in which rearrangements of the two domains of Tim44 drive unidirectional import of proteins into mitochondrial matrix from cytosol.

Tim44 recruits different subunits of the import motor to the translocation channel of the TIM23 complex, including the ATP-consuming subunit Ssc1. Ssc1 is an essential protein that belongs to Hsp70 family of molecular chaperones. A small population of Ssc1 is recruited to the matrix side of the TIM23 complex where it is involved in protein translocation. The majority of Ssc1 is present in the matrix where it plays an essential role in folding of proteins. Both functions of Ssc1 depend on ATP-hydrolysis driven conformational changes of the nucleotide binding domain (NBD) and the substrate binding domain (SBD) that are stimulated by cochaperones. I developed a method to analyse the conformation of Ssc1 inside mitochondria. The analysis carried out revealed that the two domains are undocked from each other in the presence of ATP and are found in both docked and undocked state when mitochondrial ATP was depleted prior to the analysis. Comparison of these results with previously analysed conformations of Ssc1 *in vitro* suggests that, *in organello*, the conformation of Ssc1 in the presence of ATP is similar to substrate-bound state of Ssc1 *in vitro*. Ssc1 thus appears to be exhaustively engaged in chaperoning function inside the mitochondrial matrix. Analysis of conformation of Ssc1 in mitochondria lacking active co-chaperones showed Ssc1 trapped in specific conformational states due to blockage in specific steps of the chaperone cycle. This newly developed method provides first hints into the conformational dynamics of Ssc1 under physiologically relevant conditions and opens the way for a more systematic analysis.

## 6. Zusammenfassung

Mitochondrien besitzen ein eigenes Genom und einen vollständigen Genexpressionsapparat. Dennoch kodiert die mitochondriale DNA nur für eine geringe Anzahl an Proteinen, sodass ca. 99% der Proteine, die in Mitochondrien vorzufinden sind, im Zellkern kodiert sind. Diese werden als Vorstufenproteine im Zytosol translatiert und anschließend mit Hilfe von mehreren Proteinkomplexen, sogenannten Translokasen, in die verschiedenen Subkompartimente der Mitochondrien transportiert. Über 50% der mitochondrialen Proteine werden mit Hilfe des TIM23 Komplexes importiert, welcher die zentrale Proteintranslokase der inneren Mitochondrienmembran darstellt. Der TIM23 Komplex nutzt die Energie des Membranpotentials und ATP in der Mitochondrienmatrix, um Proteine über die innere Membran zu transportieren oder in diese zu inserieren. Der Komplex besteht aus mindestens 11 verschiedenen Proteinuntereinheiten, die funktionell als Rezeptoren und/oder Bestandteile des Translokationskanals und des Importmotors eingeteilt werden können. Diese Arbeit liefert neue Erkenntnisse über die molekularen Mechanismen der Proteintranslokation in die mitochondriale Matrix durch den TIM23 Komplex.

Tim44 ist eine Komponente des TIM23 Komplexes, die auf der Matrixseite der inneren Membran zu finden ist. Dort ist Tim44 ideal positioniert, um den Translokationskanal in der inneren Membran mit dem zur Matrix-exponierten Importmotor zu verbinden. Die durchgeführte Arbeit demonstriert, dass die Zweidomänen-Struktur von Tim44 eine essentielle Rolle in der Kommunikation zwischen Translokationskanal und Importmotor spielt. Die N-terminale Domäne von Tim44 interagiert mit den Komponenten des Importmotors, wohingegen die C-terminale Domäne mit dem eintretenden Vorstufenprotein und der Kanaluntereinheit Tim17 interagiert. Die Relevanz der C-terminalen Domäne wird außerdem durch die Beobachtung untermauert, dass Träger der Mutation P308Q in der C-terminalen Domäne des humanen Tim44 familiären Schilddrüsenkrebs entwickelten. Die entsprechende Mutation in Hefe, P282Q, zeigte keine Wachstums- oder Importdefekte, jedoch war das rekombinant exprimierte und aufgereinigte Protein weniger stabil als das Wildtyp-Protein, was potentielle Hinweise auf die molekularen Mechanismen der Krankheit liefert. Um die Bindungsstelle von Tim17 an Tim44 zu ermitteln, wurde die verfügbare Kristallstruktur der C-terminalen Domäne

von Tim44 genutzt, um konservierte, Oberflächen-exponierte Aminosäurereste zu identifizieren. Mutation von D345 und Q372 erzeugte einen Wachstumsdefekt in Hefe und eine gestörte Interaktion zwischen dem Kanal und dem Importmotor des TIM23 Komplexes. Eine direkte Beteiligung der untersuchten Aminosäuren an der Tim17-Tim44-Interaktion konnte durch die Mutationsanalyse jedoch nicht nachgewiesen werden. In Tim17 wurde eine Schleife zwischen den Transmembransegmenten TM3 und TM4 als Bindungsstelle an Tim44 gefunden. Bei genauerer Untersuchung der Oberflächenstruktur der C-terminalen Domäne von Tim44 wurde zudem eine Oberflächenregion identifiziert, die sich *in vivo* in unmittelbarer Nähe von mitochondrialem Hsp70 (mtHsp70 oder Ssc1) befindet.

Insgesamt etabliert die vorliegende Arbeit, dass die zwei Domänen von Tim44 verschiedene Interaktionspartner innerhalb des TIM23 Komplexes besitzen. Basierend auf diesen Erkenntnissen wird ein Modell vorgeschlagen, in dem die Umlagerungen der zwei Domänen von Tim44 den unidirektionalen Proteinimport vom Zytosol in die mitochondriale Matrix antreiben.

Tim44 rekrutiert verschiedene Untereinheiten des Importmotors zum Translokationskanal des TIM23 Komplexes, einschließlich der ATP-verbrauchenden Untereinheit Ssc1. Ssc1 ist ein essentielles Protein, das zur Hsp70-Familie der molekularen Chaperone gehört. Ein Teil von Ssc1 wird zur Matrixseite des TIM23 Komplexes rekrutiert, wo es an der Proteintranslokation beteiligt ist. Der überwiegende Anteil befindet sich jedoch in der Mitochondrienmatrix und spielt dort eine essentielle Rolle bei der Faltung von Proteinen. Beide Funktionen von Ssc1 sind abhängig von Konformationsänderungen der Nukleotidbindungsdomäne (NBD) und der Substratbindungsdomäne (SBD), die durch die Hydrolyse von ATP angetrieben und von Co-Chaperonen stimuliert werden. In dieser Arbeit wurde eine Methode etabliert, um die Konformation von Ssc1 innerhalb von Mitochondrien zu analysieren. Die durchgeführte Analyse ergab, dass die zwei Domänen in Anwesenheit von ATP voneinander entkoppelt sind und in ATP-depletierten Mitochondrien sowohl im gekoppelten, als auch im entkoppelten Zustand vorliegen. Der Vergleich dieser Ergebnisse mit bereits analysierten *in vitro* Konformationen von Ssc1 deutet darauf hin, dass die Konformation von Ssc1 *in organello* in Anwesenheit von ATP ähnlich zu der substratgebundenen Konformation von Ssc1 *in vitro* ist. Ssc1 scheint daher in der mitochondrialen Matrix vollständig in die Chaperonfunktion involviert zu sein. Die

Konformationsanalyse von Ssc1 in Mitochondrien, die keine aktiven Co-Chaperone enthielten, zeigte Ssc1 in spezifischen Konformationen fixiert, die aufgrund der Blockade des Chaperonzyklus entstehen. Diese neuentwickelte Methode liefert daher erste Hinweise auf die konformationelle Dynamik von Ssc1 unter physiologisch relevanten Bedingungen und ebnet den Weg für eine detailliertere systematische Analyse.

## 7. References

- Abbaci, M., Barberi-Heyob, M., Blondel, W., Guillemin, F., and Didelon, J. (2008). Advantages and limitations of commonly used methods to assay the molecular permeability of gap junctional intercellular communication. *BioTechniques* *45*, 33-52, 56-62.
- Ahting, U., Thieffry, M., Engelhardt, H., Hegerl, R., Neupert, W., and Nussberger, S. (2001). Tom40, the pore-forming component of the protein-conducting TOM channel in the outer membrane of mitochondria. *The Journal of cell biology* *153*, 1151-1160.
- Ahting, U., Thun, C., Hegerl, R., Typke, D., Nargang, F.E., Neupert, W., and Nussberger, S. (1999). The TOM core complex: the general protein import pore of the outer membrane of mitochondria. *The Journal of cell biology* *147*, 959-968.
- Alder, N.N., Jensen, R.E., and Johnson, A.E. (2008). Fluorescence mapping of mitochondrial TIM23 complex reveals a water-facing, substrate-interacting helix surface. *Cell* *134*, 439-450.
- Bajaj, R., Munari, F., Becker, S., and Zweckstetter, M. (2014). Interaction of the intermembrane space domain of Tim23 protein with mitochondrial membranes. *The Journal of biological chemistry* *289*, 34620-34626.
- Bajar, B.T., Wang, E.S., Zhang, S., Lin, M.Z., and Chu, J. (2016). A Guide to Fluorescent Protein FRET Pairs. *Sensors* *16*.
- Baker, M.J., Mooga, V.P., Guiard, B., Langer, T., Ryan, M.T., and Stojanovski, D. (2012). Impaired folding of the mitochondrial small TIM chaperones induces clearance by the i-AAA protease. *Journal of molecular biology* *424*, 227-239.
- Baker, M.J., Webb, C.T., Stroud, D.A., Palmer, C.S., Frazier, A.E., Guiard, B., Chacinska, A., Gulbis, J.M., and Ryan, M.T. (2009). Structural and functional requirements for activity of the Tim9-Tim10 complex in mitochondrial protein import. *Molecular biology of the cell* *20*, 769-779.
- Banci, L., Bertini, I., Calderone, V., Cefaro, C., Ciofi-Baffoni, S., Gallo, A., Kallergi, E., Lionaki, E., Pozidis, C., and Tokatlidis, K. (2011). Molecular recognition and substrate mimicry drive the electron-transfer process between MIA40 and ALR. *Proceedings of the National Academy of Sciences of the United States of America* *108*, 4811-4816.
- Banci, L., Bertini, I., Cefaro, C., Cenacchi, L., Ciofi-Baffoni, S., Felli, I.C., Gallo, A., Gonnelli, L., Luchinat, E., Sideris, D., *et al.* (2010). Molecular chaperone function of Mia40 triggers consecutive induced folding steps of the substrate in mitochondrial protein import. *Proceedings of the National Academy of Sciences of the United States of America* *107*, 20190-20195.
- Banci, L., Bertini, I., Cefaro, C., Ciofi-Baffoni, S., Gallo, A., Martinelli, M., Sideris, D.P., Ktrakili, N., and Tokatlidis, K. (2009). MIA40 is an oxidoreductase that catalyzes oxidative protein folding in mitochondria. *Nature structural & molecular biology* *16*, 198-206.
- Banerjee, R., Gladkova, C., Mapa, K., Witte, G., and Mokranjac, D. (2015). Protein translocation channel of mitochondrial inner membrane and matrix-exposed import motor communicate via two-domain coupling protein. *eLife* *4*, e11897.
- Banerjee, R., Jayaraj, G.G., Peter, J.J., Kumar, V., and Mapa, K. (2016). Monitoring conformational heterogeneity of the lid of DnaK substrate-binding domain during its chaperone cycle. *The FEBS journal* *283*, 2853-2868.
- Bausewein, T., Mills, D.J., Langer, J.D., Nitschke, B., Nussberger, S., and Kuhlbrandt, W. (2017). Cryo-EM Structure of the TOM Core Complex from *Neurospora crassa*. *Cell* *170*, 693-700 e697.
- Becker, T., Wenz, L.S., Kruger, V., Lehmann, W., Muller, J.M., Goroncy, L., Zufall, N., Lithgow, T., Guiard, B., Chacinska, A., *et al.* (2011). The mitochondrial import protein Mim1 promotes biogenesis of multispinning outer membrane proteins. *The Journal of cell biology* *194*, 387-395.
- Bertelsen, E.B., Chang, L., Gestwicki, J.E., and Zuiderweg, E.R. (2009). Solution conformation of wild-type *E. coli* Hsp70 (DnaK) chaperone complexed with ADP and substrate. *Proceedings of the National Academy of Sciences of the United States of America* *106*, 8471-8476.

- Berthold, J., Bauer, M.F., Schneider, H.C., Klaus, C., Dietmeier, K., Neupert, W., and Brunner, M. (1995). The MIM complex mediates preprotein translocation across the mitochondrial inner membrane and couples it to the mt-Hsp70/ATP driving system. *Cell* 81, 1085-1093.
- Beverly, K.N., Sawaya, M.R., Schmid, E., and Koehler, C.M. (2008). The Tim8-Tim13 complex has multiple substrate binding sites and binds cooperatively to Tim23. *Journal of molecular biology* 382, 1144-1156.
- Bien, M., Longen, S., Wagener, N., Chwalla, I., Herrmann, J.M., and Riemer, J. (2010). Mitochondrial disulfide bond formation is driven by intersubunit electron transfer in Erv1 and proofread by glutathione. *Molecular cell* 37, 516-528.
- Blamowska, M., Sichting, M., Mapa, K., Mokranjac, D., Neupert, W., and Hell, K. (2010). ATPase domain and interdomain linker play a key role in aggregation of mitochondrial Hsp70 chaperone Ssc1. *The Journal of biological chemistry* 285, 4423-4431.
- Blobel, G. (1980). Intracellular protein topogenesis. *Proceedings of the National Academy of Sciences of the United States of America* 77, 1496-1500.
- Bohnert, M., Rehling, P., Guiard, B., Herrmann, J.M., Pfanner, N., and van der Laan, M. (2010). Cooperation of stop-transfer and conservative sorting mechanisms in mitochondrial protein transport. *Current biology : CB* 20, 1227-1232.
- Bolliger, L., Deloche, O., Glick, B.S., Georgopoulos, C., Jenö, P., Kronidou, N., Horst, M., Morishima, N., and Schatz, G. (1994). A mitochondrial homolog of bacterial GrpE interacts with mitochondrial hsp70 and is essential for viability. *The EMBO journal* 13, 1998-2006.
- Bonora, E., Evangelisti, C., Bonichon, F., Tallini, G., and Romeo, G. (2006). Novel germline variants identified in the inner mitochondrial membrane transporter TIMM44 and their role in predisposition to oncocytic thyroid carcinomas. *British journal of cancer* 95, 1529-1536.
- Bradford, M.M. (1976). A rapid and sensitive method for the quantitation of microgram quantities of protein utilizing the principle of protein-dye binding. *Analytical biochemistry* 72, 248-254.
- Burri, L., Vascotto, K., Fredersdorf, S., Tiedt, R., Hall, M.N., and Lithgow, T. (2004). Zim17, a novel zinc finger protein essential for protein import into mitochondria. *The Journal of biological chemistry* 279, 50243-50249.
- Cabral, F., and Schatz, G. (1978). Identification of cytochrome c oxidase subunits in nuclear yeast mutants lacking the functional enzyme. *The Journal of biological chemistry* 253, 4396-4401.
- Callegari, S., Richter, F., Chojnacka, K., Jans, D.C., Lorenzi, I., Pacheu-Grau, D., Jakobs, S., Lenz, C., Urlaub, H., Dudek, J., *et al.* (2016). TIM29 is a subunit of the human carrier translocase required for protein transport. *FEBS letters* 590, 4147-4158.
- Casadaban, M.J., and Cohen, S.N. (1980). Analysis of gene control signals by DNA fusion and cloning in *Escherichia coli*. *Journal of molecular biology* 138, 179-207.
- Chacinska, A., Koehler, C.M., Milenkovic, D., Lithgow, T., and Pfanner, N. (2009). Importing mitochondrial proteins: machineries and mechanisms. *Cell* 138, 628-644.
- Chacinska, A., Lind, M., Frazier, A.E., Dudek, J., Meisinger, C., Geissler, A., Sickmann, A., Meyer, H.E., Truscott, K.N., Guiard, B., *et al.* (2005). Mitochondrial presequence translocase: switching between TOM tethering and motor recruitment involves Tim21 and Tim17. *Cell* 120, 817-829.
- Chacinska, A., Pfannschmidt, S., Wiedemann, N., Kozjak, V., Sanjuan Szklarz, L.K., Schulze-Specking, A., Truscott, K.N., Guiard, B., Meisinger, C., and Pfanner, N. (2004). Essential role of Mia40 in import and assembly of mitochondrial intermembrane space proteins. *The EMBO journal* 23, 3735-3746.
- Chacinska, A., van der Laan, M., Mehnert, C.S., Guiard, B., Mick, D.U., Hutu, D.P., Truscott, K.N., Wiedemann, N., Meisinger, C., Pfanner, N., *et al.* (2010). Distinct forms of mitochondrial TOM-TIM supercomplexes define signal-dependent states of preprotein sorting. *Molecular and cellular biology* 30, 307-318.
- Chen, S., Schultz, P.G., and Brock, A. (2007). An improved system for the generation and analysis of mutant proteins containing unnatural amino acids in *Saccharomyces cerevisiae*. *Journal of molecular biology* 371, 112-122.
- Ciesielski, G.L., Plotka, M., Manicki, M., Schilke, B.A., Dutkiewicz, R., Sahi, C., Marszalek, J., and Craig, E.A. (2013). Nucleoid localization of Hsp40 Mdj1 is important for its function in maintenance of mitochondrial DNA. *Biochimica et biophysica acta* 1833, 2233-2243.

- D'Silva, P., Liu, Q., Walter, W., and Craig, E.A. (2004). Regulated interactions of mtHsp70 with Tim44 at the translocon in the mitochondrial inner membrane. *Nature structural & molecular biology* *11*, 1084-1091.
- D'Silva, P.D., Schilke, B., Walter, W., Andrew, A., and Craig, E.A. (2003). J protein cochaperone of the mitochondrial inner membrane required for protein import into the mitochondrial matrix. *Proceedings of the National Academy of Sciences of the United States of America* *100*, 13839-13844.
- D'Silva, P.R., Schilke, B., Hayashi, M., and Craig, E.A. (2008). Interaction of the J-protein heterodimer Pam18/Pam16 of the mitochondrial import motor with the translocon of the inner membrane. *Molecular biology of the cell* *19*, 424-432.
- Daum, G., Bohni, P.C., and Schatz, G. (1982a). Import of proteins into mitochondria. Cytochrome b2 and cytochrome c peroxidase are located in the intermembrane space of yeast mitochondria. *The Journal of biological chemistry* *257*, 13028-13033.
- Daum, G., Gasser, S.M., and Schatz, G. (1982b). Import of proteins into mitochondria. Energy-dependent, two-step processing of the intermembrane space enzyme cytochrome b2 by isolated yeast mitochondria. *The Journal of biological chemistry* *257*, 13075-13080.
- de la Cruz, L., Bajaj, R., Becker, S., and Zweckstetter, M. (2010). The intermembrane space domain of Tim23 is intrinsically disordered with a distinct binding region for presequences. *Protein science : a publication of the Protein Society* *19*, 2045-2054.
- Demishtein-Zohary, K., Gunsel, U., Marom, M., Banerjee, R., Neupert, W., Azem, A., and Mokranjac, D. (2017). Role of Tim17 in coupling the import motor to the translocation channel of the mitochondrial presequence translocase. *eLife* *6*.
- Demishtein-Zohary, K., Marom, M., Neupert, W., Mokranjac, D., and Azem, A. (2015). GxxxG motifs hold the TIM23 complex together. *The FEBS journal* *282*, 2178-2186.
- Dickerson, R.E. (1971). The structures of cytochrome c and the rates of molecular evolution. *Journal of molecular evolution* *1*, 26-45.
- Dietmeier, K., Honlinger, A., Bomer, U., Dekker, P.J., Eckerskorn, C., Lottspeich, F., Kubrich, M., and Pfanner, N. (1997). Tom5 functionally links mitochondrial preprotein receptors to the general import pore. *Nature* *388*, 195-200.
- Dimmer, K.S., Papic, D., Schumann, B., Sperl, D., Krumpe, K., Walther, D.M., and Rapaport, D. (2012). A crucial role for Mim2 in the biogenesis of mitochondrial outer membrane proteins. *Journal of cell science* *125*, 3464-3473.
- Donzeau, M., Kaldi, K., Adam, A., Paschen, S., Wannier, G., Guiard, B., Bauer, M.F., Neupert, W., and Brunner, M. (2000). Tim23 links the inner and outer mitochondrial membranes. *Cell* *101*, 401-412.
- Dower, W.J., Miller, J.F., and Ragsdale, C.W. (1988). High efficiency transformation of *E. coli* by high voltage electroporation. *Nucleic acids research* *16*, 6127-6145.
- Duchniewicz, M., Germaniuk, A., Westermann, B., Neupert, W., Schwarz, E., and Marszalek, J. (1999). Dual role of the mitochondrial chaperone Mdj1p in inheritance of mitochondrial DNA in yeast. *Molecular and cellular biology* *19*, 8201-8210.
- Emtage, J.L., and Jensen, R.E. (1993). MAS6 encodes an essential inner membrane component of the yeast mitochondrial protein import pathway. *The Journal of cell biology* *122*, 1003-1012.
- Endo, T., and Yamano, K. (2010). Transport of proteins across or into the mitochondrial outer membrane. *Biochimica et biophysica acta* *1803*, 706-714.
- Endo, T., Yamano, K., and Kawano, S. (2011). Structural insight into the mitochondrial protein import system. *Biochimica et biophysica acta* *1808*, 955-970.
- Fraga, H., Papaleo, E., Vega, S., Velazquez-Campoy, A., and Ventura, S. (2013). Zinc induced folding is essential for TIM15 activity as an mtHsp70 chaperone. *Biochimica et biophysica acta* *1830*, 2139-2149.
- Gambill, B.D., Voos, W., Kang, P.J., Miao, B., Langer, T., Craig, E.A., and Pfanner, N. (1993). A dual role for mitochondrial heat shock protein 70 in membrane translocation of preproteins. *The Journal of cell biology* *123*, 109-117.
- Gebert, M., Schrempp, S.G., Mehnert, C.S., Heisswolf, A.K., Oeljeklaus, S., Ieva, R., Bohnert, M., von der Malsburg, K., Wiese, S., Kleinschroth, T., *et al.* (2012). Mgr2 promotes coupling of

- the mitochondrial presequence translocase to partner complexes. *The Journal of cell biology* *197*, 595-604.
- Gebert, N., Chacinska, A., Wagner, K., Guiard, B., Koehler, C.M., Rehling, P., Pfanner, N., and Wiedemann, N. (2008). Assembly of the three small Tim proteins precedes docking to the mitochondrial carrier translocase. *EMBO reports* *9*, 548-554.
- Gebert, N., Gebert, M., Oeljeklaus, S., von der Malsburg, K., Stroud, D.A., Kulawiak, B., Wirth, C., Zahedi, R.P., Dolezal, P., Wiese, S., *et al.* (2011). Dual function of Sdh3 in the respiratory chain and TIM22 protein translocase of the mitochondrial inner membrane. *Molecular cell* *44*, 811-818.
- Geissler, A., Rassow, J., Pfanner, N., and Voos, W. (2001). Mitochondrial import driving forces: enhanced trapping by matrix Hsp70 stimulates translocation and reduces the membrane potential dependence of loosely folded preproteins. *Molecular and cellular biology* *21*, 7097-7104.
- Gevorkyan-Airapetov, L., Zohary, K., Popov-Celeketic, D., Mapa, K., Hell, K., Neupert, W., Azem, A., and Mokranjac, D. (2009). Interaction of Tim23 with Tim50 Is essential for protein translocation by the mitochondrial TIM23 complex. *The Journal of biological chemistry* *284*, 4865-4872.
- Glaser, F., Pupko, T., Paz, I., Bell, R.E., Bechor-Shental, D., Martz, E., and Ben-Tal, N. (2003). ConSurf: identification of functional regions in proteins by surface-mapping of phylogenetic information. *Bioinformatics* *19*, 163-164.
- Glick, B.S., Brandt, A., Cunningham, K., Muller, S., Hallberg, R.L., and Schatz, G. (1992). Cytochromes c1 and b2 are sorted to the intermembrane space of yeast mitochondria by a stop-transfer mechanism. *Cell* *69*, 809-822.
- Goswami, A.V., Chittoor, B., and D'Silva, P. (2010). Understanding the functional interplay between mammalian mitochondrial Hsp70 chaperone machine components. *The Journal of biological chemistry* *285*, 19472-19482.
- Gratzer, S., Lithgow, T., Bauer, R.E., Lamping, E., Paltauf, F., Kohlwein, S.D., Haucke, V., Junne, T., Schatz, G., and Horst, M. (1995). Mas37p, a novel receptor subunit for protein import into mitochondria. *The Journal of cell biology* *129*, 25-34.
- Grumbt, B., Stroobant, V., Terziyska, N., Israel, L., and Hell, K. (2007). Functional characterization of Mia40p, the central component of the disulfide relay system of the mitochondrial intermembrane space. *The Journal of biological chemistry* *282*, 37461-37470.
- Handa, N., Kishishita, S., Morita, S., Akasaka, R., Jin, Z., Chrzas, J., Chen, L., Liu, Z.J., Wang, B.C., Sugano, S., *et al.* (2007). Structure of the human Tim44 C-terminal domain in complex with pentaethylene glycol: ligand-bound form. *Acta crystallographica Section D, Biological crystallography* *63*, 1225-1234.
- Hartl, F.U., Bracher, A., and Hayer-Hartl, M. (2011). Molecular chaperones in protein folding and proteostasis. *Nature* *475*, 324-332.
- Heiss, G. (2011). Single-molecule microscopy study of nano-systems.
- Hell, K., Herrmann, J., Pratje, E., Neupert, W., and Stuart, R.A. (1997). Oxa1p mediates the export of the N- and C-termini of pCoxII from the mitochondrial matrix to the intermembrane space. *FEBS letters* *418*, 367-370.
- Herlan, M., Vogel, F., Bornhovd, C., Neupert, W., and Reichert, A.S. (2003). Processing of Mgm1 by the rhomboid-type protease Pcp1 is required for maintenance of mitochondrial morphology and of mitochondrial DNA. *The Journal of biological chemistry* *278*, 27781-27788.
- Herrmann, J.M., Neupert, W., and Stuart, R.A. (1997). Insertion into the mitochondrial inner membrane of a polytopic protein, the nuclear-encoded Oxa1p. *The EMBO journal* *16*, 2217-2226.
- Herzig, S., and Shaw, R.J. (2018). AMPK: guardian of metabolism and mitochondrial homeostasis. *Nature reviews Molecular cell biology* *19*, 121-135.
- Hines, V., Brandt, A., Griffiths, G., Horstmann, H., Brutsch, H., and Schatz, G. (1990). Protein import into yeast mitochondria is accelerated by the outer membrane protein MAS70. *The EMBO journal* *9*, 3191-3200.
- Hohr, A.I.C., Lindau, C., Wirth, C., Qiu, J., Stroud, D.A., Kutik, S., Guiard, B., Hunte, C., Becker, T., Pfanner, N., *et al.* (2018). Membrane protein insertion through a mitochondrial beta-barrel gate. *Science* *359*.

- Honlinger, A., Bomer, U., Alconada, A., Eckerskorn, C., Lottspeich, F., Dietmeier, K., and Pfanner, N. (1996). Tom7 modulates the dynamics of the mitochondrial outer membrane translocase and plays a pathway-related role in protein import. *The EMBO journal* *15*, 2125-2137.
- Ieva, R., Schrempp, S.G., Opalinski, L., Wollweber, F., Hoss, P., Heisswolf, A.K., Gebert, M., Zhang, Y., Guiard, B., Rospert, S., *et al.* (2014). Mgr2 functions as lateral gatekeeper for preprotein sorting in the mitochondrial inner membrane. *Molecular cell* *56*, 641-652.
- Jarvis, P., and Lopez-Juez, E. (2013). Biogenesis and homeostasis of chloroplasts and other plastids. *Nature reviews Molecular cell biology* *14*, 787-802.
- Jensen, R.E., and Dunn, C.D. (2002). Protein import into and across the mitochondrial inner membrane: role of the TIM23 and TIM22 translocases. *Biochimica et biophysica acta* *1592*, 25-34.
- Jores, T., Klinger, A., Gross, L.E., Kawano, S., Flinner, N., Duchardt-Ferner, E., Wohnert, J., Kalbacher, H., Endo, T., Schleiff, E., *et al.* (2016). Characterization of the targeting signal in mitochondrial beta-barrel proteins. *Nature communications* *7*, 12036.
- Josyula, R., Jin, Z., Fu, Z., and Sha, B. (2006). Crystal structure of yeast mitochondrial peripheral membrane protein Tim44p C-terminal domain. *Journal of molecular biology* *359*, 798-804.
- Kang, Y., Baker, M.J., Liem, M., Louber, J., McKenzie, M., Atukorala, I., Ang, C.S., Keerthikumar, S., Mathivanan, S., and Stojanovski, D. (2016). Tim29 is a novel subunit of the human TIM22 translocase and is involved in complex assembly and stability. *eLife* *5*.
- Kityk, R., Kopp, J., Sinning, I., and Mayer, M.P. (2012). Structure and dynamics of the ATP-bound open conformation of Hsp70 chaperones. *Molecular cell* *48*, 863-874.
- Koehler, C.M. (2004). The small Tim proteins and the twin Cx3C motif. *Trends in biochemical sciences* *29*, 1-4.
- Kolmakov, K., Belov, V.N., Bierwagen, J., Ringemann, C., Muller, V., Eggeling, C., and Hell, S.W. (2010). Red-emitting rhodamine dyes for fluorescence microscopy and nanoscopy. *Chemistry* *16*, 158-166.
- Kovermann, P., Truscott, K.N., Guiard, B., Rehling, P., Sepuri, N.B., Muller, H., Jensen, R.E., Wagner, R., and Pfanner, N. (2002). Tim22, the essential core of the mitochondrial protein insertion complex, forms a voltage-activated and signal-gated channel. *Molecular cell* *9*, 363-373.
- Kozany, C., Mokranjac, D., Sichting, M., Neupert, W., and Hell, K. (2004). The J domain-related cochaperone Tim16 is a constituent of the mitochondrial TIM23 preprotein translocase. *Nature structural & molecular biology* *11*, 234-241.
- Kozjak, V., Wiedemann, N., Milenkovic, D., Lohaus, C., Meyer, H.E., Guiard, B., Meisinger, C., and Pfanner, N. (2003). An essential role of Sam50 in the protein sorting and assembly machinery of the mitochondrial outer membrane. *The Journal of biological chemistry* *278*, 48520-48523.
- Krieger, F., Moglich, A., and Kiefhaber, T. (2005). Effect of proline and glycine residues on dynamics and barriers of loop formation in polypeptide chains. *Journal of the American Chemical Society* *127*, 3346-3352.
- Krimmer, T., Rassow, J., Kunau, W.H., Voos, W., and Pfanner, N. (2000). Mitochondrial protein import motor: the ATPase domain of matrix Hsp70 is crucial for binding to Tim44, while the peptide binding domain and the carboxy-terminal segment play a stimulatory role. *Molecular and cellular biology* *20*, 5879-5887.
- Kubo, Y., Tsunehiro, T., Nishikawa, S., Nakai, M., Ikeda, E., Toh-e, A., Morishima, N., Shibata, T., and Endo, T. (1999). Two distinct mechanisms operate in the reactivation of heat-denatured proteins by the mitochondrial Hsp70/Mdj1p/Yge1p chaperone system. *Journal of molecular biology* *286*, 447-464.
- Kumazaki, K., Chiba, S., Takemoto, M., Furukawa, A., Nishiyama, K., Sugano, Y., Mori, T., Dohmae, N., Hirata, K., Nakada-Nakura, Y., *et al.* (2014a). Structural basis of Sec-independent membrane protein insertion by YidC. *Nature* *509*, 516-520.
- Kumazaki, K., Kishimoto, T., Furukawa, A., Mori, H., Tanaka, Y., Dohmae, N., Ishitani, R., Tsukazaki, T., and Nureki, O. (2014b). Crystal structure of Escherichia coli YidC, a membrane protein chaperone and insertase. *Scientific reports* *4*, 7299.
- Kunkele, K.P., Heins, S., Dembowski, M., Nargang, F.E., Benz, R., Thieffry, M., Walz, J., Lill, R., Nussberger, S., and Neupert, W. (1998). The preprotein translocation channel of the outer membrane of mitochondria. *Cell* *93*, 1009-1019.

- Kutik, S., Stojanovski, D., Becker, L., Becker, T., Meinecke, M., Kruger, V., Prinz, C., Meisinger, C., Guiard, B., Wagner, R., *et al.* (2008). Dissecting membrane insertion of mitochondrial beta-barrel proteins. *Cell* *132*, 1011-1024.
- Kuzmenko, A., Tankov, S., English, B.P., Tarassov, I., Tenson, T., Kamenski, P., Elf, J., and Hauryliuk, V. (2011). Single molecule tracking fluorescence microscopy in mitochondria reveals highly dynamic but confined movement of Tom40. *Scientific reports* *1*, 195.
- Laemmli, U.K. (1970). Cleavage of structural proteins during the assembly of the head of bacteriophage T4. *Nature* *227*, 680-685.
- Landau, M., Mayrose, I., Rosenberg, Y., Glaser, F., Martz, E., Pupko, T., and Ben-Tal, N. (2005). ConSurf 2005: the projection of evolutionary conservation scores of residues on protein structures. *Nucleic acids research* *33*, W299-302.
- Lewrenz, I., Rietzschel, N., Guiard, B., Lill, R., van der Laan, M., and Voos, W. (2013). The functional interaction of mitochondrial Hsp70s with the escort protein Zim17 is critical for Fe/S biogenesis and substrate interaction at the inner membrane preprotein translocase. *The Journal of biological chemistry* *288*, 30931-30943.
- Li, J., and Sha, B. (2015). The structure of Tim50(164-361) suggests the mechanism by which Tim50 receives mitochondrial presequences. *Acta crystallographica Section F, Structural biology communications* *71*, 1146-1151.
- Lithgow, T., Junne, T., Suda, K., Gratzer, S., and Schatz, G. (1994). The mitochondrial outer membrane protein Mas22p is essential for protein import and viability of yeast. *Proceedings of the National Academy of Sciences of the United States of America* *91*, 11973-11977.
- Liu, Q., D'Silva, P., Walter, W., Marszalek, J., and Craig, E.A. (2003). Regulated cycling of mitochondrial Hsp70 at the protein import channel. *Science* *300*, 139-141.
- Liu, Q., and Hendrickson, W.A. (2007). Insights into Hsp70 chaperone activity from a crystal structure of the yeast Hsp110 Sse1. *Cell* *131*, 106-120.
- Liu, Q., Krzewska, J., Liberek, K., and Craig, E.A. (2001). Mitochondrial Hsp70 Ssc1: role in protein folding. *The Journal of biological chemistry* *276*, 6112-6118.
- Lutz, T., Neupert, W., and Herrmann, J.M. (2003). Import of small Tim proteins into the mitochondrial intermembrane space. *The EMBO journal* *22*, 4400-4408.
- Malhotra, K., Modak, A., Nangia, S., Daman, T.H., Gunsell, U., Robinson, V.L., Mokranjac, D., May, E.R., and Alder, N.N. (2017). Cardiolipin mediates membrane and channel interactions of the mitochondrial TIM23 protein import complex receptor Tim50. *Science advances* *3*, e1700532.
- Malhotra, K., Sathappa, M., Landin, J.S., Johnson, A.E., and Alder, N.N. (2013). Structural changes in the mitochondrial Tim23 channel are coupled to the proton-motive force. *Nature structural & molecular biology* *20*, 965-972.
- Mapa, K. (2009). Conformational Dynamics of the Mitochondrial TIM23 Preprotein Translocase.
- Mapa, K., Sikor, M., Kudryavtsev, V., Waegemann, K., Kalinin, S., Seidel, C.A., Neupert, W., Lamb, D.C., and Mokranjac, D. (2010). The conformational dynamics of the mitochondrial Hsp70 chaperone. *Molecular cell* *38*, 89-100.
- Marada, A., Allu, P.K., Murari, A., PullaReddy, B., Tammineni, P., Thiriveedi, V.R., Danduprolu, J., and Sepuri, N.B. (2013). Mge1, a nucleotide exchange factor of Hsp70, acts as an oxidative sensor to regulate mitochondrial Hsp70 function. *Molecular biology of the cell* *24*, 692-703.
- Marom, M., Azem, A., and Mokranjac, D. (2011a). Understanding the molecular mechanism of protein translocation across the mitochondrial inner membrane: still a long way to go. *Biochimica et biophysica acta* *1808*, 990-1001.
- Marom, M., Dayan, D., Demishtein-Zohary, K., Mokranjac, D., Neupert, W., and Azem, A. (2011b). Direct interaction of mitochondrial targeting presequences with purified components of the TIM23 protein complex. *The Journal of biological chemistry* *286*, 43809-43815.
- Marom, M., Safonov, R., Amram, S., Avneon, Y., Nachliel, E., Gutman, M., Zohary, K., Azem, A., and Tsfadia, Y. (2009). Interaction of the Tim44 C-terminal domain with negatively charged phospholipids. *Biochemistry* *48*, 11185-11195.
- Martinez-Caballero, S., Grigoriev, S.M., Herrmann, J.M., Campo, M.L., and Kinnally, K.W. (2007). Tim17p regulates the twin pore structure and voltage gating of the mitochondrial protein import complex TIM23. *The Journal of biological chemistry* *282*, 3584-3593.

- Mayer, A., Nargang, F.E., Neupert, W., and Lill, R. (1995). MOM22 is a receptor for mitochondrial targeting sequences and cooperates with MOM19. *The EMBO journal* *14*, 4204-4211.
- Mayer, M.P. (2013). Hsp70 chaperone dynamics and molecular mechanism. *Trends in biochemical sciences* *38*, 507-514.
- Meier, S., Neupert, W., and Herrmann, J.M. (2005). Conserved N-terminal negative charges in the Tim17 subunit of the TIM23 translocase play a critical role in the import of preproteins into mitochondria. *The Journal of biological chemistry* *280*, 7777-7785.
- Miao, B., Davis, J.E., and Craig, E.A. (1997). Mge1 functions as a nucleotide release factor for Ssc1, a mitochondrial Hsp70 of *Saccharomyces cerevisiae*. *Journal of molecular biology* *265*, 541-552.
- Mick, D.U., Dennerlein, S., Wiese, H., Reinhold, R., Pacheu-Grau, D., Lorenzi, I., Sasarman, F., Weraarpachai, W., Shoubbridge, E.A., Warscheid, B., *et al.* (2012). MITRAC links mitochondrial protein translocation to respiratory-chain assembly and translational regulation. *Cell* *151*, 1528-1541.
- Milenkovic, D., Kozjak, V., Wiedemann, N., Lohaus, C., Meyer, H.E., Guiard, B., Pfanner, N., and Meisinger, C. (2004). Sam35 of the mitochondrial protein sorting and assembly machinery is a peripheral outer membrane protein essential for cell viability. *The Journal of biological chemistry* *279*, 22781-22785.
- Miyata, N., Tang, Z., Conti, M.A., Johnson, M.E., Douglas, C.J., Hasson, S.A., Damoiseaux, R., Chang, C.A., and Koehler, C.M. (2017). Adaptation of a Genetic Screen Reveals an Inhibitor for Mitochondrial Protein Import Component Tim44. *The Journal of biological chemistry* *292*, 5429-5442.
- Moczko, M., Gartner, F., and Pfanner, N. (1993). The protein import receptor MOM19 of yeast mitochondria. *FEBS letters* *326*, 251-254.
- Model, K., Meisinger, C., and Kuhlbrandt, W. (2008). Cryo-electron microscopy structure of a yeast mitochondrial preprotein translocase. *Journal of molecular biology* *383*, 1049-1057.
- Model, K., Prinz, T., Ruiz, T., Radermacher, M., Krimmer, T., Kuhlbrandt, W., Pfanner, N., and Meisinger, C. (2002). Protein translocase of the outer mitochondrial membrane: role of import receptors in the structural organization of the TOM complex. *Journal of molecular biology* *316*, 657-666.
- Mokranjac, D., Berg, A., Adam, A., Neupert, W., and Hell, K. (2007). Association of the Tim14.Tim16 subcomplex with the TIM23 translocase is crucial for function of the mitochondrial protein import motor. *The Journal of biological chemistry* *282*, 18037-18045.
- Mokranjac, D., Bourenkov, G., Hell, K., Neupert, W., and Groll, M. (2006). Structure and function of Tim14 and Tim16, the J and J-like components of the mitochondrial protein import motor. *The EMBO journal* *25*, 4675-4685.
- Mokranjac, D., and Neupert, W. (2009). Thirty years of protein translocation into mitochondria: unexpectedly complex and still puzzling. *Biochimica et biophysica acta* *1793*, 33-41.
- Mokranjac, D., and Neupert, W. (2010). The many faces of the mitochondrial TIM23 complex. *Biochimica et biophysica acta* *1797*, 1045-1054.
- Mokranjac, D., Paschen, S.A., Kozany, C., Prokisch, H., Hoppins, S.C., Nargang, F.E., Neupert, W., and Hell, K. (2003a). Tim50, a novel component of the TIM23 preprotein translocase of mitochondria. *The EMBO journal* *22*, 816-825.
- Mokranjac, D., Sichtung, M., Neupert, W., and Hell, K. (2003b). Tim14, a novel key component of the import motor of the TIM23 protein translocase of mitochondria. *The EMBO journal* *22*, 4945-4956.
- Mokranjac, D., Sichtung, M., Popov-Celeketic, D., Berg, A., Hell, K., and Neupert, W. (2005). The import motor of the yeast mitochondrial TIM23 preprotein translocase contains two different J proteins, Tim14 and Mdj2. *The Journal of biological chemistry* *280*, 31608-31614.
- Mokranjac, D., Sichtung, M., Popov-Celeketic, D., Mapa, K., Gevorkyan-Airapetov, L., Zohary, K., Hell, K., Azem, A., and Neupert, W. (2009). Role of Tim50 in the transfer of precursor proteins from the outer to the inner membrane of mitochondria. *Molecular biology of the cell* *20*, 1400-1407.

- Mordas, A., and Tokatlidis, K. (2015). The MIA pathway: a key regulator of mitochondrial oxidative protein folding and biogenesis. *Accounts of chemical research* 48, 2191-2199.
- Moro, F., Okamoto, K., Donzeau, M., Neupert, W., and Brunner, M. (2002). Mitochondrial protein import: molecular basis of the ATP-dependent interaction of MtHsp70 with Tim44. *The Journal of biological chemistry* 277, 6874-6880.
- Nakai, M., and Endo, T. (1995). Identification of yeast MAS17 encoding the functional counterpart of the mitochondrial receptor complex protein MOM22 of *Neurospora crassa*. *FEBS letters* 357, 202-206.
- Nakai, M., Kato, Y., Ikeda, E., Toh-e, A., and Endo, T. (1994). Yge1p, a eukaryotic Grp-E homolog, is localized in the mitochondrial matrix and interacts with mitochondrial Hsp70. *Biochemical and biophysical research communications* 200, 435-442.
- Neal, S.E., Dabir, D.V., Wijaya, J., Boon, C., and Koehler, C.M. (2017). Osm1 facilitates the transfer of electrons from Erv1 to fumarate in the redox-regulated import pathway in the mitochondrial intermembrane space. *Molecular biology of the cell* 28, 2773-2785.
- Neupert, W., and Herrmann, J.M. (2007). Translocation of proteins into mitochondria. *Annual review of biochemistry* 76, 723-749.
- Nunnari, J., Fox, T.D., and Walter, P. (1993). A mitochondrial protease with two catalytic subunits of nonoverlapping specificities. *Science* 262, 1997-2004.
- Nunnari, J., and Suomalainen, A. (2012). Mitochondria: in sickness and in health. *Cell* 148, 1145-1159.
- Ott, M., Prestele, M., Bauerschmitt, H., Funes, S., Bonnefoy, N., and Herrmann, J.M. (2006). Mba1, a membrane-associated ribosome receptor in mitochondria. *The EMBO journal* 25, 1603-1610.
- Pais, J.E., Schilke, B., and Craig, E.A. (2011). Reevaluation of the role of the Pam18:Pam16 interaction in translocation of proteins by the mitochondrial Hsp70-based import motor. *Molecular biology of the cell* 22, 4740-4749.
- Papic, D., Krumpke, K., Dukanovic, J., Dimmer, K.S., and Rapaport, D. (2011). Multispan mitochondrial outer membrane protein Ugo1 follows a unique Mim1-dependent import pathway. *The Journal of cell biology* 194, 397-405.
- Pareek, G., Krishnamoorthy, V., and D'Silva, P. (2013). Molecular insights revealing interaction of Tim23 and channel subunits of presequence translocase. *Molecular and cellular biology* 33, 4641-4659.
- Paschen, S.A., Waizenegger, T., Stan, T., Preuss, M., Cyrklaff, M., Hell, K., Rapaport, D., and Neupert, W. (2003). Evolutionary conservation of biogenesis of beta-barrel membrane proteins. *Nature* 426, 862-866.
- Pfeffer, S., Woellhaf, M.W., Herrmann, J.M., and Forster, F. (2015). Organization of the mitochondrial translation machinery studied in situ by cryoelectron tomography. *Nature communications* 6, 6019.
- Polier, S., Dragovic, Z., Hartl, F.U., and Bracher, A. (2008). Structural basis for the cooperation of Hsp70 and Hsp110 chaperones in protein folding. *Cell* 133, 1068-1079.
- Popov-Celeketic, D., Mapa, K., Neupert, W., and Mokranjac, D. (2008a). Active remodelling of the TIM23 complex during translocation of preproteins into mitochondria. *The EMBO journal* 27, 1469-1480.
- Popov-Celeketic, D., Waagemann, K., Mapa, K., Neupert, W., and Mokranjac, D. (2011). Role of the import motor in insertion of transmembrane segments by the mitochondrial TIM23 complex. *EMBO reports* 12, 542-548.
- Popov-Celeketic, J., Waizenegger, T., and Rapaport, D. (2008b). Mim1 functions in an oligomeric form to facilitate the integration of Tom20 into the mitochondrial outer membrane. *Journal of molecular biology* 376, 671-680.
- Preuss, M., Leonhard, K., Hell, K., Stuart, R.A., Neupert, W., and Herrmann, J.M. (2001). Mba1, a novel component of the mitochondrial protein export machinery of the yeast *Saccharomyces cerevisiae*. *The Journal of cell biology* 153, 1085-1096.
- Preuss, M., Ott, M., Funes, S., Luirink, J., and Herrmann, J.M. (2005). Evolution of mitochondrial oxa proteins from bacterial YidC. Inherited and acquired functions of a conserved protein insertion machinery. *The Journal of biological chemistry* 280, 13004-13011.

- Prip-Buus, C., Westerman, B., Schmitt, M., Langer, T., Neupert, W., and Schwarz, E. (1996). Role of the mitochondrial DnaJ homologue, Mdj1p, in the prevention of heat-induced protein aggregation. *FEBS letters* 380, 142-146.
- Qi, R., Sarbeng, E.B., Liu, Q., Le, K.Q., Xu, X., Xu, H., Yang, J., Wong, J.L., Vorvis, C., Hendrickson, W.A., *et al.* (2013). Allosteric opening of the polypeptide-binding site when an Hsp70 binds ATP. *Nature structural & molecular biology* 20, 900-907.
- Qian, X., Gebert, M., Hopker, J., Yan, M., Li, J., Wiedemann, N., van der Laan, M., Pfanner, N., and Sha, B. (2011). Structural basis for the function of Tim50 in the mitochondrial presequence translocase. *Journal of molecular biology* 411, 513-519.
- Qiu, J., Wenz, L.S., Zerbes, R.M., Oeljeklaus, S., Bohnert, M., Stroud, D.A., Wirth, C., Ellenrieder, L., Thornton, N., Kutik, S., *et al.* (2013). Coupling of mitochondrial import and export translocases by receptor-mediated supercomplex formation. *Cell* 154, 596-608.
- Rahman, B., Kawano, S., Yunoki-Esaki, K., Anzai, T., and Endo, T. (2014). NMR analyses on the interactions of the yeast Tim50 C-terminal region with the presequence and Tim50 core domain. *FEBS letters* 588, 678-684.
- Ramesh, A., Peleh, V., Martinez-Caballero, S., Wollweber, F., Sommer, F., van der Laan, M., Schroda, M., Alexander, R.T., Campo, M.L., and Herrmann, J.M. (2016). A disulfide bond in the TIM23 complex is crucial for voltage gating and mitochondrial protein import. *The Journal of cell biology* 214, 417-431.
- Rapaport, D. (2005). How does the TOM complex mediate insertion of precursor proteins into the mitochondrial outer membrane? *The Journal of cell biology* 171, 419-423.
- Rapaport, D., and Neupert, W. (1999). Biogenesis of Tom40, core component of the TOM complex of mitochondria. *The Journal of cell biology* 146, 321-331.
- Rehling, P., Brandner, K., and Pfanner, N. (2004). Mitochondrial import and the twin-pore translocase. *Nature reviews Molecular cell biology* 5, 519-530.
- Rehling, P., Model, K., Brandner, K., Kovermann, P., Sickmann, A., Meyer, H.E., Kuhlbrandt, W., Wagner, R., Truscott, K.N., and Pfanner, N. (2003). Protein insertion into the mitochondrial inner membrane by a twin-pore translocase. *Science* 299, 1747-1751.
- Rojo, E.E., Stuart, R.A., and Neupert, W. (1995). Conservative sorting of F<sub>0</sub>-ATPase subunit 9: export from matrix requires delta pH across inner membrane and matrix ATP. *The EMBO journal* 14, 3445-3451.
- Rowley, N., Prip-Buus, C., Westermann, B., Brown, C., Schwarz, E., Barrell, B., and Neupert, W. (1994). Mdj1p, a novel chaperone of the DnaJ family, is involved in mitochondrial biogenesis and protein folding. *Cell* 77, 249-259.
- Ryan, K.R., Leung, R.S., and Jensen, R.E. (1998). Characterization of the mitochondrial inner membrane translocase complex: the Tim23p hydrophobic domain interacts with Tim17p but not with other Tim23p molecules. *Molecular and cellular biology* 18, 178-187.
- Ryan, K.R., Menold, M.M., Garrett, S., and Jensen, R.E. (1994). SMS1, a high-copy suppressor of the yeast mas6 mutant, encodes an essential inner membrane protein required for mitochondrial protein import. *Molecular biology of the cell* 5, 529-538.
- Sakuragi, S., Liu, Q., and Craig, E. (1999). Interaction between the nucleotide exchange factor Mge1 and the mitochondrial Hsp70 Ssc1. *The Journal of biological chemistry* 274, 11275-11282.
- Schendzielorz, A.B., Schulz, C., Lytovchenko, O., Clancy, A., Guiard, B., Ieva, R., van der Laan, M., and Rehling, P. (2017). Two distinct membrane potential-dependent steps drive mitochondrial matrix protein translocation. *The Journal of cell biology* 216, 83-92.
- Schilke, B.A., Hayashi, M., and Craig, E.A. (2012). Genetic analysis of complex interactions among components of the mitochondrial import motor and translocon in *Saccharomyces cerevisiae*. *Genetics* 190, 1341-1353.
- Schiller, D., Cheng, Y.C., Liu, Q., Walter, W., and Craig, E.A. (2008). Residues of Tim44 involved in both association with the translocon of the inner mitochondrial membrane and regulation of mitochondrial Hsp70 tethering. *Molecular and cellular biology* 28, 4424-4433.
- Schneider, H.C., Berthold, J., Bauer, M.F., Dietmeier, K., Guiard, B., Brunner, M., and Neupert, W. (1994). Mitochondrial Hsp70/MIM44 complex facilitates protein import. *Nature* 371, 768-774.

- Sherman, E.L., Go, N.E., and Nargang, F.E. (2005). Functions of the small proteins in the TOM complex of *Neurospora crassa*. *Molecular biology of the cell* *16*, 4172-4182.
- Shiota, T., Imai, K., Qiu, J., Hewitt, V.L., Tan, K., Shen, H.H., Sakiyama, N., Fukasawa, Y., Hayat, S., Kamiya, M., *et al.* (2015). Molecular architecture of the active mitochondrial protein gate. *Science* *349*, 1544-1548.
- Shpilka, T., and Haynes, C.M. (2018). The mitochondrial UPR: mechanisms, physiological functions and implications in ageing. *Nature reviews Molecular cell biology* *19*, 109-120.
- Sichting, M., Mokranjac, D., Azem, A., Neupert, W., and Hell, K. (2005). Maintenance of structure and function of mitochondrial Hsp70 chaperones requires the chaperone Hsp1. *The EMBO journal* *24*, 1046-1056.
- Sikor, M., Mapa, K., von Voithenberg, L.V., Mokranjac, D., and Lamb, D.C. (2013). Real-time observation of the conformational dynamics of mitochondrial Hsp70 by spFRET. *The EMBO journal* *32*, 1639-1649.
- Sikorski, R.S., and Hieter, P. (1989). A system of shuttle vectors and yeast host strains designed for efficient manipulation of DNA in *Saccharomyces cerevisiae*. *Genetics* *122*, 19-27.
- Slutsky-Leiderman, O., Marom, M., Iosefson, O., Levy, R., Maoz, S., and Azem, A. (2007). The interplay between components of the mitochondrial protein translocation motor studied using purified components. *The Journal of biological chemistry* *282*, 33935-33942.
- Smith, J.J., and Aitchison, J.D. (2013). Peroxisomes take shape. *Nature reviews Molecular cell biology* *14*, 803-817.
- Sollner, T., Griffiths, G., Pfaller, R., Pfanner, N., and Neupert, W. (1989). MOM19, an import receptor for mitochondrial precursor proteins. *Cell* *59*, 1061-1070.
- Sollner, T., Pfaller, R., Griffiths, G., Pfanner, N., and Neupert, W. (1990). A mitochondrial import receptor for the ADP/ATP carrier. *Cell* *62*, 107-115.
- Stiller, S.B., Hopker, J., Oeljeklaus, S., Schutze, C., Schrempp, S.G., Vent-Schmidt, J., Horvath, S.E., Frazier, A.E., Gebert, N., van der Laan, M., *et al.* (2016). Mitochondrial OXA Translocase Plays a Major Role in Biogenesis of Inner-Membrane Proteins. *Cell metabolism* *23*, 901-908.
- Stojanovski, D., Bragoszewski, P., and Chacinska, A. (2012). The MIA pathway: a tight bond between protein transport and oxidative folding in mitochondria. *Biochimica et biophysica acta* *1823*, 1142-1150.
- Stroud, D.A., Becker, T., Qiu, J., Stojanovski, D., Pfannschmidt, S., Wirth, C., Hunte, C., Guiard, B., Meisinger, C., Pfanner, N., *et al.* (2011). Biogenesis of mitochondrial beta-barrel proteins: the POTRA domain is involved in precursor release from the SAM complex. *Molecular biology of the cell* *22*, 2823-2833.
- Suomalainen, A., and Battersby, B.J. (2018). Mitochondrial diseases: the contribution of organelle stress responses to pathology. *Nature reviews Molecular cell biology* *19*, 77-92.
- Tamura, Y., Harada, Y., Shiota, T., Yamano, K., Watanabe, K., Yokota, M., Yamamoto, H., Sesaki, H., and Endo, T. (2009). Tim23-Tim50 pair coordinates functions of translocators and motor proteins in mitochondrial protein import. *The Journal of cell biology* *184*, 129-141.
- Terziyska, N., Grumbt, B., Bien, M., Neupert, W., Herrmann, J.M., and Hell, K. (2007). The sulfhydryl oxidase Erv1 is a substrate of the Mia40-dependent protein translocation pathway. *FEBS letters* *581*, 1098-1102.
- Terziyska, N., Lutz, T., Kozany, C., Mokranjac, D., Mesecke, N., Neupert, W., Herrmann, J.M., and Hell, K. (2005). Mia40, a novel factor for protein import into the intermembrane space of mitochondria is able to bind metal ions. *FEBS letters* *579*, 179-184.
- Ting, S.Y., Schilke, B.A., Hayashi, M., and Craig, E.A. (2014). Architecture of the TIM23 inner mitochondrial translocon and interactions with the matrix import motor. *The Journal of biological chemistry* *289*, 28689-28696.
- Ting, S.Y., Yan, N.L., Schilke, B.A., and Craig, E.A. (2017). Dual interaction of scaffold protein Tim44 of mitochondrial import motor with channel-forming translocase subunit Tim23. *eLife* *6*.
- Truscott, K.N., Kovermann, P., Geissler, A., Merlin, A., Meijer, M., Driessen, A.J., Rassow, J., Pfanner, N., and Wagner, R. (2001). A presequence- and voltage-sensitive channel of the mitochondrial preprotein translocase formed by Tim23. *Nature structural biology* *8*, 1074-1082.
- Truscott, K.N., Voos, W., Frazier, A.E., Lind, M., Li, Y., Geissler, A., Dudek, J., Muller, H., Sickmann, A., Meyer, H.E., *et al.* (2003). A J-protein is an essential subunit of the presequence

- translocase-associated protein import motor of mitochondria. *The Journal of cell biology* *163*, 707-713.
- Vafai, S.B., and Mootha, V.K. (2012). Mitochondrial disorders as windows into an ancient organelle. *Nature* *491*, 374-383.
- van der Laan, M., Chacinska, A., Lind, M., Perschil, I., Sickmann, A., Meyer, H.E., Guiard, B., Meisinger, C., Pfanner, N., and Rehling, P. (2005). Pam17 is required for architecture and translocation activity of the mitochondrial protein import motor. *Molecular and cellular biology* *25*, 7449-7458.
- van der Laan, M., Wiedemann, N., Mick, D.U., Guiard, B., Rehling, P., and Pfanner, N. (2006). A role for Tim21 in membrane-potential-dependent preprotein sorting in mitochondria. *Current biology : CB* *16*, 2271-2276.
- Waegemann, K., Popov-Celeketic, D., Neupert, W., Azem, A., and Mokranjac, D. (2015). Cooperation of TOM and TIM23 complexes during translocation of proteins into mitochondria. *Journal of molecular biology* *427*, 1075-1084.
- Wagner, K., Gebert, N., Guiard, B., Brandner, K., Truscott, K.N., Wiedemann, N., Pfanner, N., and Rehling, P. (2008). The assembly pathway of the mitochondrial carrier translocase involves four preprotein translocases. *Molecular and cellular biology* *28*, 4251-4260.
- Waizenegger, T., Habib, S.J., Lech, M., Mokranjac, D., Paschen, S.A., Hell, K., Neupert, W., and Rapaport, D. (2004). Tob38, a novel essential component in the biogenesis of beta-barrel proteins of mitochondria. *EMBO reports* *5*, 704-709.
- Waizenegger, T., Schmitt, S., Zivkovic, J., Neupert, W., and Rapaport, D. (2005). Mim1, a protein required for the assembly of the TOM complex of mitochondria. *EMBO reports* *6*, 57-62.
- Wallace, D.C. (2005). A mitochondrial paradigm of metabolic and degenerative diseases, aging, and cancer: a dawn for evolutionary medicine. *Annual review of genetics* *39*, 359-407.
- Wang, X., and Chen, X.J. (2015). A cytosolic network suppressing mitochondria-mediated proteostatic stress and cell death. *Nature* *524*, 481-484.
- Webb, C.T., Gorman, M.A., Lazarou, M., Ryan, M.T., and Gulbis, J.M. (2006). Crystal structure of the mitochondrial chaperone TIM9.10 reveals a six-bladed alpha-propeller. *Molecular cell* *21*, 123-133.
- Weiss, C., Niv, A., and Azem, A. (2002). Two-step purification of mitochondrial Hsp70, Ssc1p, using Mge1(His)(6) immobilized on Ni-agarose. *Protein expression and purification* *24*, 268-273.
- Weiss, C., Oppliger, W., Vergeres, G., Demel, R., Jenö, P., Horst, M., de Kruijff, B., Schatz, G., and Azem, A. (1999). Domain structure and lipid interaction of recombinant yeast Tim44. *Proceedings of the National Academy of Sciences of the United States of America* *96*, 8890-8894.
- Wenz, L.S., Ellenrieder, L., Qiu, J., Bohnert, M., Zufall, N., van der Laan, M., Pfanner, N., Wiedemann, N., and Becker, T. (2015). Sam37 is crucial for formation of the mitochondrial TOM-SAM supercomplex, thereby promoting beta-barrel biogenesis. *The Journal of cell biology* *210*, 1047-1054.
- Westermann, B., Gaume, B., Herrmann, J.M., Neupert, W., and Schwarz, E. (1996). Role of the mitochondrial DnaJ homolog Mdj1p as a chaperone for mitochondrially synthesized and imported proteins. *Molecular and cellular biology* *16*, 7063-7071.
- Westermann, B., and Neupert, W. (1997). Mdj2p, a novel DnaJ homolog in the mitochondrial inner membrane of the yeast *Saccharomyces cerevisiae*. *Journal of molecular biology* *272*, 477-483.
- Westermann, B., Prip-Buus, C., Neupert, W., and Schwarz, E. (1995). The role of the GrpE homologue, Mge1p, in mediating protein import and protein folding in mitochondria. *The EMBO journal* *14*, 3452-3460.
- Wickner, W., and Schekman, R. (2005). Protein translocation across biological membranes. *Science* *310*, 1452-1456.
- Wiedemann, N., and Pfanner, N. (2017). Mitochondrial Machineries for Protein Import and Assembly. *Annual review of biochemistry* *86*, 685-714.
- Wrobel, L., Sokol, A.M., Chojnacka, M., and Chacinska, A. (2016). The presence of disulfide bonds reveals an evolutionarily conserved mechanism involved in mitochondrial protein translocase assembly. *Scientific reports* *6*, 27484.

- Wrobel, L., Topf, U., Bragoszewski, P., Wiese, S., Sztolsztener, M.E., Oeljeklaus, S., Varabyova, A., Lirski, M., Chroscicki, P., Mroczek, S., *et al.* (2015). Mistargeted mitochondrial proteins activate a proteostatic response in the cytosol. *Nature* 524, 485-488.
- Wu, Y., and Sha, B. (2006). Crystal structure of yeast mitochondrial outer membrane translocator member Tom70p. *Nature structural & molecular biology* 13, 589-593.
- Yamamoto, H., Esaki, M., Kanamori, T., Tamura, Y., Nishikawa, S., and Endo, T. (2002). Tim50 is a subunit of the TIM23 complex that links protein translocation across the outer and inner mitochondrial membranes. *Cell* 111, 519-528.
- Yamano, K., Yatsukawa, Y., Esaki, M., Hobbs, A.E., Jensen, R.E., and Endo, T. (2008). Tom20 and Tom22 share the common signal recognition pathway in mitochondrial protein import. *The Journal of biological chemistry* 283, 3799-3807.
- Yano, M., Terada, K., and Mori, M. (2004). Mitochondrial import receptors Tom20 and Tom22 have chaperone-like activity. *The Journal of biological chemistry* 279, 10808-10813.
- Young, J.C., Hoogenraad, N.J., and Hartl, F.U. (2003). Molecular chaperones Hsp90 and Hsp70 deliver preproteins to the mitochondrial import receptor Tom70. *Cell* 112, 41-50.
- Zhu, X., Zhao, X., Burkholder, W.F., Gragerov, A., Ogata, C.M., Gottesman, M.E., and Hendrickson, W.A. (1996). Structural analysis of substrate binding by the molecular chaperone DnaK. *Science* 272, 1606-1614.
- Zhuravleva, A., Clerico, E.M., and Gierasch, L.M. (2012). An interdomain energetic tug-of-war creates the allosterically active state in Hsp70 molecular chaperones. *Cell* 151, 1296-1307.

# Abbreviations

A	Antibody
AAC	ADP/ATP carrier
ADP	adenosine diphosphate
Amp	Ampicillin
APS	ammonium persulfate
ATP	adenosine triphosphate
ATPase	adenosine triphosphatase
Avg	Average
BN-PAGE	blue native polyacrylamide gel electrophoresis
Bpa	p-benzoyl-L-phenylalanine
BSA	bovine serum albumin
C-	carboxy-
CBB	coomassie brilliant blue
Cc-	C core
CNBr	cyanogen bromide
CV	column volume
Cyt c	cytochrome c
DHFR	dihydrofolate reductase
DiSC <sub>3</sub> (5)	(3,3'-Dipropylthiadicarbocyanine Iodide)
DMSO	dimethyl sulfoxide

DNA	deoxyribonucleic acid
dNTP	deoxyribonucleoside triphosphate
DSG	disuccinimidyl glutarate
DSS	disuccinimidyl suberate
DTT	Dithiotreitol
$\Delta\Psi$	membrane potential
<i>E. coli</i>	<i>Escherichia coli</i>
EDTA	Ethylendiaminetetraacetate
F1 $\beta$	F1 $\beta$ subunit of the ATP synthase
FL	full length
5-FOA	5-fluoroorotic acid
fp	forward primer
FRET	Förster Resonance Energy Transfer
gDNA	genomic DNA
GPD	glyceraldehyde-3-phosphate dehydrogenase
HEPES	(4-(2-hydroxyethyl)-1-piperazineethanesulfonic acid)
His	Histidine
Hsp	heat shock protein
IgG	immunoglobuline G
IM	inner membrane
IMP	inner membrane peptidase
IMS	intermembrane space

IP	Immunoprecipitation
IPTG	isopropyl- $\beta$ D-thiogalactopyranoside
kDa	Kilodalton
LB	Luria Bertani
MPP	mitochondrial processing peptidase
Mt	Mitochondrial
MTS	matrix targeting signal
MTX	Methotrexate
N-	amino-
<i>N. crassa</i>	<i>Neurospora crassa</i>
NADH	nicotinamide adenine dinucleotide
NADPH	nicotinamide adenine dinucleotide phosphate
NBD	nucleotide binding domain
NEF	nucleotide exchange factor
Ni-NTA	nickel-nitrilotriacetic acid
NMR	nuclear magnetic resonance
OD <sub>x</sub>	optical density at x nm wavelength
OM	outer membrane
OXA	oxidase assembly
PAGE	polyacrylamide gel electrophoresis
PAS	Protein A-Sepharose
PCR	polymerase chain reaction

PEG	polyethylene glycol
PI	pre-immune serum
PK	proteinase K
PMSF	phenylmethylsulfonyl fluoride
POTRA	polypeptide transport-associated
pre	presequence of precursor protein
PVDF	polyvinylidene difluoride
pre-X	presequence-X (gene or protein)
prom-X-f	promoter-X (gene)-flank
RNA	ribonucleic acid
RNase	Ribonuclease
rp	reverse primer
RT	room temperature
<i>S. cerevisiae</i>	<i>Saccharomyces cerevisiae</i>
SAM	sorting and assembly machinery
SBD	substrate binding domain
SD	synthetic defined
SDS	sodium dodecyl sulphate
spFRET	single pair FRET
std dev	standard deviation
TAE	Tris base, acetic acid, EDTA
TBS	Tris-buffered saline

## Abbreviations

---

TCA	trichloroacetic acid
TEMED	N,N,N',N'-tetramethylene-1,2-diamine
TIM	translocase of inner mitochondrial membrane
TIRF	Total Internal Reflection Fluorescence
TM	transmembrane segment
T <sub>m</sub>	melting temperature
TOB	topogenesis of mitochondrial outer membrane $\beta$ -barrel proteins
TOM	translocase of outer mitochondrial membrane
TPR	tetratricopeptide repeat
Tris	tris(hydroxymethyl)aminomethane
UTR	untranslated region
v/v	volume per volume
w/v	weight per volume
WT	wild type
YPD	Yeast-Extract-Peptone-Dextrose
YPG	Yeast-Extract-Peptone-Glycerol
YPGal	Yeast-Extract-Peptone-Galactose
YPLac	Yeast-Extract-Peptone-Lactate

## Publications from this thesis

**Banerjee, R.**, Gladkova, C., Mapa, K., Witte, G., and Mokranjac, D. (2015). Protein translocation channel of mitochondrial inner membrane and matrix-exposed import motor communicate via two-domain coupling protein. *eLife* 4, e11897.

Demishtein-Zohary, K., Günsel, U., Marom, M., **Banerjee, R.**, Neupert, W., Azem, A., and Mokranjac, D. (2017). Role of Tim17 in coupling the import motor to the translocation channel of the mitochondrial presequence translocase. *eLife* 6, e22696

**Banerjee, R.\***, Günsel, U.\*, and Mokranjac, D. (2017). Chemical crosslinking in intact mitochondria. *Methods Mol Biol.*, 1567:139-154.

**Banerjee, R.**, Trauschke, V., Lamb, D., and Mokranjac, D. Conformational dynamics of mitochondrial Hsp70 inside mitochondria. (manuscript in preparation)

\*Equally contributing authors

# Eidesstattliche Versicherung

Banerjee, Rupa

Ich erkläre hiermit an Eides statt,  
dass ich die vorliegende Dissertation mit dem Thema

Molecular mechanisms of protein translocation across mitochondrial  
inner membrane

selbständig verfasst, mich außer der angegebenen keiner weiteren Hilfsmittel bedient und alle Erkenntnisse, die aus dem Schrifttum ganz oder annähernd übernommen sind, als solche kenntlich gemacht und nach ihrer Herkunft unter Bezeichnung der Fundstelle einzeln nachgewiesen habe.

Ich erkläre des Weiteren, dass die hier vorgelegte Dissertation nicht in gleicher oder in ähnlicher Form bei einer anderen Stelle zur Erlangung eines akademischen Grades eingereicht wurde.

Munich, 12.11.18

Ort, Datum

Rupa Banerjee

Unterschrift Doktorandin